The Inflamed Gut: An Integrative Approach to Understanding the Impact of Inflammation on Bacteriophage-Host Dynamics.

by

Keah Veronica Chambers Higgins

A dissertation submitted to the Graduate Faculty of
Auburn University
in partial fulfillment of the
requirements for the Degree of
Doctor of Philosophy

Auburn, Alabama
May 2, 2020

Keywords: Intestinal microbiota, intestinal phageome,
intestinal inflammation, bacteriophage dynamics, obesity

Approved by

Elizabeth Hiltbold Schwartz, Chair, Associate Professor of Biology
Laurie Stevison, Assistant Professor of Biology
Mark Liles, Professor of Biology
Stuart Price, Professor of Pathobiology

Abstract

The intestinal microbiome is a diverse and dynamic microbial ecosystem residing within the gastrointestinal tract. The mammalian intestine is home to both commensal and opportunistic pathogenic microorganisms. The immune system within the intestine has a unique challenge in maintaining homeostasis while providing protection from invading pathogens. The intestinal microbiome consists primarily of organisms from the domain Bacteria, with smaller populations of Archaea, Eukaryota, and Viruses. The healthy bacteriome profile is dominated by the phylum Bacteroidetes. Members of the Firmicutes, Proteobacteria and Actinobacteria phyla are also major components of the bacteriome. This intestinal microbiota in the 'healthy state' contributes to the healthy functionality of metabolic, digestive, endocrine, immune, and neurological function of the host. Inversely, the microbiota can negatively impact the host when the relative abundance of these consortia becomes altered, a condition generally known as dysbiosis. For example, the dysbiotic profile of intestinal microbiota in obesity consistently reflects an increased abundance of Firmicutes, altering the Bacteroidetes:Firmicutes ratio. Dysbiotic bacteriome profiles have also been linked to increased susceptibility of development of intestinal inflammation, colitis. Within the last 10 years, researchers have grown a respect for the intestinal bacteriome, but there are other components within the intestinal microbiome that could contribute, directly or indirectly, to the homeostasis of the intestinal microbiome. Namely, the bacteriophage within the intestinal microbiome, phageome, have recently been shown to display modulation in response to both environmental influences (diet) and internal influences (immune system induced stress). The phageome has been described as more diverse in people who have Inflammatory Bowel Disease (IBD). While the field has made progress towards understanding bacteriophage role in microecosystems, it is not well understood how these changes occur in an

established microbiome or how the abundance dynamics of the phageome progress overtime following external or internal influence. The goal of this study was to understand the longitudinal impact of dietary intervention and intestinal inflammation and how these influences affect bacteriophage abundance and functionality in the microbiome. To do this, intestinal bacteria and bacteriophage abundance changes were monitored following high-fat western diet (WD) feeding using shotgun metagenomic sequencing. Additionally, an *in vitro* study was conducted using a fecal bacterial and bacteriophage isolate to understand the role the mammalian host plays on bacteriophage infectivity rates. These isolates were used in modified adsorption constant kinetic assays and one-step growth curves both in the presence and absence of inflammatory derived products. Overall, components of the phageome are affected by the diet in various ways. The phageome of WD-fed mice display rapid shifts in abundance profiles of bacteriophage genera which appeared to proceed apparent abundance changes of the host. We found that most bacteriophage display abundance patterns that coincide with predicted bacteriophage behavior. For example, temperate bacteriophage displayed a rise in abundance alongside their putative host which is likely explained by replication of host genome containing prophage. Interestingly, the abundance dynamics of bacteriophage do not always follow the abundance dynamics of their host. The *in vitro* experiments conducted showed that reactive oxygen and chlorine species led to delayed adsorption, delays in time to burst and reduction of progeny produced. At the conclusion of this work, we have shown that bacteriophage are affected in a similar manner to bacteria to external and internal influences on the intestinal microbiome. The abundance dynamics experienced by the phageome could play a role in development of dysbiosis and perpetuation of disease.

Acknowledgments

Over the course of my program, I have had the opportunity to interact and work with many amazing people. To these people, thank you will never encompass the true gratitude I have in my heart for all you have done to help me get to the finish line. Thank you all for being a part of this chapter of my story.

I first want to thank my major advisor Dr. Elizabeth Schwartz for always providing heart-felt advice, support, patience, and guidance throughout my graduate career. I want to take the time to thank all the other members of my graduate advisory committee. Dr. Mark Liles, thank you for all of your advice and helping me get my start in metagenomics. I want to express my gratitude to Dr. Stuart Price for providing me with training in bacteriophage isolation and culturing techniques. I want to express my appreciation to Dr. Laurie Stevison for giving me the tools that enabled me to skillfully utilize bioinformatics in my study. I am so grateful to have been mentored by all individuals on my committee and these few sentences do not speak to the magnitude of impact they had on my overall journey here at Auburn.

Of all the things I have experienced over the last 5 years, the vast majority of the most memorable moments included the closest people to me here at Auburn, my lab mates. These people were not just the 4 other people who shared the same small office in our lab. These are friends who have become family. Peter Rogers is one of the most creative and intelligent people I know, but he often would use this to challenge our thinking and keep us on our toes. Adesola Olatunda, my BFF number 1, was always there for me with her calm voice of reassurance but was never afraid to tell me when I was wrong. Robert Johnson was always looking to help me even if it was getting coffee or just to agree on colors of appliances. Haley Hallowell, my collaborator for life, I honestly could have not gotten here without you and you will forever have

a special place in my heart. The friendships that have developed with these individuals who I have had the pleasure of working with over the last 5 years have made all the hardships worth it.

I am also indebted to countless undergraduate students who, either voluntarily or for credit, participated in various aspects of my research. Thank you to all the students who helped with the husbandry of the Mangalica pigs. I especially want to thank all the undergraduate students involved with the work on PF-2, namely Tillie Drost, Chad Hamm, Ben Nelson, Faith Anderson, Karin Chapelle, Sydney Bergstresser, Jack Landrum, Baker Smith, Madeliene Bruderer and Archie Landrum, for troubleshooting and conducting phage experiments over and over again until I was finally happy. I have enjoyed every minute of our unique experiment environment.

Not only was I blessed with a wonderful lab environment, but also with a whole support network of people here at Auburn. Thank you, Dr. Michael Greene, for allowing me to collaborate with you and Lauren Woodie. To Dr. Richard Sorrentino, thank you so much for everything you taught me regarding teaching and for encouraging me to go for it to the fullest in everything I do. My gratitude also goes to Dr. Michael Miller for his assistance in helping me obtain the image on *PF2.* Thank you to numerous other faculty members for all the support, reagents, advice, insight and laughs, namely Dr. Paul Cobine, Dr. Jason Upton, Dr. Scott Santos, Dr. Kate Buckley, Dr. Carla Shoemaker, Dr. Mary Mendonca. I am also so grateful to my department, faculty and staff, for numerous travel awards and being extremely supportive of their graduate students. Of note, thank you to Paula Norrell, Joann Broach and Michele Smith for rapidly addressing every request and concern I had with kindness and a smile. Kirby Norrell, thank you for always being there for me and for showing genuine care that is so hard to come by these days. Finally, to countless friends thank you for the comradery, laughs and support: Alinne

Perra, Alexandra Colombara, Abby Beaty, Sarah Martin, Megan Powers, Pricilla Barger, Kaitlyn Murphy and Kate Stillion just to name a few.

Thank you to every member of my family both immediate and extended for your undying support, love, encouragement, and prayers. I especially want to acknowledge my parents, Kai and Kecia Chambers, for all the sacrifices, love and support they have provided me over the course of my studies and entire life. To my siblings, Rhett and Kayli Chambers, and their families (Ashley, Merritt, Reid and Rhodes Chambers), thank you for always believing in me more than I believed in myself. To my husband, Christopher, thank you for the insurmountable things you have done (and put up with) over the course of our relationship and time during graduate school. Through the chaos of this life, I am thankful you are by my side no matter what. To my ever-present heavenly father, thank you for being my refuge and peace in the storm of mental chaos. I would not have been able to complete this journey without your unfailing love.

Table of Contents

List of Tables

List of Figures

List of Abbreviations

IBD	Inflammatory Bowel Disease
WD	Western Diet
GI	Gastrointestinal
H_2O_2	hydrogen peroxide
HOCl	hypochlorous acid

Chapter 1

Literature Review

Introduction to the Intestinal Microbiome

All complex metazoans are colonized by a ubiquitous layer of microbial organisms that are present at all external surfaces of the host, specifically mucosal surfaces and skin [1]. This collection of microbial symbionts, known as the microbiota, and the environment they inhabit collectively make up the microbiome [2]. Within the last twenty years, there has been an exponential expansion in our understanding of the symbiotic nature of the microbiota via high-throughput DNA sequencing technologies coupled with advances in bioinformatics. These strategies were developed following completion of the Human Genome Project [3] and subsequent initiation of the Human Microbiome Project [4] in the early 2000s. This allowed for the emergence of an investigative field seeking to identify the organisms of the microbiome, characterize interactions between the microbiome and host, and determine influence of the microbiome on the pathophysiology of disease. New approaches in the field of microbiome research have allowed us to resolve our understanding of its role in human biology and disease [4]. Although many sites on a given host harbor a resident microbial community, no site has been more intriguing or puzzling than that of the intestinal microbiome.

The gastrointestinal tract of organisms, ranging from insects to humans, is inhabited by many symbiotic bacteria, archaea, eukaryotes, and viruses that compose the intestinal microbiota [5]. These approximately 100 trillion microbial constituents are representative of 5000 distinct species belonging to 6-10 major phyla [1]. The collective gene pool of the intestinal microbiota is

comprised of over 3 million microbial genes, which is 150 times more than genes identified within the human genome [6]. The assortment of microbial genes in the intestinal microbiome has substantial potential for metabolic functions comparable to the magnitude observed in the liver [1]. Many members of the intestinal microbiota obtain nutrients from substances ingested by the host, and in turn, the host benefits from the metabolites produced by the microbiota. The intestinal microbiota also contributes to the host by providing essential nutrients such as biotin and vitamin K, facilitating the digestion of complex dietary fiber by fermentation, and generation of butyric acid, which is a major source of fuel for the gut epithelia [1,7,8]. Beyond its metabolic contributions, the microbiota has also displayed the ability to interact with and influence components of the immune, endocrine, and neurological systems. Metabolites and cellular components of the microbiota are recognized by host cells, facilitating crosstalk between the microbiome and host. When in homeostasis, this crosstalk provides positive regulation of various organ systems [9]. Mice void of microorganisms (germ-free) have displayed reduction in intestinal secretory IgA, developmental defects in gut-associated lymphoid tissue and smaller Peyer's patches and mesenteric lymph nodes [10,11]. For example, the presence of the microbiota in the intestine has been linked to maintenance of the epithelial barrier integrity and regulation of gut motility [1,12]. This crosstalk first became evident in studies of germ-free animals. Investigators determined that stimuli derived from the intestinal microbiota acts to regulate secretion of bone morphogenetic protein 2 (BMP2) secreted by muscularis macrophages. BMP2 activates a receptor on enteric neurons that in turn induces secretion of colony stimulatory factor 1. This perpetuates a positive feedback loop to both induce peristalsis and maintain healthy macrophage development [5]. Although most cellular components of the intestinal system have developed by the time of birth, the intestinal neural networks and immune system do not reach functional

maturation until the host is exposed to the intestinal microbiome [13]. In this way, the intestinal microbiota is an active participant in host physiology.

The composition of the microbiota is regulated by a variety of stimuli such as diet, route of birth delivery, nutrient availability, antibiotic usage, age, and stress [14–16]. Organisms of the same species and lifestyle typically have a common core group of microbial symbionts. The defined core group of the healthy human and mouse intestinal microbiota includes large populations of Phylum Bacteroidetes and Firmicutes and smaller populations of Actinobacteria and Proteobacteria [17,18]. Members of two most abundant Phyla, Bacteroidetes and Firmicutes, have been directly linked to production of metabolites that contribute to the healthy colonic environment. For example, *Bacteroides thetaiotaomicron* has the capacity to metabolize plant polysaccharides and members of the genus *Clostridium* are one of many microorganisms that generate butyrate [18,19]. The relative proportion of these bacteria within the whole is crucial to maintaining the production of beneficial products. Furthermore, increasing evidence has linked the composition of the intestinal microbiota and the development of disease, such as obesity [20]. In obese individuals, the balance of the top two phyla is reversed, with Firmicutes comprising a larger proportion than Bacteroidetes [14,21]. Diets high in lipids and carbohydrates, such as the Western diet, can induce compositional changes in the intestinal microbiota that correlate to those characterized in obesity [2,20,21]. There is also evidence that defined microbial communities can induce increased energy harvest and induce the obese phenotype in the mammalian host [20–22]. However, it has not been determined if the intestinal microbiota or diet has more influence on the development of obesity in the mammalian host over other contributing factors. Most of the work evaluating the intestinal microbiota and obesity has focused on bacterial constituents as

they comprise the majority of the intestinal microbiome. Yet, other microbial populations, such as bacteriophage, also have the potential to impact host physiology.

Bacteriophage – silent modulators of the microbiome

Nonbacterial members of the intestinal microbiome have been neglected until recently, mainly due to the lack of diagnostic tools for the assessment of nonbacterial genomes [12]. However, these communities have displayed evidence that they too are contributing members of the healthy gut microbiome. One such community is the virome, or the viral components of the microbiome [12]. The virome is comprised of both eukaryotic and prokaryotic viruses. The dominant member of the intestinal virome are viruses belonging to the order Caudovirales, otherwise known as bacteriophages [12]. Caudovirales are tailed bacteriophages with double-stranded DNA genomes. Caudovirales is divided into Podoviridae, Siphoviridae, and Myoviridae families [12]. Originally, bacteriophage were utilized as anti-bacterial agents following identification by Twort and d'Herelle, independently [23]. Bacteriophage are viruses that target bacteria as a host and require host cellular machinery to reproduce. Bacteriophage can also be classified as either virulent or temperate.

Virulent bacteriophage operate through a purely lytic infection cycle, killing their host as new virions burst from the cell. Temperate bacteriophage however, have evolved mechanisms that allow them to undergo either a lytic infection cycle or undergo lysogeny [23]. Lysogeny is a life cycle in which phage integrate their genome into the host's or form an episome and enter a phase of latency [23]. During the latent phase of lysogeny, both host and bacteriophage genomes are replicated, but little phage gene expression is detected. Under stress or other external stimuli, latent bacteriophage can become activated, resulting in a shift to the lytic cycle [23].

Infection begins with adsorption of the phage particle or virion to its host cell through specific receptor recognition. This is followed by delivery of the phage nucleic acid into the infected cell. At the conclusion of infection, all bacteriophage undergo lytic infection cycle where progeny phage particles are released from the host cell in a process that most often involves host cell lysis via bacteriophage-derived proteins [23]. New insights into bacteriophage dynamics have shown that the choice of infection cycle is not as predictable as previously thought, especially in the setting of microbial ecosystem [24–26].

Bacteriophage were featured in early genetic experiments that facilitated the birth of molecular biology during the mid-twentieth century. They were utilized in the ground-breaking Hershey and Chase experiment that identified DNA as the genetic material which is now considered basic knowledge of the nature of life at the molecular level [23]. It seems fitting that there is a resurgence of investigations into bacteriophage in the new age of genetic exploration facilitated by next generation DNA sequencing. The advent of high-throughput sequencing and bioinformatics has allowed researchers access to a multitude of data regarding genetic relatedness, identification of genetic mutations in disease, and allowed for meaningful characterization of microbial communities. Early work on characterization of microbial communities focused on bacterial constituents, as 16S ribosomal classification techniques made it easier to isolate and classify them. Recently, the virome, specifically the bacteriophage communities or phageome, has gained attention from those studying the intestinal microbiota. Although an exhaustive classification is still lacking, researchers have evidence that the phageome can maintain stability over time in healthy conditions and it is responsive to environmental stimuli [16,23,26,27]. Recent studies have described a common set of virus-like particles that are shared among more than one-half of all people tested, called the core

phageome. Yet, the phageome has displayed unique signatures between individuals regardless of genetic relatedness [23,24]. Bacteriophage represent the most abundant member of the intestinal virome and some suggest the highly abundant bacteriophage could be involved in shaping the healthy gut microbiome as well as having a role in pathogenic conditions [23].

Researchers now postulate that bacteriophage have the potential to directly shape bacterial communities. This could be accomplished by 1) killing the bacterial host or 2) rewiring bacterial metabolism and pathogenicity through horizontal transfer of genetic information [23]. Traditionally, bacteriophages are thought to infect bacteria purely out of the need to reproduce and kill host populations upon induction. In fact, virulent bacteriophages often display "kill the winner" dynamics: targeting the most prevalent or fastest growing bacterial population. However, new discoveries have provided more insight into bacteriophage biology which expands our knowledge of the possibilities of bacteriophage behavior. For example, prophage integration could enable the host to resist super-infection, encode toxins that foster bacterial pathogenesis or alter bacterial metabolism though phage-encoded genes [23]. Additionally, recent studies have described the quorum sensing-like mechanism of *Bacillus* phage phi3T that coordinates lysogeny decisions. It is thought that this form of communication allows bacteriophage to coordinate lysis in order to successfully undergo reproduction through replication of the host and lysogenize the host after so many replication cycles to ensure viable host remain for the next infection cycle [23]. These mechanisms point to the ability of bacteriophage to regulate bacterial populations in the microbiome which could consequently influence human health and disease.

Dietary Impact on the Intestinal Microbiome

Among the major environmental stimuli, nutrient availability appears to be one of the most relevant, not only in the composition of the intestinal microbiome, but also microbial ecosystems as a whole. For example, healthy diets, such as those high in plant products, are associated with a colonic bacteriome profile dominated by the phylum Bacteroidetes with Firmicutes being close in relative abundance [28]. Microbial balance and composition are important factors to maintaining optimal metabolic functionality and efficiency in the intestinal microbiome. For example, the intestinal microbiome associated with diets high in plant polysaccharides shows a high abundance of *Bacteroides thetaiotaomicron* [18]. Additionally, *B. thetaiotaomicron's* polyfructose-containing glycan degradation is enhanced in the presence of the methanogen *Methanobrevibacter smithii* which is also shown to be prevalent in these conditions [29]. Recently, the intestinal microbiome's role in metabolism has been shown to extend beyond food digestion and nutrient adsorption to include regulatory influences of the central nervous and endocrine systems [1]. In contrast to homeostatic conditions, deviations from the healthy state of the intestinal microbiome, termed dysbiosis, can greatly contribute to the development of metabolic disorders and disease.

Alterations in the intestinal microbiota can influence metabolic diseases by potentially 1) increasing caloric extraction from intestinal contents resulting in increased adiposity, 2) inducing low grade chronic inflammation either directly or via Leaky Gut syndrome, 3) generating toxic metabolites from dietary components or 4) via indirect regulation of host metabolic functionality [1,30]. The mechanisms by which the microbiome influences metabolic disease is said to be a direct consequence of altered microbial metabolism and interactions with the intestinal immune system. For example, diets rich in saturated fat are correlated with elevated levels of Gram-negative bacteria, which leads to elevated luminal LPS levels [1,21,31]. This can lead to increases in systemic

circulating LPS originating from translocation across the gut, a condition termed “leaky gut syndrome”. Leaky gut syndrome can contribute to the development of metabolic endotoxemia, characterized by low-grade chronic inflammation, metabolic disease and insulin resistance [1].

High fat diets have not only been linked to higher abundance of Gram-negative organisms, but also to display a shift from Bacteroidetes-dominant to a more even abundance of Bacteroidetes and Firmicutes in the intestinal bacteriome profiles. The proportional shifts displayed in Phylum profiles in these individuals is related to a bloom in the class Bacilli and reduction in Bacteroidia and Clostridia in relative abundance [32]. Dysregulation or dysbiosis of microorganisms can lead to alteration to the metabolic profile and could result in generation or overaccumulation of toxic metabolites from the host diet. For instance, amino acid deamination and decarboxylation in bacteria produces ammonia and amines [33], respectively. High ammonia concentrations have been correlated with tumorigenesis [33]. Additionally, bacterial degradation of cysteine and methionine leads to the formation of hydrogen sulfide which has been linked to inhibition of butyrate oxidation in colonocytes [33]. Finally, the intestinal microbiota induces indirect regulation of host metabolic functionality, such as in the case of suppressed Fiaf expression. Under conditions of over consumption, the microbiota induces suppression of Fiaf expression which ultimately induces fat deposition in the host [1,30]. This is one mechanism by which the intestinal microbiota influences host physiology and promotes obesity.

There is an ever-growing concern of obesity rates in developed countries. Obesity is associated with increased adiposity, metabolic dysregulation, development of low-grade chronic inflammation, and dysbiosis of the intestinal microbiome [9,34]. Obese individuals are also more likely to develop other conditions such as diabetes, IBD, and congestive heart failure [14,21,35]. While diet has been shown to be a major modulator of intestinal microbial composition and of

obesity, the intestinal microbiota has been shown to have their own role in the development of obesity. Riduara, et al. supported this idea by demonstrating that the obese phenotype can be conferred via fecal microbiota transfer from an obese donor to a germ-free organism [20]. Dietary patterns have also been associated with a change in the virome community to a new state. Recent studies in dietary influences on viral community structure reported that individuals on the same diet had similar intestinal viral consortia [36]. The role of bacteriophage and of the host immune response on the composition of the microbiota requires further study to be better understood.

Intestinal inflammation and its Effect on the Intestinal Microbiome

Correct interplay between the intestinal microbiome and the host has been demonstrated to be essential to human health [12]. Maintaining homeostasis of this complex system has resulted in the development of a specialized immune system. The mucosal immune system is responsible for rapidly detecting and clearing transient pathogens while also ensuring tolerance of beneficial microorganisms. The mucosal immune system has intricate systems of recognition facilitated through toll-like and nod-like pattern recognition receptors that allow for detection and monitoring of the microbiota [1]. Studies in germ-free mice have illustrated the necessity of microbial interactions during the development of both the innate and adaptive immune systems. Yet, multiple mouse models of inflammatory disease have also demonstrated the necessity of the presence of the intestinal microbiota in the development of various inflammatory diseases ranging from colitis to arthritis [1].

Inflammatory diseases share the common symptom of inflammation. Inflammation is a mechanism of the immune system that provides defense against pathogenic threats and contributes to the repair of damaged tissue. The intestinal immune system has the additional

challenge of warding off invaders while minimizing harm to beneficial microorganisms and host tissues [1]. Intestinal inflammation can occur on a variety of levels. Acute inflammation is usually short term and involves signaling of proinflammatory cytokines to recruit granulocytes [37]. Chronic inflammation denotes a persistent immune response as seen in conditions including inflammatory bowel disease (IBD) and obesity [37]. Chronic inflammation is denoted by a shift in immune effector cells from granulocytes to mononuclear cell types due to a shift in the cytokine profiles [37]. Low-grade chronic inflammation, like that of obesity, rarely results in overt symptoms or damage to the tissue [37,38]. On the other hand, chronic intestinal inflammation seen in IBD can result in overall topological distortion of the gastrointestinal tract [37]. Many commensal bacteria are unable to maintain residency in the presence of constant immune pressures and intestinal damage [39,40]. Microorganisms that are adapted to surviving these pressures, namely opportunistic or true pathogens will bloom and express virulence factors upon detection of host tissue infiltration [41]. Ultimately, the host immune response to pathogenic threats can perpetuate the clinical presentation of these disorders.

Bacteria have evolved global regulatory systems for adaptation to both environmental and inflammatory stress. These regulatory systems aid in detecting and initiating responses to stressors-including pH, nutrient depletion, and oxidation that could destroy necessary proteins and nucleic acids [42]. Global regulatory systems of bacteria usually autoregulate and increase or decrease necessary gene expression based on the level of the stress applied to the system [42–44]. A well-documented example of a global regulatory system responsive to stressors is that of heat shock. Unfolded proteins and oxidative damage resulting from exposure to inflammatory products can induce transcription of a large set of heat shock proteins in bacteria that act to mediate potential damage, also referred to as the SOS response [43,44]. After production of pro-

inflammatory cytokines, such as IFNγ, TNF-α, and IL-1, the brain induces fever, lethargy, and a decrease in appetite [43]. A rapid increase in environmental temperature can leave bacteria vulnerable to protein denaturation. The pro-inflammatory cytokines also stimulate immune cells to migrate to the affected area. Consequently, biproducts of the immune system can act to clear infection as well as disrupt resident microorganisms. For example, neutrophils are among the first immune cells to arrive at inflammatory sites. These are potent immune cells that, in addition to being phagocytic, contain machinery and enzymes to produce oxygen and chlorine radicles. These conditions can aid in controlling infection but can cause oxidative damage to symbiotic commensals. It has been established that induction of bacterial SOS functions result in phage repressor inactivation in temperate bacteriophage [45]. It is possible that similar reactions may contribute to bacteriophage composition changes during intestinal microbiome dysbiosis.

Where interactions between the bacteriome and immune system have been explored, it is still unclear which mechanisms of the immune system contribute to the alteration of bacteriophage diversity and abundance. Intestinal inflammation does impact bacteriophage populations within the intestinal microbiome [24,25]. Members of the defined core phageome were significantly depleted or absent in IBD patients as compared to healthy counterparts [24]. Additionally, Norman, *et al.* reported that during times of intestinal inflammation, such as IBD, bacteriophage richness increased as bacterial diversity decreased [25]. Elevated abundance of bacteriophages could be connected with bacterial dysbiosis and perpetuation of inflammation via lysis of host organisms and subsequent release of pathogen-associated molecular patterns or triggering the immune response directly [25,46]. Unlike bacteria, bacteriophage share a purely mutualistic relationship to the mammalian host. Bacteriophage not only provide microbial regulation but have also been reported to confer a type of innate resistance to bacterial infection

by populating the mucin layer over mucosal surfaces [47]. Early studies in bacteriophage therapy have defined the immunogenic nature of bacteriophage and how the immune system responds to systemic bacteriophage prevalence. For example, bacteriophage are rapidly detectable in multiple organ systems, including the central nervous system, following treatment and are cleared within 30 minutes by the liver if their host is not located [48]. The bacteriophage particles are immunogenic enough to elicit immunoglobulin production in infants which has now been linked to a TLR9-dependent mechanism [25,46]. Yet, knowledge of how the immune system affects bacteriophage infectivity during intestinal inflammation is lacking in the literature.

Brief History of Project Development

This work was inspired by experiments investigating the intestinal microbiota in a natural model of obesity, the Mangalica pig. We found that the intestinal microbiota of obese Mangalica pigs had a slightly larger representation of viral sequences, primarily bacteriophage, than their lean counterparts. Upon discussing these finding with Dr. Stuart Price, I was afforded the opportunities to learn 'the ways of the phage'. After numerous rounds of tears and bacteriophage isolation, these techniques allowed for the isolation of the *Escherichia coli* bacteriophage, *PF-2,* from Mangalica pig samples. Bacteriophage culturing techniques were crucial to the years of work spent on the development of the *in vitro* protocols discussed in Chapter 4. The preliminary study with Mangalica pigs led to a secondary study seeking to characterize the timeline of the development of obesity. Around the same time, Dr. Michael Greene was conducting a study with similar experimental methods in a mouse model. The mouse system allowed us to answer the same scientific questions with better accuracy and resolution due to the numerous reagents available to study both the microbiome and immune response.

Hypothesis and Goals

The overall hypothesis of this project is the phageome has the capacity to respond to environmental influences independent of their bacterial host. This hypothesis was addressed with three major goals: First, we determined the kinetics of microbiome response to high-fat diet by monitoring the intestinal bacteriome and phageome in relation to the metabolic features of obesity; Second, we described the variety of detailed phage:host interactions following exposure to the high-fat diet; Finally, we determined the impact of inflammatory products on the infectivity and replication of bacteriophage and its enteric host in vitro.

References

1. Chassaing, B., Aitken, J. D., Gewirtz, A. T. & Vijay-Kumar, M. Gut Microbiota Drives Metabolic Disease in Immunologically Altered Mice. in Advances in Immunology vol. 116 93–112 (Academic Press Inc., 2012).

2. Turnbaugh, P. J. et al. The effect of diet on the human gut microbiome: a metagenomic analysis in humanized gnotobiotic mice. Sci. Transl. Med. 1, 6ra14 (2009).

3. Lander, E. S. et al. Initial sequencing and analysis of the human genome. Nature 409, 860–921 (2001).

4. A review of 10 years of human microbiome research activities at the US National Institutes of Health, Fiscal Years 2007-2016. Microbiome vol. 7 31 (2019).

5. Muller, P. A. et al. Crosstalk between muscularis macrophages and enteric neurons regulates gastrointestinal motility. Cell 158, 300–313 (2014).

6. Weinstock, G. M. Genomic approaches to studying the human microbiota. Nature vol. 489 250–256 (2012).

7. Wagatsuma, K. et al. Diversity of Gut Microbiota Affecting Serum Level of Undercarboxylated Osteocalcin in Patients with Crohn's Disease. Nutrients 11, (2019).

8. HAMER, H. M. et al. Review article: the role of butyrate on colonic function. Aliment. Pharmacol. Ther. 27, 104–119 (2007).

9. Cani, P. D. Human gut microbiome: hopes, threats and promises. Gut gutjnl-2018-316723 (2018) doi:10.1136/gutjnl-2018-316723.

10. HOSHI, H. et al. Lymph Follicles and Germinal Centers in Popliteal lymph Nodes and Other Lymphoid Tissues of Germ-Free and Conventional Rats. Tohoku J. Exp. Med. 166, 297–307 (1992).

11. Hapfelmeier, S. et al. Reversible microbial colonization of germ-free mice reveals the dynamics of IgA immune responses. Science (80-.). 328, 1705–1709 (2010).

12. Lopetuso, L. R., Ianiro, G., Scaldaferri, F., Cammarota, G. & Gasbarrini, A. Gut Virome and Inflammatory Bowel Disease. Inflamm. Bowel Dis. 22, 1708–1712 (2016).

13. Obata, Y. & Pachnis, V. The Effect of Microbiota and the Immune System on the Development and Organization of the Enteric Nervous System. Gastroenterology vol. 151 836–844 (2016).

14. Trosvik, P., Stenseth, N. C. & Rudi, K. Convergent temporal dynamics of the human infant gut microbiota. ISME J. 4, 151–158 (2010).

15. Hepworth, M. R. et al. Group 3 innate lymphoid cells mediate intestinal selection of commensal bacteria-specific CD4+ T cells. Science (80-.). 348, 1031–1035 (2015).

16. Virgin, H. W. The virome in mammalian physiology and disease. Cell vol. 157 142–150 (2014).

17. Human Microbiome Project Consortium. Structure, function and diversity of the healthy human microbiome. Nature 486, 207–214 (2012).

18. Edwards, L. A. et al. Aberrant response to commensal Bacteroides thetaiotaomicron in Crohn's disease: An ex vivo human organ culture study. Inflamm. Bowel Dis. 17, 1201–1208 (2011).

19. Duncan, S. H. et al. Reduced dietary intake of carbohydrates by obese subjects results in decreased concentrations of butyrate and butyrate-producing bacteria in feces. Appl. Environ. Microbiol. 73, 1073–8 (2007).

20. Ridaura, V. K. et al. Gut microbiota from twins discordant for obesity modulate metabolism in mice. Science 341, 1241214 (2013).

21. Ley, R. E., Turnbaugh, P. J., Klein, S. & Gordon, J. I. Microbial ecology: Human gut microbes associated with obesity. Nature 444, 1022–1023 (2006).

22. Turnbaugh, P. J. et al. An obesity-associated gut microbiome with increased capacity for energy harvest. Nature 444, 1027–1031 (2006).

23. Ofir, G. & Sorek, R. Contemporary Phage Biology: From Classic Models to New Insights. Cell (2018) doi:10.1016/j.cell.2017.10.045.

24. Manrique, P. et al. Healthy human gut phageome. Proc. Natl. Acad. Sci. U. S. A. 113, 10400–10405 (2016).

25. Norman, J. M. et al. Disease-specific alterations in the enteric virome in inflammatory bowel disease. Cell 160, 447–60 (2015).

26. Minot, S. et al. The human gut virome: inter-individual variation and dynamic response to diet. Genome Res. 21, 1616–25 (2011).

27. Reyes, A. et al. Viruses in the faecal microbiota of monozygotic twins and their mothers. Nature 466, 334–338 (2010).

28. Huttenhower, C. et al. Structure, function and diversity of the healthy human microbiome. Nature 486, 207–214 (2012).

29. Kobyliak, N., Virchenko, O. & Falalyeyeva, T. Pathophysiological role of host microbiota in the development of obesity. Nutr. J. 15, 43 (2016).

30. Parekh, P. J., Arusi, E., Vinik, A. I. & Johnson, D. A. The role and influence of gut microbiota in pathogenesis and management of obesity and metabolic syndrome. Frontiers in Endocrinology vol. 5 (2014).

31. Thaiss, C. A. et al. Hyperglycemia drives intestinal barrier dysfunction and risk for enteric infection. Science (80-.). 359, (2018).

32. Howe, A. et al. Divergent responses of viral and bacterial communities in the gut microbiome to dietary disturbances in mice. ISME J. 10, 1217–1227 (2016).

33. Vernocchi, P., Del Chierico, F. & Putignani, L. Gut microbiota profiling: Metabolomics based approach to unravel compounds affecting human health. Frontiers in Microbiology vol. 7 (2016).

34. Sun, L. et al. Insights into the role of gut microbiota in obesity: pathogenesis, mechanisms, and therapeutic perspectives. Protein Cell 9, 397 (2018).

35. Duncan, S. H. et al. Human colonic microbiota associated with diet, obesity and weight loss. Int. J. Obes. 32, 1720–1724 (2008).

36. Minot, S. et al. The human gut virome: inter-individual variation and dynamic response to diet. Genome Res. 21, 1616–1625 (2011).

37. Ryan, G. B. & Majno, G. Acute inflammation. A review. Am. J. Pathol. 86, 183–276 (1977).

38. Goldman, H. Acute versus chronic colitis: How and when to distinguish by biopsy. Gastroenterology vol. 86 (1984).

39. Samanta, A. K., Torok, V. A., Percy, N. J., Abimosleh, S. M. & Howarth, G. S. Microbial fingerprinting detects unique bacterial communities in the faecal microbiota of rats with experimentally-induced colitis. J. Microbiol. 50, 218–225 (2012).

40. Wen, Z. & Fiocchi, C. Inflammatory bowel disease: Autoimmune or immune-mediated pathogenesis? in Clinical and Developmental Immunology vol. 11 195–204 (2004).

41. Skaar, E. P. The Battle for Iron between Bacterial Pathogens and Their Vertebrate Hosts. PLoS Pathog. 6, e1000949 (2010).

42. Ron, E. Z. Bacterial Stress Response. in The Prokaryotes 1012–1027 (Springer New York, 2006). doi:10.1007/0-387-30742-7_32.

43. Wilson, B. A., Salyers, A. A., Whitt, D. D. & Winkler, M. E. Bacterial Pathogenesis. Bacterial Pathogenesis (American Society of Microbiology, 2011). doi:10.1128/9781555816162.

44. Bacterial Stress Responses, Second Edition. Bacterial Stress Responses, Second Edition (American Society of Microbiology, 2011). doi:10.1128/9781555816841.

45. Smith, C. L. & Oishi, M. Early events and mechanisms in the induction of bacterial SOS functions: Analysis of the phage repressor inactivation process in vivo. Proc. Natl. Acad. Sci. U. S. A. 75, 1657–1661 (1978).

46. Gogokhia, L. et al. Expansion of Bacteriophages Is Linked to Aggravated Intestinal Inflammation and Colitis. Cell Host Microbe 25, 285-299.e8 (2019).

47. Barr, J. J. et al. Bacteriophage adhering to mucus provide a non–host-derived immunity. Proc. Natl. Acad. Sci. 110, 10771–10776 (2013).

48. Appelmans, R. Le dosage du bactériophage. Compt Rend Soc Biol 85, 701 (1921).

Chapter 2

Integrative Longitudinal Analysis of Metabolic Phenotype and Microbiota Changes During the Development of Obesity

Abstract

In the United States, obesity has increased at an alarming rate over the past two decades. The prevalence of obesity has increased from 30.5% in 2000 to 40.4% in 2018. Although increased body mass is the main association with diet-induced obesity, it is not the only component that makes an obese individual unhealthy. Diet-induced comorbidities, such as Type II Diabetes Mellitus (T2DM) and non-alcoholic fatty liver disease (NAFLD), are commonly seen in obese individuals. While the bacterial consortia present at the endpoint of obesity are known to be distinct from lean individuals, we do not know at what point the change in the microbial populations occurs. Also, we know little about how other domains of the microbiota, namely viral populations, are affected during the progression of obesity. Thus, our goal in this study was to monitor changes in the microbiome and metabolic profile following western diet feeding. We accomplished this goal by taking metabolic data collected from Promethion Metabolic cages and metagenomic shotgun sequencing of fecal samples from a mouse model of diet-induced obesity over the course of 12 weeks. We found that after just 2 weeks on a western diet, the animals weighed significantly more and were less metabolically stable than their chow fed counterparts. This phenotype persisted at 8 and 12 weeks and was accompanied by significant insulin resistance at the time of sacrifice. Additionally, temporal shifts in not only the bacterial communities, but in bacteriophage communities were seen starting at the 2 weeks post WD-

feeding. Changes in the bacteriophage genera were observed as well as shifts in the microbiota over the course of our study in individuals fed a WD compared to a normal chow diet. Our study highlights the dynamic nature of the microbiota in response to dietary changes and correlated these events with the metabolic status of the mammalian host following WD feeding.

Introduction

The worldwide obesity rate has almost tripled since 1975 in the United States. Nearly 40% of the adult population was considered obese as recently as 2016 as compared to 15% between 1976-1980 [1,2]. A main cause for this rapid rise is the prevalence and popularity of food high in saturated fats and added sugars [3,4]. Individuals consuming a high-fat western diet (WD) are prone to developing diseases comorbid with obesity such as Type-II Diabetes Mellitus (T2DM), non-alcoholic fatty liver disease and cardiovascular disease, as well as gastrointestinal (GI) maladies such as irritable bowel disease and colon cancer [5–7]. The comorbidity of GI disease and obesity prompted investigations into potential links between the two disorders. Among the potential connections that have received a lot of attention are diet-induced alterations within the intestinal microbiota.

The intestinal microbiome is a diverse and dynamic microbial ecosystem residing within the GI tract. It consists primarily of organisms from the domain Bacteria, with smaller populations of Archaea, Eukaryota, and Viruses. Healthy diets, such as those high in plant polysaccharides, drive a colonic bacteriome profile dominated by the phylum Bacteroidetes [8]. Members of the Firmicutes, Proteobacteria and Actinobacteria phyla are also common components of the bacteriome [9]. The resident commensal bacteria carry out important functions for the host such as synthesis of vitamins and short chain fatty acids (SCFA), degradation of host dietary oxalates, and transformation of host derived bile acids, amongst many other metabolic functions [10,11]. However, the microbiota can negatively impact the host when the relative abundance of microbial populations becomes altered, a condition generally known as dysbiosis [10]. For example, the dysbiotic profile of the intestinal microbiota in obesity consistently reflects an increased abundance of Firmicutes, altering the Bacteroidetes:Firmicutes ratio [8,12]. However,

this has been mainly described at the endpoint of obesity. Thus, the kinetics with which microbial dysbiosis progresses during the development of obesity remains poorly defined. Additionally, many of these studies focus on phylum-level community profiles. Observing the more detailed dynamics of organisms at lower classification levels might better inform how shifts in the intestinal bacteriome relate to metabolic disease.

While much is known about the bacterial constituents within the microbiome, there is a substantial gap in our understanding of how other microbiome constituents, such as bacteriophage populations, change in abundance or composition during the development of obesity [8,13]. Bacteriophages are viruses that target bacteria and enter one of two lifestyles: lysogenic or lytic. Temperate bacteriophages may reside within the bacteria as a lysogen, or quickly replicate and lyse the host in a lytic cycle [14]. Virulent phages, however, do not possess the genes necessary to carry out lysogeny and are purely lytic [15]. Given the predator/prey relationship of phages and their host bacteria, diet-induced changes in intestinal environment are likely to drastically alter bacteriophage populations, and vice versa. One study utilizing gnotobiotic mice demonstrated that introduction of specific bacteriophage by oral gavage can induce compositional changes, in both bacteria and bacteriophage populations, shaping the intestinal bacteriome and microbiome [16]. Bacteriophage populations, collectively known as the phageome, have also displayed diet-induced disturbances [12,17]. However, our understanding of diet-induced longitudinal changes in bacteria/bacteriophage dynamics remains incomplete. Bacteriophages represent an attractive target for tailoring the gut bacteriome by targeting and culling populations of specific bacteria while leaving other commensal bacteria unaffected. Therefore, it is critical to understand their role in the development and progression of metabolic disease.

In the current study, we explore microbial population dynamics in a mouse model of diet-induced obesity. We collected fecal samples from animals at five time points on a chow or high fat Western Diet (WD) to determine how these populations changed as obesity and metabolic disease developed. Metabolic disruptions were apparent in animals after two weeks of high-fat feeding, yet microbial population shifts began after just two days. Additionally, we found that after twelve weeks on WD, bacteriophage populations separated into groups that correlated either with an obese metabolic profile or a lean metabolic profile. Interestingly, most bacteriophage genera correlated to metabolic data similar to their putative bacterial host family, but this was not always the case. Our study highlights a novel connection between diet-induced metabolic functionality and the intestinal microbiome.

Materials and Methods

Experimental Approach

Animals and Diets

Male C57BL/6J mice from Jackson Laboratories (Bar Harbor, ME) were singly housed in standard microisolator cages at the Veterinary Research Building, College of Veterinary Medicine, Auburn University. The room was maintained at an ambient temperature of 22°C ± 2°C on a 12:12 light:dark cycle with zeitgeber time (ZT) 0 representing lights on and ZT12 representing lights off. All experimental procedures were approved by the Auburn University Animal Care and Use Committee. Animals were fed standard rodent chow for 1-week during acclimation to the facility. After which, animals were split into groups receiving either the standard chow diet with tap water (Chow) or a High-Fat Western Diet with tap water (WD). The chow diet (Teklad Global Rodent Diet 2018) contained 24% of calories from protein,

18% from fat, and 58% from carbohydrate. The WD diet was based on the AIN-93G diet and consisted of 44% carbohydrate, 16% protein, and 40% fat, 30% of which was provided from lard, 30% from butterfat, 30% from Crisco, 7% from soybean oil and 3% from corn oil. All dietary groups were given food and water *ad libitum*.

Metabolic Cages

Promethion Mouse Cages (Sable Systems, Las Vegas, NV) were utilized to house animals for metabolic screening and phenotyping. Animals were transferred from their home cages and singly housed in the metabolic cages at three time points (2-, 4- and 12-weeks after diets began). The animals were kept in the cages for 3 consecutive days with the 1st day committed to environment acclimatization and the 2nd and 3rd days for data collection. All animals were returned to their home cage after completion of metabolic phenotyping. Animal activity was measured by the Promethion XYZ Beambreak Activity Monitor. Food, water, and body weight were measured by Promethion precision MM-1 Load Cell sensors. The amount food and water withdrawn from the hoppers was measured and analyzed. The body mass monitors were plastic tubes that also functioned as in-cage enrichment and nesting devices. Water vapor, CO_2, and O_2 were analyzed by the Promethion GA-3 gas-analyzer to provide detailed respirometry data. Energy expenditure (EE) was calculated in kilocalories (kcal) by utilizing the Weir equation: $60*(0.003941*VO_2\ (n) +0.001106*VCO_2\ (n))$ in which VO_2 is the oxygen uptake and VCO_2 is the carbon dioxide output, both of which are measured in ml/min. Respiratory exchange ratio (RER) was determined by measuring gas exchange within the metabolic cages to identify the substrate being primarily utilized for energy within the body. Specifically, RER is the ratio of CO_2 produced to the volume of O_2 consumed (RER = VCO_2 /

VO_2) where a RER ~ 0.7 indicates lipid utilization and a RER ~ 1.0 indicates carbohydrate utilization. All metabolic phenotyping data were analyzed using ExpeData software (version 1.8.2; Sable Systems) with Universal Macro Collection (version 10.1.3; Sable Systems).

Fecal Sample Collection

Collection of fecal matter was performed at the initiation of diet change (Day 0) as well at four other time points following WD feeding: 2 days, 2-, 8-, and 12-weeks. Animals were removed from their home cages and placed in sterile microisolator cages without bedding for 3 hours. Food and water were provided to the animals during this time. Mice were then returned to resident cages and feces were collected from the sterile cages for DNA extraction and shotgun metagenomic sequencing.

Tissue Collection and Analysis

Upon completion of the study, all animals were fasted and then sacrificed via CO_2 asphyxiation and quickly decapitated by guillotine to allow trunk blood collection. Tissues including the liver and visceral (epididymal and retroperitoneal) and subcutaneous (inguinal) white adipose depots were excised and weighed. Final blood glucose was measured by an Accu-Chek blood glucose meter. Serum insulin levels were determined by an insulin ELISA assay (Crystal Chem, Inc., Downers Grove, IL) and data were analyzed for insulin resistance using the HOMA-IR score (HOMA-IR = (26 * fasting serum insulin * fasting blood glucose)/405).

Shotgun metagenomic sequencing-based Microbiome Profiling

Immediately following collection, DNA was extracted from fecal samples using the Omega E.N.Z.A. Stool DNA kit. Extracted DNA samples were pooled (2/sample) and shotgun metagenomic sequencing was performed by Hudson Alpha (Huntsville, AL). Whole genome sequencing was performed using an Illumina HiSeq v4 with a 2 x 125 paired-end sequencing 200 million reads. Metagenomic sequences were evaluated for quality using FastX toolkit [18]. Low quality sequences (Q-score less than 30) and sequencing adapters were removed using Trimmomatic [19]. Sequences were then uploaded to the Metagenomic Rapid Annotation Server (MG-RAST) version 4.0.3 for taxonomic and functional annotation [20]. Briefly, sequences were paired, filtered for quality, dereplicated, filtered for host-specific sequences (*Mus musculus,* UMD v3.0), and annotated. Annotated profiles of each sample are publicly available at the MG-RAST repository (https://www.mg-rast.org/mgmain.html?mgpage=project&project=mgp81921). Taxonomic classifications were annotated using the GenBank repository with the minimum cutoff parameters of $1x10^{-5}$ e-value and alignment length of 15. Density plots, calculated by total annotated hits, were used to set stringent uniform percent identity thresholds while maintaining an accurate measurement of the microbial populations. The percent identity was set to a minimum of 80% identity for bacterial and functional annotations and 70% identity for bacteriophage (Order Caudovirales) annotations. At these parameters, we were able to provide a conservative estimate of taxa while excluding ambiguous sequences. Current databases are not complete for viral genera classification due to variations in taxonomic classification strategies. Therefore, species within the order Caudovirales, as annotated by MG-RAST, were cross-referenced with the International Committee on Taxonomy of Viruses taxonomic database or other documentation detailing classification of the bacteriophage [21] (See Appendix 1 for

annotation reference database). From this, we were able to update viral species into current taxonomic genera in order to describe the types of bacteriophage present and how they fluctuate following dietary change. Descriptions of genera present in our samples are outlined in Appendix 1. Taxonomic classification hits were then normalized based on the total hit count. Rarefaction curves depicting alpha diversity were generated using the MG-RAST server.

Statistics

Statistical analysis

Final body and tissue weights along with serum measures were analyzed using a one-way ANOVA with a Newman-Keuls *post-hoc* test. The percent body weight change and 24-hour cycle data were assessed by a repeated measures two-way ANOVA so that animals in one diet group could be compared with animals in another diet group across dietary weeks or circadian time points. The above statistical analyses were performed using SigmaPlot with significance determined at $p < 0.05$. Multiple linear regression analysis (ANCOVA) was employed to assess the impact of body mass on metabolic cage parameters and energy expenditure was adjusted accordingly. Utilization of the National Mouse Metabolic Phenotyping Centers (MMPC) Energy Expenditure analysis page (https://www.mmpc.org/shared/regression.aspx) allowed for the assessment of body weight as a covariate on energy expenditure with significance determined at $p < 0.05$. Significance for all measures was determined at $p < 0.05$ and all data are presented as Mean ± SE.

Microbiome statistical analysis

Three pooled samples for each diet group at each collection point were used to calculate changes of relative abundance in the microbiome. Relative abundance was used to calculate means and standard deviations of each treatment groups at each time point using the statistical program GraphPad Prism v4. Using the R studio statistical platform [22], t-tests were performed to identify significant difference in relative abundance of microbial taxa. Non-metric multidimensional scaling (n*MDS*) ordination was generated in R studio using the *vegan* package [23]. To generate the nMDS, raw bacterial hits were used to compute a sample dissimilarity matrix using the Bray-Curtis dissimilarity index. This matrix was then used to compute an ordination of the samples in two dimensions. The *vegan* package was also used to calculate Shannon's Diversity Index scores. Then, the Pielou's Evenness Index was calculated by dividing the Shannon's Diversity Index score by the log of unique species amount. Mann-Kendall Trend tests were performed on diversity and evenness scores separately using the *randtest* package [24]. Pearson correlation coefficients were calculated using relative abundance and metabolic readouts at 12 weeks following dietary exposure in R studio using the package *psych* [25]. Pearson correlation plots were generated in R studio using the package *ggcorplot* [26] using a correlation coefficient threshold of an absolute value of 0.6.

Results

Obesity pathophysiology

Body weight was tracked over the course of the 12-week experiment (Fig 2.1). Animals fed the WD had a significantly higher percent body weight change compared to chow starting at week 2 ($p < 0.01$) and persisting throughout the duration of the 12-week experiment ($p < 0.001$).

The change in body weight was mainly due to an increase in body fat as the WD-fed group had significantly heavier visceral and subcutaneous (Sub-Q) fat pad weights (Table 2.1, visceral: $p < 0.001$; Sub-Q: $p < 0.01$). Although weights were significantly increased by WD feeding, there was no effect of WD on fasting blood glucose. Serum insulin levels, however, were significantly elevated in the WD-fed group after 12 weeks (Table 2.1, $p < 0.01$). Insulin resistance was determined using the HOMA-IR equation and revealed that the WD-fed animals were insulin resistant compared to the Chow-fed animals (Table 2.1, $p < 0.01$).

Metabolic rhythm and flexibility

To examine the changes in average EE within the light and dark phases, we measured EE at each ZT over a 24-hour cycle. Although diurnal rhythmicity was observed in both dietary groups, the WD induced significant disruptions as early as 2 weeks. The WD-fed group exhibited elevated average EE when compared to Chow during the inactive (day) period from ZT4-ZT11 (Fig 2.2A, $p < 0.01$). At 4 weeks, the WD-fed group continued to demonstrate elevated average EE during the day, specifically at ZT3, ZT6 and ZT8-11 (Fig 2.2B, $p < 0.05$). By 12 weeks, the WD-fed group exhibited significantly elevated average EE for the entirety of the day cycle (Fig 2.2C, $p < 0.01$). Additionally, we observed a dip in the average EE in from ZT18-22, which was not as pronounced in the WD-fed group. Consequently, the EE of the WD-fed group was significantly elevated during that time (Fig 2.2C, $p < 0.05$).

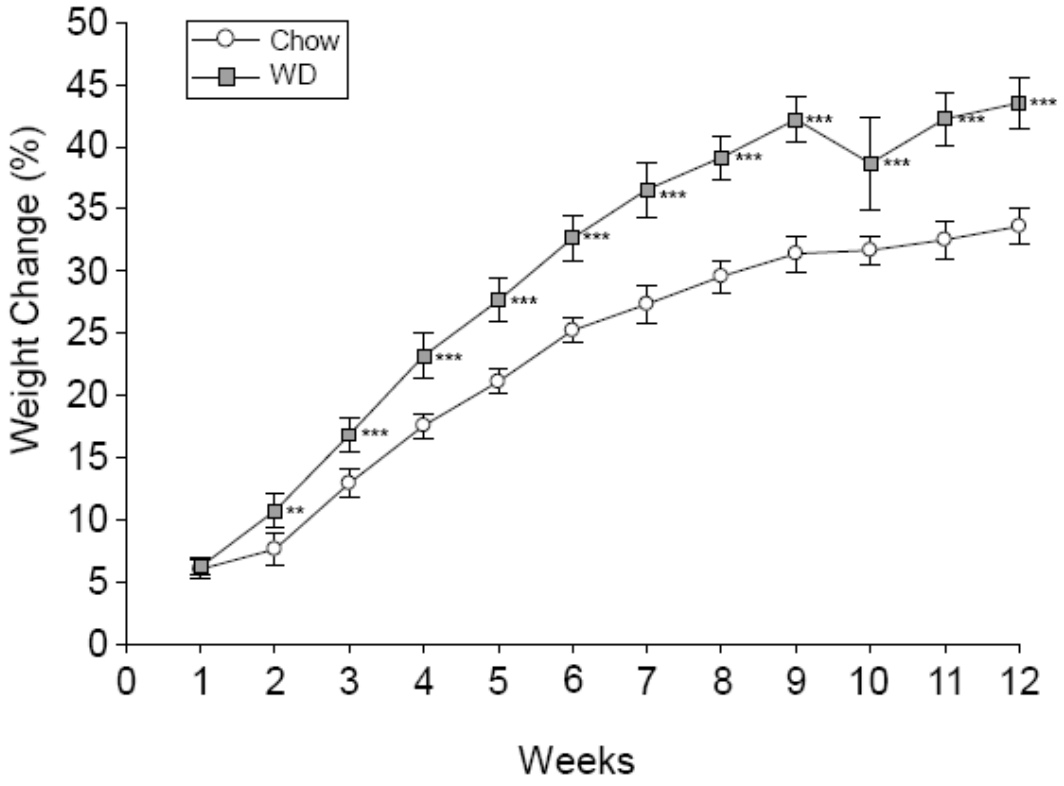

Figure 2.1. Percent body weight change. Weekly percent weight change over time is shown for the Chow and WD groups. Group differences over the course of dietary treatment were analyzed by ANOVA. All data points are shown as group mean ± SE. (* $p < 0.05$, ** $p < 0.01$, *** $p < 0.001$ compared to Chow)

TABLE 2.1. Final body weight, tissue weights normalized to body weight and serum measures for the three dietary groups.

	Chow	WD
Final Body (g)	27.4 ± 0.426[a]	39.8 ± 1.58[b]
Normalized eWAT (g)	0.024 ± 0.002[a]	0.060 ± 0.004[b]
Normalized rWAT (g)	0.006 ± 0.001[a]	0.017 ± 0.003[b]
Normalized iWAT (g)	0.009 ± 0.0004[a]	0.026 ± 0.004[b]
Normalized Liver (g)	0.046 ± 0.003	0.048 ± 0.002
Insulin (ng/mL)	0.814 ± 0.246[a]	2.27 ± 0.367[a]
Glucose (mg/dL)	164 ± 11.4	171 ± 14.7
HOMA-IR	8.84 ± 2.71[a]	26.2 ± 4.82[a]

Data are presented as mean ± SE. Differing superscript letters indicate differences between dietary conditions $P<0.05$.

Across all three experimental time points, a diurnal rhythm was observed in the RER of Chow-fed mice: greater metabolism of lipids during the inactive, day phase and more carbohydrate utilization during the active, night phase (Fig 2.3A-C). At week 2 and persisting through week 12, this rhythm was significantly dampened in the WD fed group with near constant lipid utilization across the time points. At 2 weeks, WD-fed animals demonstrated a significantly elevated RER from ZT4-ZT7 and a significantly decreased RER from ZT13-17 and ZT22-ZT24 (Fig 2.3A, $p < 0.05$). Four-weeks after diets began, RER in the WD-fed group was significantly decreased from Chow-fed animals starting at ZT12 and continuing to ZT24 (Fig 2.3B, $p < 0.05$). Lastly, after 12 weeks of dietary exposure, we observed results similar to week 4 during ZT13-ZT18 with the WD-fed animals exhibiting a significantly decreased RER (Fig 2.3C, $p <0.05$). These data suggest that the WD significantly impacted metabolic diurnal rhythms as well as metabolic flexibility. These effects were observed as early as 2 weeks and persisted through 4 and 12 weeks of WD feeding.

Diurnal activity and feeding behavior

We observed a typical murine diurnal rhythm in our animals with elevated activity during the night phase and decreased activity during the day (Supplementary Figure 1A-C). Diet did not appear to have an effect on activity at the 2-week time point (Supplementary Fig 1A). Similarly, 4-weeks of WD consumption did not induce large-scale changes in diurnal activity (Supplementary Fig 1B). However, at the 12-week experimental time point, we observed a significant drop in activity in the WD-fed group from ZT13-ZT15 (Supplementary Fig 1C, $p < 0.05$). However, this did not cause a significant decrease in activity when averaged across the entire night cycle.

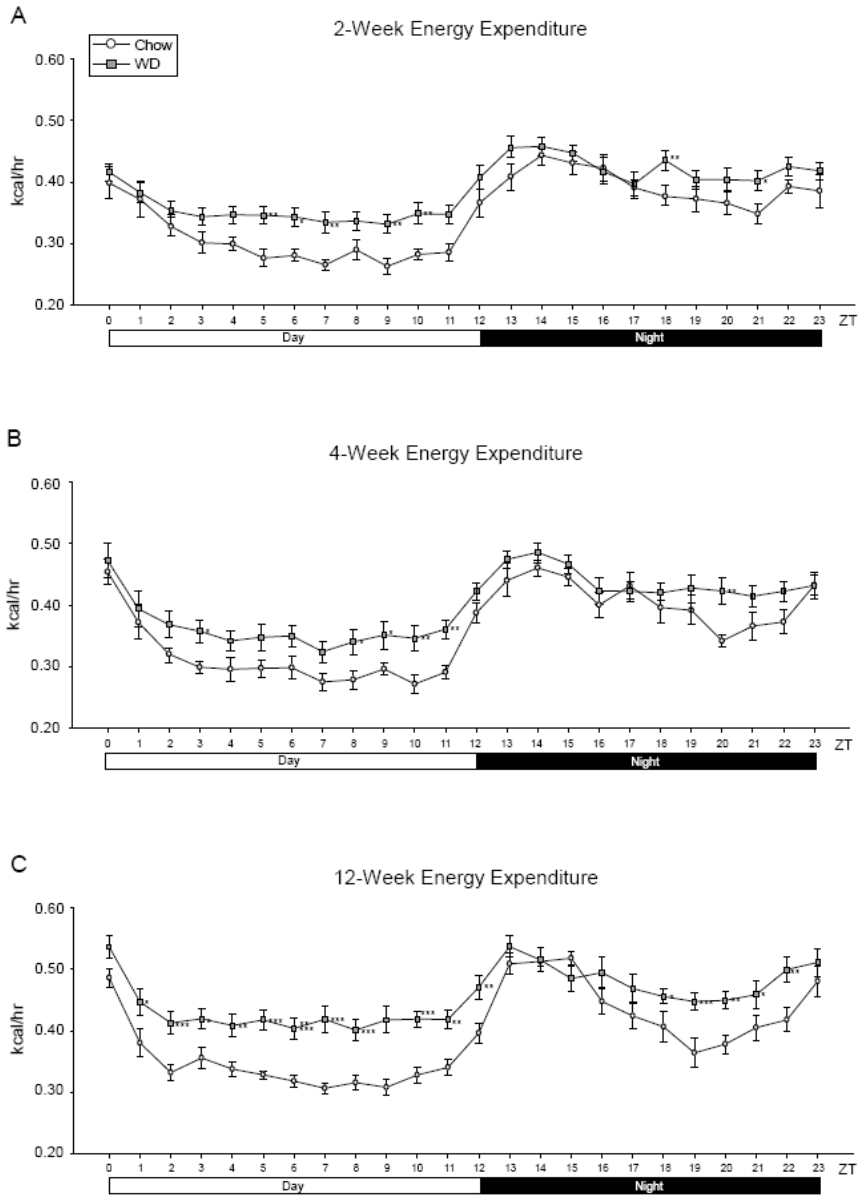

Figure 2.2. Energy expenditure at 2-, 4- and 12-weeks. A. Mean circadian analysis of energy expenditure at each hour in the 24-hour cycle in the Chow and WD groups after 2-weeks of dietary exposure. B. Mean circadian analysis of energy expenditure at each hour in the 24-hour cycle in the Chow and WD groups after 4-weeks of dietary exposure. C. Mean circadian analysis of energy expenditure at each hour in the 24-hour cycle in the Chow and WD groups after 12-weeks of dietary exposure. All data points are shown as group mean ± SE. (* $p < 0.05$, ** $p < 0.01$, *** $p < 0.001$ compared to Chow)

After 2-weeks on the diets, the WD-fed group consumed significantly more food and water by weight than the Chow-fed group during the day (Supplementary Fig 2A, left and middle panels, $p < 0.05$). Kilocalorie consumption was found to be significantly greater in the WD-fed group during all three time points (Supplementary Fig 2A, right panel, $p < 0.05$). At the 4-week time point, the WD-fed group consumed more grams of food during the day, but less food during the night than the Chow-fed groups (Supplementary Fig 2B, left panel, $p < 0.01$). This translated into greater kilocalorie consumption in the WD-fed animals during the day and total (Supplementary Fig 2B, right panel, $p < 0.01$). Twelve weeks after diets began, the WD-fed group did not consume more food by weight than the Chow-fed animals. However, kcal consumption was significantly elevated in the WD-fed group compared to Chow-fed group for the day, night and 24-hour total data points due to caloric density of the food (Supplementary Fig 2C, right panel, $p < 0.05$). There was not a significant difference in water consumption between the Chow-fed and WD-fed groups at 4 or 12 weeks.

Diet-Induced Changes in the Enteric Microbiota

To identify WD-induced changes in the enteric microbiota, we used shotgun metagenomic sequencing of fecal material at each indicated timepoint. First, to ensure that we had adequate depth of sequencing, estimates of alpha diversity and depth of sampling were assessed using rarefaction curves (Supplementary figure 3A-E). Each sample at each time point reached a plateau, (indicating more sequences than OTUs) signifying adequate depth of sampling and alpha diversity.

We next assessed global changes in the enteric microbiome in the WD-fed vs. Chow-fed mice. To achieve this, we analyzed the composition of the enteric microbiota over time by means

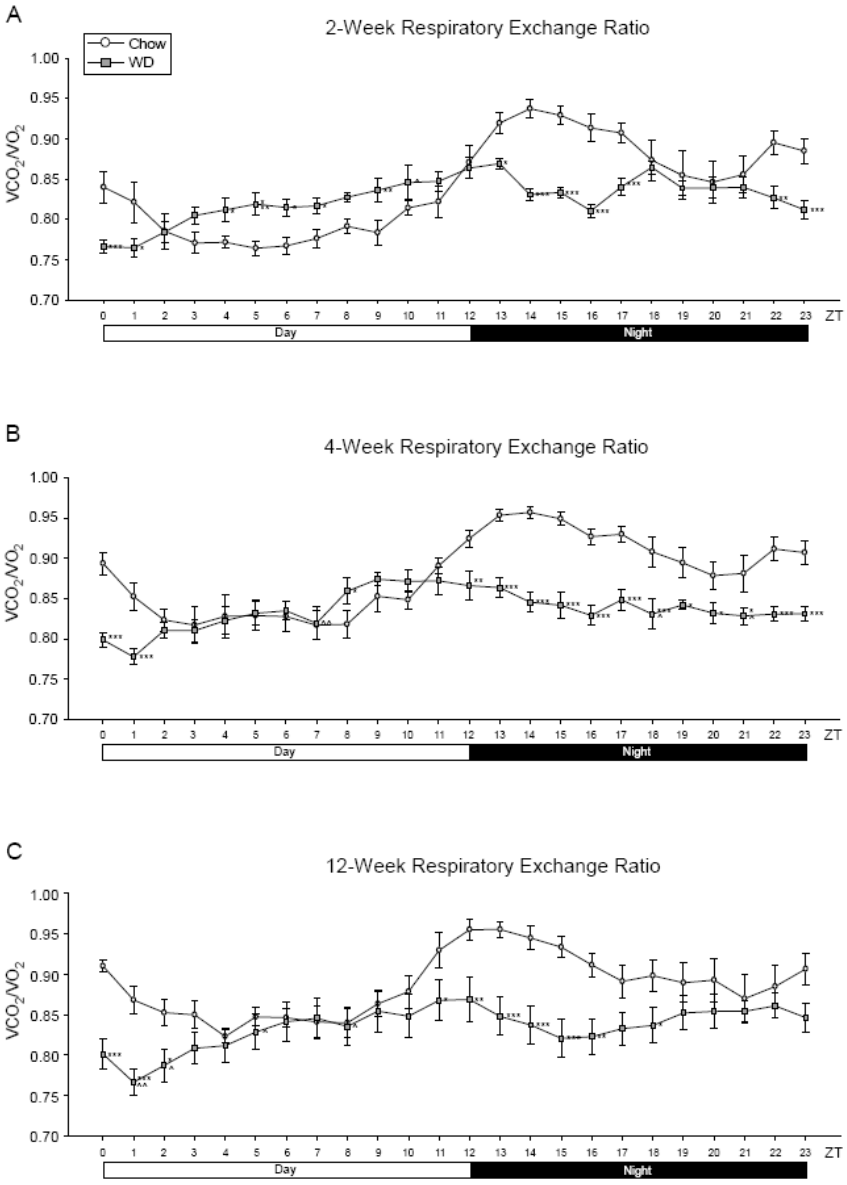

Figure 2.3. Respiratory equivalent ratio at 2-, 4- and 12-weeks. A. Mean circadian analysis of respiratory equivalent ratio at each hour in the 24-hour cycle in the Chow and WD groups after 2-weeks of dietary exposure. B. Mean circadian analysis of respiratory equivalent ratio at each hour in the 24-hour cycle in the Chow and WD groups after 4-weeks of dietary exposure. C. Mean circadian analysis of respiratory equivalent ratio at each hour in the 24-hour cycle in the Chow and WD groups after 12-weeks of dietary exposure. All data points are shown as group mean ± SE. (* $p < 0.05$, ** $p < 0.01$, *** $p < 0.001$ compared to Chow)

of non-metric dimensional scaling (nMDS) ordination plots based on the Bray-Curtis dissimilarity index (Figure 2.4). This method provides a similar visualization of the data as a principle component analysis (PCA) without the biases associated with a PCA concerning low abundance organisms [27]. The fit or stress of the nMDS denotes how well the ordination consolidates the observed distances among the samples. The fit associated with our analysis was 0.156 for both Figure 2.4A and 2.4B. This is considered a good fit for this analysis, where 0.3 or greater would be considered poor. In Figure 2.4A, the nMDS ordination plot factored by diet revealed one predominant central cluster (Chow diet) with the other diet (WD) scattered in a radiating pattern, indicating increasing dissimilarity. To further examine the dissimilarity between the two diet groups, an nMDS ordination plot factored by diet and time was constructed (Figure 2.4B). This showed the progression of increasing changes within the intestinal microbiome over time in those animals fed a WD (Figure 2.4B). As early as two weeks (and less dramatically so, at day two) (Supplemental Figure 7), we observed separation of WD-fed from Chow-fed groups indicating dissimilarity of their enteric microbiota (Supplemental Figure 5). This trend of increasing dissimilarity continued throughout the duration of the experiment, corresponding to increasing body weights and metabolic changes in the mice fed a WD.

Next, we assessed how the dissimilarity depicted in the nMDS plots corresponded to microbial diversity and evenness. Taxonomic heterogeneity was assessed by the Shannon-Weiner Diversity Index, which accounts for both richness (number of different OTUs) and evenness (distribution of individuals among OTUs). Additionally, Pielou's Evenness Index was used determine whether changes in the Shannon-Weiner Diversity Index were derived from changes in evenness or diversity of taxa. We observed a significant decrease in bacterial diversity and evenness in the WD-fed group compared to Chow-fed group, but primarily at 12

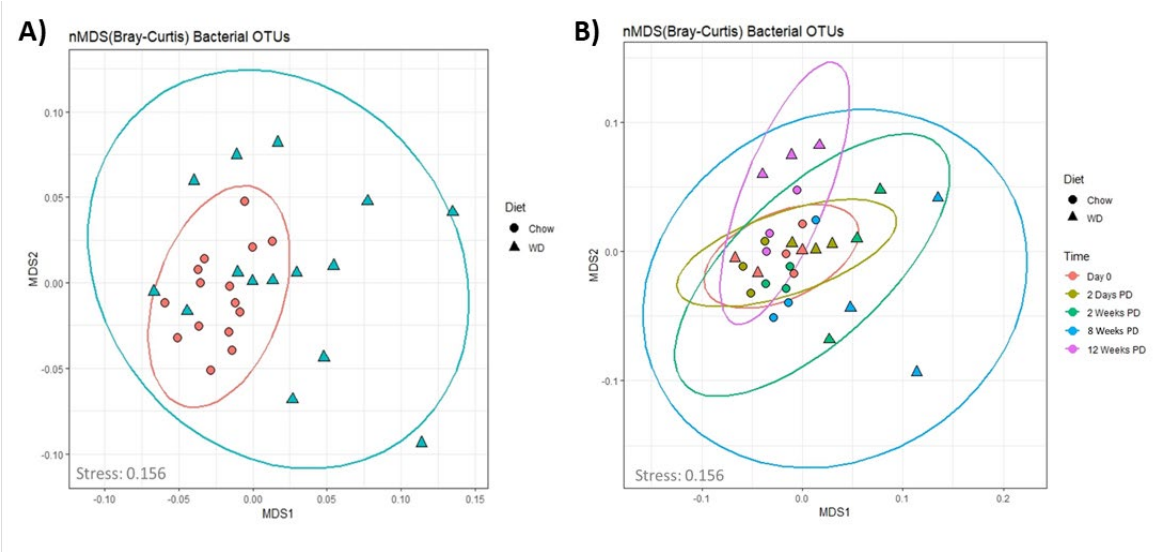

Figure 2.4. An nMDS ordination of the microbiota samples A) by diet and B) over time. The taxonomic profiles of the samples were used to compute the sample dissimilarity matrix using Bray-Curtis dissimilarity index. The matrix was used to compute an ordination of the samples in two dimensions (MDS1 and MDS2). The stress associated with this ordination is 0.156. The shapes in plot B denote the diet (Chow and WD), where the color denotes the time point (0 days, 2 days and 2, 8 and 12 weeks on the diets).

weeks on diet ($p = 0.006$; $p = 0.008$) (Supplemental Figure 4A, 4C). A Mann-Kendall trend analysis was also performed to evaluate the overall trend in changes in diversity and evenness over time. This analysis revealed a significant downward trend in diversity (S = -59, $p = 0.01$) and evenness (S = -55, $p = 0.02$) in WD-fed mice. This indicates the intestinal microbiota of mice fed a WD progressively declines in species richness and proportionality of bacterial communities over time.

To better understand the relationships between bacterial dysbiosis and metabolic phenotype at 12 weeks, Pearson's correlation coefficients were calculated to determine relationships between bacterial diversity, bacterial evenness and metabolic readouts. Both bacterial diversity and evenness were inversely related to parameters that increased during the development of obesity, specifically HOMA-IR, body weight, visceral fat weight, and Day EE (Supplemental Figure 4E; Appendix 2). Night RER, which is reduced in WD-fed mice, was positively correlated with bacterial diversity and evenness. In summary, decreases in enteric bacterial diversity and evenness, indicators of dysbiosis, were observed in mice fed a WD and correlated strongly with the metabolic phenotype of obesity.

Our next goal was to determine which microbial populations most significantly contributed to the dissimilarity seen in WD-associated microbiota. Relative abundance plots of microbial taxa illustrate the temporal shifts in relative abundance of the intestinal microbial communities in WD-fed vs. Chow-fed mice (Supplemental Figure 6). The composition of the microbiota in each group at day zero resembled the well-documented, healthy consortia of microorganisms [28]. Prominent bacterial phyla in the Chow-fed group (Supplemental Figure 6, Day 0) included members of the four well know bacterial phyla: Firmicutes (60 ± 8.5%), Bacteroidetes (33.460 ± 7.1%), Proteobacteria (1.675 ± 0.2%), and Actinobacteria

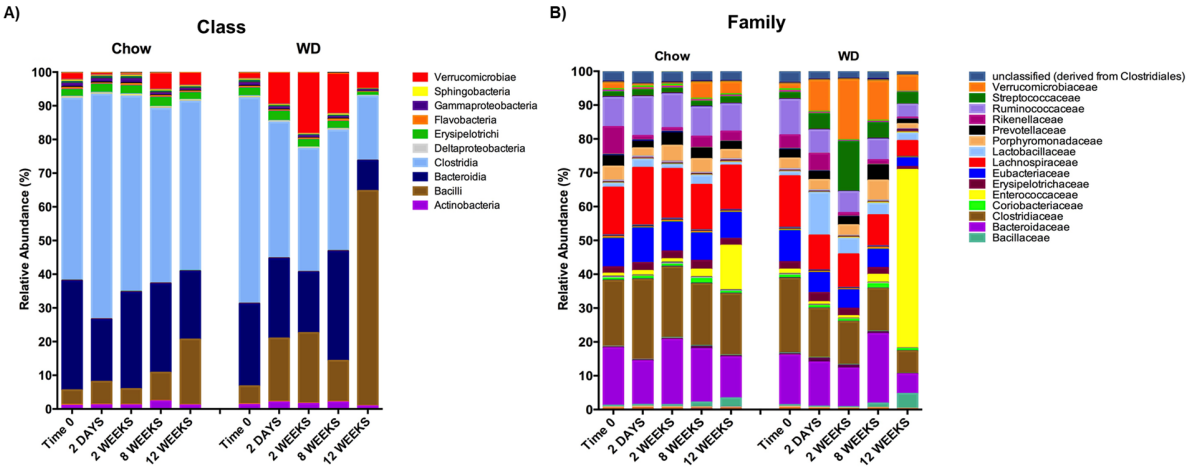

Figure 2.5. Changes in relative abundance of microbial composition after administration of the Western diet. A) Class and B) Family level bacterial composition in mice fed Chow or WD after 2 days, 2, 8 and 12 weeks of dietary exposure. The mean relative abundance (%) of bacterial phyla are shown.

(1.012 ± 0.2%), which are consistent with previous reports[29,30]. The microbial composition remained relatively stable throughout the 12-week experiment for mice fed a Chow diet. On the other hand, shifts in relative abundance profiles of WD-fed mice samples were detected as early as day 2. For example, Proteobacteria showed a significant reduction in abundance in the WD-fed group vs. Chow-fed group ($p = 0.02$). Proteobacteria continued to be significantly decreased in WD-fed group at 2 weeks ($p = 0.0005$) and 12 weeks ($p = 0.002$). Conversely, the phylum Verrucomicrobia began to increase after 2 days from 1.467 ± 2.4% to 9.182 ± 4.6% in the WD-fed group. The increase in Verrucomicrobia abundance was transient and began to decrease around 8 weeks. Verrucomicrobia returned to pre-diet abundance levels by 12 weeks. Notably, significant increases were observed in in Firmicutes ($p = 0.04$) at 12 weeks.

To more precisely resolve shifts in bacterial communities, we next evaluated class-level community profiles. The composition of the bacterial classes in the Chow-fed group were relatively stable throughout the experiment (Figure 2.5A). In contrast, starting as early as 2 days, we observed an increase in the class Verrucomicrobiae in the WD-fed group that peaked at 2 weeks and returned to roughly baseline levels by 12 weeks (Figure 2.5A). Other significant changes in the WD group included decreases in Clostridia at 2 weeks and most dramatically by 12 weeks ($p = 0.01$) (Figure 2.5A). The most notable change in the WD-fed group was a dramatic increase in Bacilli at 12 weeks ($p = 0.04$). Bacilli have been previously shown to be elevated in the intestinal microbiota in obese individuals [29]. Thus, even though no significant differences were noted between WD-fed and Chow-fed groups in the Firmicutes phyla, there were underlying changes in these constituents at the class level between the two groups. In addition to these changes, a significant decrease in Bacteroidia was observed in the WD-fed group at 2 weeks ($p = 0.04$) and 12 weeks ($p = 0.0007$). Additionally, Alphaproteobacteria,

Betaproteobacteria, Deltaproteobacteria, Epsilonproteobacteria and Gammaproteobacteria were significantly decreased at various time-points throughout the experiment in WD-fed groups. Thus, many subpopulations within the phylum Proteobacteria were reduced in abundance in WD-fed vs. Chow-fed mice.

Family level community profiles were assessed to obtain a more detailed view of the bacterial population dynamics on different diets. This revealed that the increase in the phylum Verrucomicrobia in WD-fed mice was predominantly due to an increase in the family Verrucomicrobiaceae (Figure 2.5B), primarily from the genera *Akkermansia* (data not shown). While Verrucomicrobiaceae relative abundance correlated well with the abundance pattern of Verrucomicrobiae, Bacillaceae did not follow the same trend as their class, Bacilli. Instead, there was a significant decrease of Bacillaceae in the WD-fed group compared to the Chow-fed mice (0.517 ± 0.02%) at 2 days (0.362 ± 0.009%, $p = 0.006$) and 2 weeks (0.338 ± 0.07%, $p = 0.01$). Enterococcaceae, specifically the Genera *Enterococcus*, appeared to be the major contributor to the increase in the class Bacilli at 12 weeks in this group ($p = 0.04$). Additionally, the increase seen in the class Bacilli could be attributed to a bloom in Streptococcaceae abundance at 2 weeks ($p = 0.005$), 8 weeks ($p = 0.01$) and 12 weeks ($p = 0.02$). Lactobacillaceae, another member of the class Bacilli, displayed an increase in relative abundance at day 2, but returned to baseline by 8 and 12 weeks. Members of the class Clostridia also displayed population divergence between WD-fed vs. Chow-fed mice which included a reduction in Clostridiaceae beginning at 2 days on WD ($p = 0.008$). Though not significant, we observed a decreasing trend in Clostridiaceae in the WD-fed group at 2, 8, and 12 weeks as compared to Chow-fed groups. Other families within the class Clostridia that were also significantly reduced included Clostridiales Family XI at 2 days ($p = 0.003$) and 2 weeks ($p = 0.03$) and Clostriales Family XVII at 2 weeks ($p = 0.05$) and 12 weeks

($p = 0.009$). Taken together, we observed reductions in many bacterial components, corresponding to the reduction of overall diversity and evenness within the intestinal microbiota, which could indicate initiation of dysbiosis as some organisms bloom as others decrease in abundance.

Diet-Induced Changes in the Enteric Phageome

We next wanted to determine how other constituents of the microbiome, namely bacteriophage populations, were impacted by WD vs. Chow diets. First, we assessed the degree of the dissimilarity by analyzing bacteriophage diversity and evenness (Supplementary Figure 4B and 4D). Similar to the trends observed in bacterial populations in WD-fed mice, we observed a reduction in the diversity and evenness of the enteric phageome over the course of the experiment. At 2 weeks, there was a significant reduction in bacteriophage OTU diversity ($p = 0.0001$) and evenness ($p = 0.0002$) in the WD-fed group (Supplementary figure 4B, 4D). The Mann-Kendall trend analysis revealed a downward trend over the course of the experiment in both diversity ($S = -65$, $p = 0.008$) and evenness ($S = -75$, $p = 0.003$) in WD-fed groups. Moreover, the reduction in the diversity and evenness of the enteric phageome preceded similar changes in bacteria following dietary exposure. Similar to our bacterial diversity and evenness correlations with metabolic readouts, bacteriophage diversity and evenness were inversely related to parameters seen to increase during obesity and at the end of our experiment, specifically HOMA-IR, body weight, visceral fat weight, and Day EE (Supplemental Figure 4E). Thus, changes in bacteriophage populations happened in tandem with changes in bacterial composition and changes in metabolic phenotype.

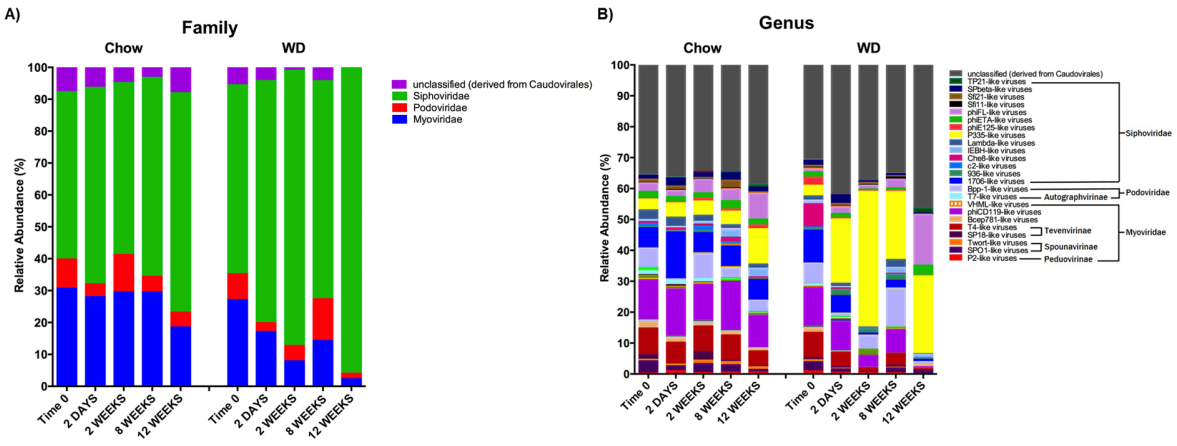

Figure 2.6. Changes in relative abundance of bacteriophage composition after administration of the Western diet. A) Family and B) Genus level viral composition derived from the order Caudovirales in mice fed Chow or WD at 2 days, 2, 8 and 12 weeks. Data shown are based on those families belonging to the order Caudovirales. The mean relative abundances (%) of viral families are shown.

The enteric phageome of Chow-fed mice remained relatively consistent throughout the experiment at the family level (Figure 2.6A). Mice fed a WD demonstrated a reduction of Myoviridae and Podoviridae as early as day 2. Myoviridae was significantly reduced in the WD-fed group at 2 weeks ($p = 0.001$) and 8 weeks ($p = 0.05$) as compared to the Chow-fed group. Myoviridae abundance continued to decline in WD-fed mice at 12 weeks (2.297 ± 0.5%), though not significant due to a decrease observed in Chow-fed mice. In contrast to Myoviridae, we noted a significant increase in relative abundance of Siphoviridae at 2 weeks ($p = 0.0001$). Taken together, WD feeding induced elevated abundance of the Siphoviridae family and reduced abundance in the Myoviridae family compared to Chow-fed mice.

Evaluating genus level bacteriophage profiles showed Chow-fed mice maintained a relatively consistent enteric phageome profile until 12 weeks (Figure 2.6B). In contrast, the WD-fed group exhibited an increase in *P335-like viruses* starting at 2 days, which was maintained through 12 weeks (Figure 2.6B), with significant increases at 2 weeks ($p = 1.78 \times 10^{-5}$) and 8 weeks ($p = 0.0001$). We also observed a significant depletion of the viral genus *phiCD119-like viruses* at 2 weeks ($p = 0.004$) in WD-fed mice. Though not significant, *phiCD119-like viruses* remained reduced in relative abundance in the WD-fed group at 8 weeks and 12 weeks. Other significant shifts in bacteriophage profiles in the WD-fed group included an increase in *phiETA-like viruses* at 8 weeks ($p = 0.01$), a decrease in *T4-like viruses* at 2 weeks ($p = 0.0006$) and a decrease in *T7-like viruses* at 2 days ($p = 0.03$). Additionally, we noticed an increase in *phiFL-like viruses* at 12 weeks. *phiFL-like viruses* are primarily temperate bacteriophage and this increase could be attributed to an increase in host species containing a prophage. The WD-induced alterations in the enteric phageome occurred as early as 2 days on diet (Figure 2.6B), preceding changes in their bacterial host abundance (Figure 2.5B).

Correlations between Diet-Induced changes in the Bacterial and Bacteriophage Consortia

To obtain a more comprehensive picture of how diet affects the relationship between specific phage genera and bacterial families, we calculated Pearson correlation coefficients between the Caudovirales genera and the 55 most abundant bacterial families at the final time point of 12 weeks (Figure 2.7). This analysis sorted bacteria and bacteriophages into two major groups, 1) a large group of bacteria that correlated positively with a large group of phages (both highlighted with green brackets) and 2) a smaller group of bacteria and bacteriophage that were positively correlated with each other (orange brackets). The two groups also had conversely negative correlations with members of the other (green vs. orange) group. This correlation grouping allowed for separation of families, most of which clustered with other families belonging to the same class. This was not true for members of the class Actinobacteria, Bacilli, and Gammaproteobacteria whose families segregated because of differential correlation. Given this information, we next determined the frequency of putative phage-host relationships between the positively correlated groups.

Upon further investigation of bacteria:bacteriophage relationships, we identified 6 (26%) of the 23 bacteriophage genera in the green grouping were strongly positively correlated (correlation coefficient of 0.6 or higher) with their putative bacterial host family (Figure 2.7). Additionally, 5 other bacteriophage genera within this grouping showed positive relationships with their preferred bacterial host family (correlation coefficients between 0.4 and 0.6) [total with above 47.8%]. Not all bacteriophage within this grouping correlated positively with putative host. Nine of the bacteriophage genera within this grouping negatively correlated with their putative host. The correlation coefficients of these bacteriophage genera with their host varied from slightly negative to strongly negative (Appendix 1). Interestingly, bacteriophage genera

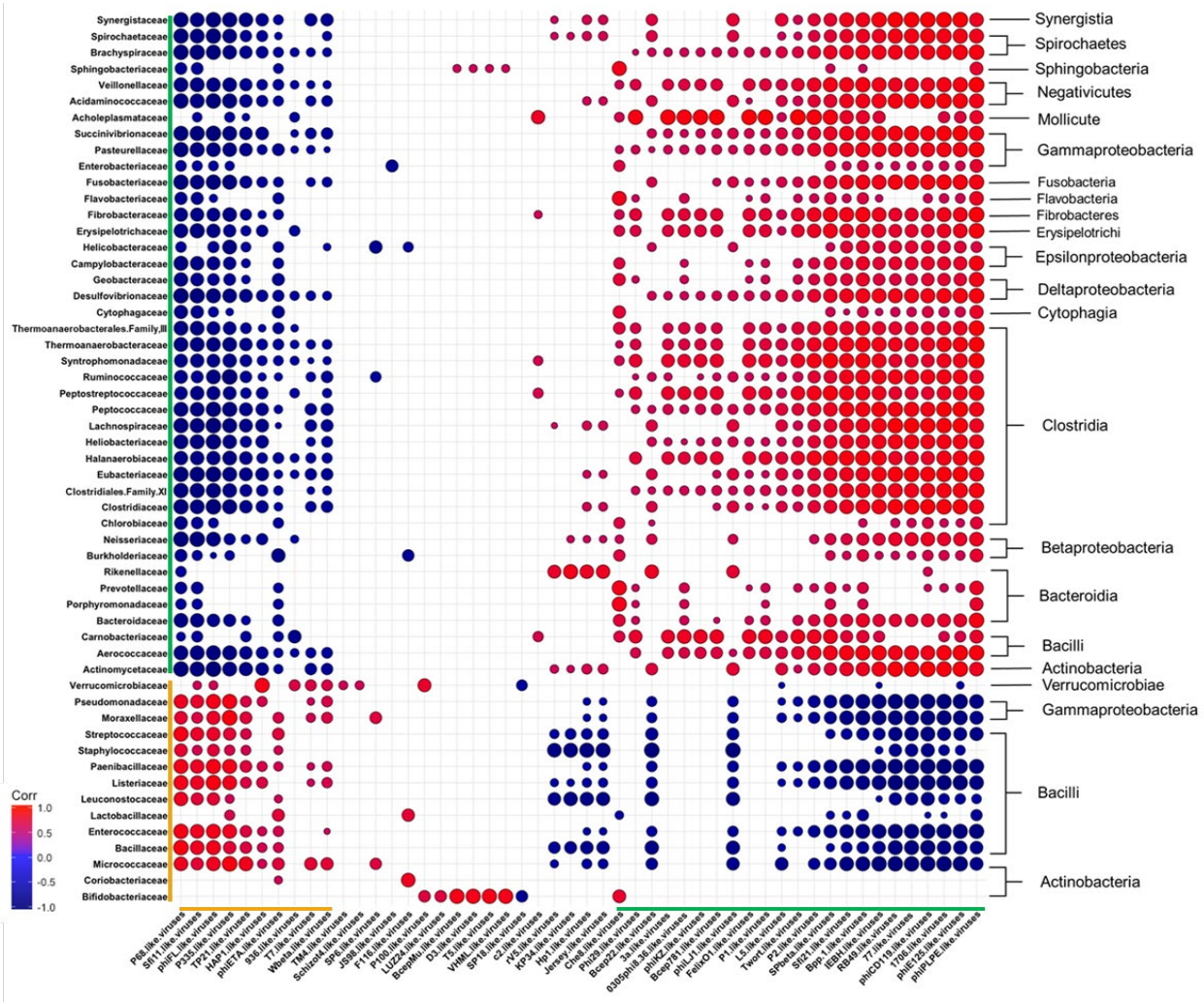

Figure 2.7. Diet Induced Bacteria-Bacteriophage Patterns in Obesity. Pearson's correlation plot of the top 55 most abundant Bacterial Families and all Bacteriophage Genera (Viral OTUs within the order Caudovirales) for mice fed Chow or WD at 12 weeks. Positive values (red circles) indicate positive correlation coefficients above 0.6, and negative values (blue circles) indicate inverse correlation coefficients below -0.6. The size and shading of the circles indicate the magnitude of the correlation, where darker shades indicate a stronger correlation than lighter shades. Correlation coefficient values outside of the threshold of 0.6 are not included in this plot. Putative host information and correlation coefficient values between bacteriophage genera and putative bacterial host family are listed in Appendix 1.

with strong negative correlations in this grouping targeted either members of Bacillaceae, Streptococcaceae or Staphylococcaceae. The green grouping showed a variety of relationships between host and bacteriophage, but the orange grouping was mainly composed of strongly positive bacteria:bacteriophage relationships. Of the 10 bacteriophage genera within the orange grouping, 6 were strongly positively correlated with their preferred bacterial host family [60%]. Additionally, 2 other bacteriophage genera within this grouping while positively correlated with their preferred bacterial host family, had weaker correlations (coefficients between 0.4 and 0.6) [total with above 80%]. Taken together, phage abundance did positively correlate with the abundance of their putative host bacteria in many cases, but not all.

Among the organisms outlined with green brackets, we see positive relationships between 6 bacteriophage and their putative bacterial host (Figure 2.7). These include bacteriophage genera who target bacterial families Pasteurellaceae (*phiPLPE-like viruses*), Burkholderiaceae (*Bpp-1-* and *phiE125-like viruses*), Clostridiaceae (*phiCD119-like viruses*) and Enterobacteriaceae (*Che8-* and *RB49-like viruses*). Many of the bacteriophage belonging to these genera are characterized as temperate. *phiCD119-like viruses*, for example, are temperate bacteriophage that target *Clostridium* species as their host [31–33]. Abundance of *phiCD119-like viruses*, and other temperate bacteriophage, is likely dependent on bacterial host abundance if they are present as integrated prophage. Five other bacteriophage genera within the green grouping were somewhat positively correlated with their preferred bacterial host family (0.4>x>0.6). These bacteriophages either targeted Enterobacteriaceae (*Felix01-, P1- and P2-like viruses*) or Burkholderiaceae (*Becp781-, Bcep22-, and P2-like viruses).* Other bacteriophage genera within the green grouping demonstrated no relationship or were negatively correlated with their putative host. In fact, Streptococcaceae-targeting bacteriophage genera *1706-* and

Sfi21-like viruses were strongly negatively correlated with their host, Streptococcaceae. Similar results were seen for Staphylococcaceae-targeting bacteriophage genera *77-like viruses* and Bacillaceae- targeting bacteriophage genera *SpBeta-* and *IEBH-like viruses.*

The orange grouping contained fewer bacterial families and bacteriophage genera than the green grouping (Figure 2.7). The majority of bacteriophage and putative host bacteria within the orange grouping showed strong positive correlations. These include Streptococcaceae-targeting *P68-, Sfi11-,* and *P335-like viruses,* Staphylococcaceae-targeting *P68- and phiETA-like viruses,* Bacillaceae-targeting *TP21-like viruses* and Enterococcaceae-targeting *phiFL-like viruses*. Many of these bacteriophage genera showed increases following WD feeding. For example, *P335-like viruses* displayed a rapid increase in relative abundance in the phageome. Bacteriophage within this genera target *Lactococcus* species as their hosts [33–37]. Consistent with this, we found a significant increase in Streptococcaceae, the taxonomic family containing the genus *Lactococcus*, in WD-fed mice starting at 2 weeks. This genus is comprised of an equivalent amount of virulent and temperate bacteriophage species. Thus, the elevation in abundance of this bacteriophage genera cannot be solely due to replication of prophage via host replication. Two other bacteriophage genera within the orange grouping were somewhat positively correlated with their preferred bacterial host family ($0.4>x>0.6$). These bacteriophages either targeted Streptococcaceae (*936-like viruses*) or Bacillaceae (*Wbeta-like viruses).* The remaining bacteriophage genera within the orange grouping were not significantly correlated with their host (Enterobacteriaceae-targeting *T7-like viruses*) or their host was not included in this analysis due to low relative abundance (Halomonadaceae-targeting *HAP1-like viruses*).

Correlations between WD induced Metabolic Phenotype and the Intestinal Bacteria and Bacteriophage populations

Next, we wanted to explore how specific bacterial families correlated with metabolic phenotypes within the WD-fed group. Interestingly, bacterial families clustered into similar groupings as those generated by correlations of bacteria and bacteriophage (again designated by orange or green brackets, Figure 2.8A). Bacterial families grouped in the orange cluster (Bacillaceae, Enterococcaceae, Lactobacillaceae, Leuconostocaceae, Listeriaceae, Paenibacillaceae, Staphylococcaceae, Streptococcaceae, Micrococcaceae, Moraxellaceae and Pseudomonadaceae) positively correlated with metabolic parameters shown to be indicative of metabolic disease, namely HOMA IR, Percent Body Weight Change, Visceral Fat Weight, and Day EE. Conversely, this orange group of bacterial families showed a strong inverse relationship with Night RER. As mentioned previously, a lower night RER (close to 0.7) during the active cycle would indicate primarily lipid utilization, characteristic of an inflexible metabolic status. These results indicate that bacterial families within the orange group positively correlate with key pathophysiological metabolic parameters associated with obesity. Thus, we can think of this group as obesity-associated.

Correlation profiles showing a negative relationship with metabolic parameters associated with obesity were apparent for the bacterial families within the green grouping, including the majority of the families belonging to the classes Actinobacteria, Bacteroidia, Betaproteobacteria, Clostridia, Cytophagia, Deltaproteobacteria, Epsilonproteobacteria, Erysipelotrichi, Fibrobacteres, Flavobacteria, Fusobacteria, Gammaproteobacteria, Negativicutes, Sphingobacteria, Spirochaetes, and Synergistia. Bacterial families within the green grouping negatively correlated with HOMA IR, Percent Body Weight Change, Visceral

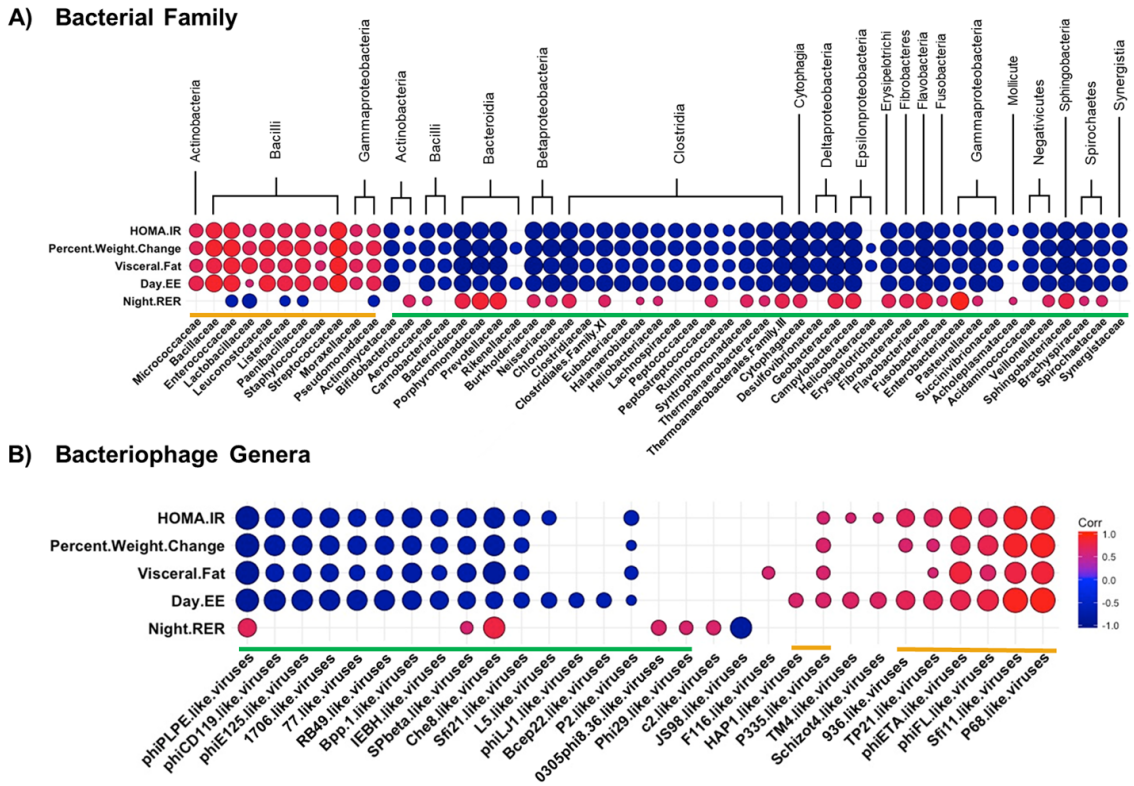

Figure 2.8. Diet Induced Bacteria/Bacteriophage – Metabolic Patterns in Obesity. Pearson's correlation plot of A) Bacterial Families (top 55 most abundant) or B) Bacteriophage Genera (Viral OTUs within the order Caudovirales) and metabolic parameters for mice fed Chow or WD for data after 12 weeks. Statistical significance was determined for all pairwise comparisons. Positive values (red circles) indicate positive correlation coefficients above 0.6, and negative values (blue circles) indicate inverse correlation coefficients below -0.6. The size and shading of the circles indicate the magnitude of the correlation, where darker shades indicate a stronger correlation than lighter shades. Correlation coefficient values outside of the threshold of 0.6 are not included in this plot.

fat weight, and Day EE and were most often positively correlated with Night RER. Hence, bacterial families grouped in green negatively correlate with key pathophysiological metabolic parameters associated with obesity.

Because strong relationships were identified between bacterial families and metabolic phenotypes, we sought to examine the relationships between bacteriophage populations in the intestinal microbiome and the metabolic phenotype observed in the WD-fed animals. Many of the bacteriophage genera that showed strong correlations to metabolic readouts correlated similarly in terms of green and orange grouped bacteriophage genera (Figure 2.8B). Orange labeled bacteriophage genera (*P335-, 936-, TP21-, phiETA-, phiFL-, Sfi11-* and *P68-like viruses)* positively correlated with HOMA IR, Percent Body Weight Change, Visceral Fat Weight, and Day EE. As these particular bacteriophage genera increase in relative abundance, phenotypic markers for body weight gain increase following dietary exposure. In contrast, green labeled bacteriophage genera (*phiPLPE-, phiCD119-, phiE125-, 1706-, 77-, RB49-, Bpp1-, IEBH-, SPbeta-, Che8-, Sfi21-like viruses,* etc.) have a negative relationship with HOMA IR, Percent Body Weight Change, Visceral Fat Weight, and Day EE revealing that as these metabolic parameters increase, there was a decrease in the relative abundance of these bacteriophage genera (Figure 2.8B). Because of the linked relationship between the bacteriophage genera and their host, correlations between bacteriophage and metabolic parameters may be a reflection of the bacterial host dynamics.

Discussion

In this study, we demonstrated that WD-feeding adversely effects the systemic metabolic profile and the intestinal microbiome. Importantly, we have also demonstrated novel

relationships between specific microbiome constituents and pathophysiological metabolic parameters associated with obesity. We described dynamic alterations to the composition of the intestinal microbiota as early as 2 days following WD feeding. Furthermore, fluctuations in the phageome were quite rapid, often preceding changes in abundance of their bacterial host. After 12-weeks of WD-feeding, constituents of the enteric microbiome, namely bacteria and bacteriophages, showed distinct correlation patterns between bacteria and bacteriophage with the metabolic phenotype, which allowed us to distinguish between a healthy microbiome and one more typical of obesity.

Our observations reflect that compositional shifts the intestinal microbiota occur within days following dietary exposure to the WD. Our data suggests that as animals consume a WD over time, the diversity of microorganisms decreases over time, with over-representation of certain organisms. This could be due to direct effects from the nutrient composition of WD or indirect effects mediated by competition between microorganisms. The composition of the microbiota between individuals on the same diet were relatively consistent, with only slight variation. Yet, changes induced by WD feeding happened rapidly and trended toward decreased diversity over time. One prominent example of rapid changes in WD-fed animals was the transient rise in Verrucomicrobia which peaked at 2 weeks and declined to levels comparable to Chow-fed counterparts by 12 weeks. This spike in Verrucomicrobia was mainly attributed to the genera *Akkermansia*, which has been shown to play a protective role during obesity. Administration of *Akkermansia muciniphila* during diet-induced obesity has been shown to improve the metabolic profile and colonic mucus layer thickness [38]. Perhaps these organisms aid in short-term protection from intestinal microbiota dysbiosis or bloom simply due to nutrient

availability following dietary exposure. Nevertheless, *Akkermansia* spp. were unable to maintain increased abundance after 8 weeks PD in our study.

At 12 weeks PD, we observed a depletion of Bacteroidetes and domination by Firmicutes in WD-fed mice. The disproportionality of Bacteroidetes:Firmicutes has been previously associated with the obese phenotype of the intestinal microbiota [8,12]. Although changes in the microbiota occurred rapidly, the shift in Bacteriodetes:Firmicutes ratio did not happen until late in our study, at 12 weeks. Instead, we observed diet-induced fluctuations in several other phyla that preceded the well-documented B:F ratio. Further, small changes were observed for bacteria at phylum level, but more dynamic shifts were detectable in relative abundance of bacteria at the class level as early as 2 days PD in WD-fed mice. The WD-fed group demonstrated a shift in bacterial profile to one dominated by Bacilli in contrast to the Chow-fed group which was dominated by Clostridia and Bacteroidia.

Many studies of the gut microbiota have been focused primarily on bacterial constituents, utilizing16S amplicon sequencing, as these do account for the majority of organisms in the gut microbiota. However, 16S amplicon sequencing has recently been described as having limited taxonomic and functional resolution as compared to shotgun metagenomics [39]. Primers used in 16S amplicon sequencing can also lead to discordant annotation results [39]. For these reasons, we chose a shotgun metagenomic sequencing approach which provides for identification of other organisms within the microbiome (namely bacteriophage) as well as enhanced resolution of both functional and taxonomic annotations. This approach, combined with the metabolic phenotype analysis, has allowed us to connect several important aspects of host-microbiome interaction in the context of WD-induced obesity. Not only have we observed changes that are consistent with

existing studies of the bacteriome in obesity [40,41], but we also bring into context changes in the phageome that occur in tandem with mammalian host metabolic changes.

In recent years, there has been a rise in appreciation of the enteric virome. This is due to technological advances in metagenomic sequencing, which has given us a reliable method to examine the complexity within this community. The experimental design of our study allowed us to follow the abundance patterns of a subset of organisms within the virome, the order Caudovirales which contains bacteriophage. Of note, our study did not use methods to quantify enveloped viruses or RNA viruses, and there may be much more to learn about these components of the enteric virome, especially in the setting of obesity. We targeted bacteriophages in order to describe the longitudinal shifts in their abundance following diet change as compared to their bacterial host. To do this, we cross-annotated species annotations, within the order Caudovirales, from the RefSeq database with the International Committee on Taxonomy of Viruses taxonomic database or other documentation detailing classification of the bacteriophage into respective genera (descriptions of genera present are outlined in Appendix 1).

In this study, we observed significant differences in the composition of bacterial consortia in response to diet change, consistent with previous reports [40,41]. We also observed shifts within the bacteriophage communities in WD-fed animals even prior to those observed in bacterial communities. Initially, we demonstrated that WD-feeding leads to increased abundance in bacteriophage belonging to the Siphoviridae family, and a decreased abundance in those belonging to the Myoviridae family. Similar changes have been observed in studies characterizing changes in intestinal bacteriophage populations during inflammation [42]. Previous studies have also reported effects of diet on composition of the virome. Howe, *et al.* demonstrated contrasting viral communities between individuals on a low fat and milk fat diet [12].

We also report dynamic changes in the phageome following WD feeding. Significant changes in community structure were demonstrated beginning at 2 days PD in our WD fed mice. Pearson correlation results also indicate intricate relationship networks between bacteria and bacteriophage following dietary exposure. One explanation for elevated bacteriophage abundance following diet change could be that viruses replicate at a much faster rate than bacteria. Bacteria typically produce one daughter cell per replication cycle where one bacteriophage can give rise to hundreds of new virions within one host cell per replication cycle. Additionally, bacteriophage require less resources for production of progeny than bacteria. When the opportunity arises, such as a bloom in target bacteria following nutrient availability, bacteriophage can benefit from the increase in viable host bacteria. In this way, a small bloom of bacteria could give rise to a rapid bloom of bacteriophage that target this host. Bacterial abundance levels could appear reduced or stagnant as bacteriophage progeny are infecting new daughter bacterial cells. This is until a plateau is reached in which bacteriophage have been reported to co-exist with host which could be a result of co-evolution of the host or virus [43–45].

Many of the bacteriophage genera correlated positively with their host, indicating that their relative abundance changed in parallel to their host. However, bacteriophage can bloom in the presence of their host as well as coexist with them [46]. We further demonstrate that bacteriophage abundance dynamics do not always follow that of their host, and this pattern was exacerbated in WD-fed mice. For example, members of the Streptococcaceae-targeting bacteriophage genera showed a wide range of responses to WD-feeding. *P335-like* and *936-like viruses* showed similar responses to diet change, directly corresponding to that of their host while *1706-like viruses* showed very different patterns of abundance than their host. The *P335-like viruses* genus is comprised of approximately equal portions of virulent and temperate bacteriophage species.

Therefore, the bloom of this bacteriophage genera could arise as a result of a combination of interactions, such as prophage integration (temperate) in the host and kill-the-winner dynamics (virulent). In the "kill-the-winner" scenario, host bacteria increase in abundance, followed by a bloom in virulent bacteriophage who target that particular host. One good example of this that we observed was the *936-like viruses,* which increased on the heels of their host Streptococcaceae. This genus of bacteriophage is strictly comprised of virulent bacteriophage species, thus an increase in abundance was likely explained by kill-the-winner dynamics alone.

Previous theories of bacteriophage ecology and abundance predict bacteriophage populations would follow that of their putative host - either due to lysogeny or kill-the-winner dynamics - which much of our findings support. However, we also noted bacteriophage genera whose abundance inversely correlated with the abundance of their bacterial host. This was exemplified by *1706-like viruses,* which are virulent bacteriophage who target Streptococcaceae, similar to *936-like* viruses. They exhibited a reduction in abundance as compared to its bacterial host in WD-fed animals, but not in Chow-fed animals. Potential explanations for this inverse correlation are: 1) it could be due to a decrease in as yet-unidentified bacterial host populations; 2) competition of different phages for the same host, perhaps some phages lose out, or 3) like a recent publication reported, phage dynamics can change in response to non-host bacteria [45]. To our knowledge, *936-like* and *1706-like viruses* both target *Lactococcus* within Streptococcaceae. Both *936-like viruses* and their host Streptococcaceae displayed detectable elevations in abundance following WD feeding. Bacteriophage persistence could also be based on sensitivities of these bacteriophage external triggers, such as metabolites or inflammatory products, within the microbiome following dietary exposure. Recent publications have also described how bacteriophage communities experience compositional changes occurring early after shifting from

a low-fat to milk-fat diet in the absence of bacterial community compositional changes within 6 weeks [12]. We demonstrated similar effects on the bacteriophage community following WD feeding where bacteriophage abundance displayed early changes from chow counterparts. In our study, we noted that many of the bacteriophage genera abundance changes preceded those of their putative bacterial host family. Ongoing studies are aimed at more closely evaluating the specific bacteria:bacteriophage dynamics following dietary exposure.

Here we show that compositional shifts in the microbiota occur prior to the onset of pathophysiological metabolic parameters associated with obesity. Families within the class Bacilli, namely Enterococcaceae, Streptococcaceae, Bacillaceae and Staphylococcaceae, showed strong positive relationships with metabolic parameters elevated in WD-fed mice. Interestingly, these families have been previously implicated in the literature as increasing the energy-harvesting capacity of the microbiota, and thus contributing to the pathophysiology of obesity [47]. Therefore, the elevation in body weight, visceral fat, and metabolic inflexibility observed in the WD-fed mice could be directly related to the elevation in these bacterial components in the intestinal microbiota. The same study noted an inverse relationship between these obese-associated bacterial families and members of the bacterial families Clostridiaceae, Rumminococcaceae, Bacteroidaceae and Prevotellaceae [47]. Similarly, we found that these families were depleted in WD-fed animals and had strong negative relationships with the metabolic parameters elevated in the WD-fed mice. Our findings support previous studies and implicate the above listed bacteria as those associated with obesity, and those representative of a leaner phenotype, respectively.

With the surge of antibiotic resistance within recent years, researchers are embracing the idea of utilizing bacteriophage as therapy for bacterial infections. One noted advantage of

bacteriophage therapy to traditional antibiotics is the reduced impact on the organism's commensal microbiome. In a similar fashion, bacteriophage could be utilized to cause depletions of certain blooms of bacterial constituents in the intestinal microbiome in order to bring about homeostasis such as during colitis or obesity. The intestinal microbiota has been previously implicated in having a causal role in the development of obesity [48]. Considering this study and other previous reports, bacteriophage therapy could be used to deplete obese-associated bacteria. Thus, an important goal for the field will be further investigating bacteria-bacteriophage dynamics and the impacts of this on the surrounding microbiome community. By evaluating the dynamic relationship between bacteriophage and their bacterial hosts following WD-feeding, our work provides an overview of the timeline of disruption of both constituents and how this relates to the pathophysiology of obesity.

References

1. World Health Organization. Overweight and obesity fact sheet. (2016).

2. Hales, C. M., Carroll, M. D., Fryar, C. D. & Ogden, C. L. Prevalence of Obesity Among Adults and Youth: United States, 2015-2016 Key findings Data from the National Health and Nutrition Examination Survey. https://www.cdc.gov/nchs/data/databriefs/db288_table.pdf#1. (2015).

3. Popkin, B. M. & Gordon-Larsen, P. The nutrition transition: Worldwide obesity dynamics and their determinants. Int. J. Obes. 28, S2–S9 (2004).

4. Popkin, B. M., Adair, L. S. & Ng, S. W. Global nutrition transition and the pandemic of obesity in developing countries. Nutr. Rev. 70, 3–21 (2012).

5. Klein, S. et al. Weight management through lifestyle modification for the prevention and management of type 2 diabetes: Rationale and strategies. A statement of the American Diabetes Association, the North American Association for the Study of Obesity, and the American Society for Clinical Nutrition. American Journal of Clinical Nutrition vol. 80 257–263 (2004).

6. Singh, S., Dulai, P. S., Zarrinpar, A., Ramamoorthy, S. & Sandborn, W. J. Obesity in IBD: Epidemiology, pathogenesis, disease course and treatment outcomes. Nature Reviews Gastroenterology and Hepatology vol. 14 110–121 (2017).

7. Goodwin, P. J. & Stambolic, V. Impact of the Obesity Epidemic on Cancer. Annu. Rev. Med. 66, 281–296 (2015).

8. Duncan, S. H. et al. Human colonic microbiota associated with diet, obesity and weight loss. Int. J. Obes. 32, 1720–1724 (2008).

9. Human Microbiome Project Consortium. Structure, function and diversity of the healthy human microbiome. Nature 486, 207–214 (2012).

10. Hollister, E. B., Gao, C. & Versalovic, J. Compositional and functional features of the gastrointestinal microbiome and their effects on human health. Gastroenterology 146, 1449–58 (2014).

11. Cantarel, B. L., Lombard, V. & Henrissat, B. Complex Carbohydrate Utilization by the Healthy Human Microbiome. PLoS One 7, e28742 (2012).

12. Howe, A. et al. Divergent responses of viral and bacterial communities in the gut microbiome to dietary disturbances in mice. ISME J. 10, 1217–1227 (2016).

13. Sonnenburg, E. D. et al. Diet-induced extinctions in the gut microbiota compound over generations. Nature 529, 212–5 (2016).

14. Ul Haq, I., Chaudhry, W. N., Akhtar, M. N., Andleeb, S. & Qadri, I. Bacteriophages and their implications on future biotechnology: A review. Virology Journal vol. 9 (2012).

15. Hepworth, M. R. et al. Group 3 innate lymphoid cells mediate intestinal selection of commensal bacteria-specific CD4+ T cells. Science (80-.). 348, 1031–1035 (2015).

16. Reyes, A., Wu, M., McNulty, N. P., Rohwer, F. L. & Gordon, J. I. Gnotobiotic mouse model of phage-bacterial host dynamics in the human gut. Proc. Natl. Acad. Sci. U. S. A. 110, 20236–41 (2013).

17. Minot, S. et al. The human gut virome: inter-individual variation and dynamic response to diet. Genome Res. 21, 1616–25 (2011).

18. FASTX-Toolkit. http://hannonlab.cshl.edu/fastx_toolkit/.

19. Bolger, A. M., Lohse, M. & Usadel, B. Trimmomatic: a flexible trimmer for Illumina sequence data. Bioinformatics 30, 2114–2120 (2014).

20. Meyer, F. et al. The metagenomics RAST server – a public resource for the automatic phylogenetic and functional analysis of metagenomes. BMC Bioinformatics 9, 386 (2008).

21. International Committee on Taxonomy of Viruses. & King, A. Virus taxonomy : ninth report of the International Committee on Taxonomy of Viruses. (Elsevier, 2011).

22. R Core Team. R: A language and environment for statistical computing. (2014).

23. Dixon, P. VEGAN, a package of R functions for community ecology. J. Veg. Sci. 14, 927–930 (2003).

24. Pohlert, T. trend: Non-Parametric Trend Tests and Change-Point Detection. R Packag. version 1.1.0 (2018).

25. Revelle, W. R. psych: Procedures for Personality and Psychological Research. (2017).

26. Kassambara, A. ggcorrplot: Visualization of a correlation matrix using ggplot2. https://github.com/kassambara/ggcorrplot (2015).

27. Zhu, C. & Yu, J. Nonmetric multidimensional scaling corrects for population structure in association mapping with different sample types. Genetics 182, 875–88 (2009).

28. Shreiner, A. B., Kao, J. Y. & Young, V. B. The gut microbiome in health and in disease. Curr. Opin. Gastroenterol. 31, 69–75 (2015).

29. Ziętak, M. et al. Altered Microbiota Contributes to Reduced Diet-Induced Obesity upon Cold Exposure. Cell Metab. 23, 1216–1223 (2016).

30. David, L. A. et al. Diet rapidly and reproducibly alters the human gut microbiome. Nature 505, (2014).

31. Hargreaves, K. R. & Clokie, M. R. J. A Taxonomic Review of Clostridium difficile Phages and Proposal of a Novel Genus, "Phimmp04likevirus". Viruses 7, 2534–41 (2015).

32. Lavigne, R. et al. Classification of Myoviridae bacteriophages using protein sequence similarity. BMC Microbiol. 9, 224 (2009).

33. ACLAME: Phages lifestyle. http://aclame.ulb.ac.be/Classification/Phages/life_style.html.

34. Labrie, S. & Moineau, S. Multiplex PCR for Detection and Identification of Lactococcal Bacteriophages. Appl. Environ. Microbiol. 66, 987–994 (2000).

35. Blatny, J. M., Godager, L., Lunde, M. & Nes, I. F. Complete genome sequence of the Lactococcus lactis temperate phage φLC3: comparative analysis of φLC3 and its relatives in lactococci and streptococci. Virology 318, 231–244 (2004).

36. Samson, J. E. & Moineau, S. Characterization of Lactococcus lactis phage 949 and comparison with other lactococcal phages. Appl. Environ. Microbiol. 76, 6843–52 (2010).

37. Christiansen, B., Johnsen, M. G., Stenby, E., Vogensen, F. K. & Hammer, K. Characterization of the lactococcal temperate phage TP901-1 and its site-specific integration. J. Bacteriol. 176, 1069–76 (1994).

38. Everard, A. et al. Cross-talk between Akkermansia muciniphila and intestinal epithelium controls diet-induced obesity. Proc. Natl. Acad. Sci. U. S. A. 110, 9066–71 (2013).

39. Jovel, J. et al. Characterization of the Gut Microbiome Using 16S or Shotgun Metagenomics. Front. Microbiol. 7, 459 (2016).

40. Hakkak, R., Korourian, S., Foley, S. L. & Erickson, B. D. Assessment of gut microbiota populations in lean and obese Zucker rats. PLoS One 12, e0181451 (2017).

41. Backhed, F. et al. The gut microbiota as an environmental factor that regulates fat storage. Proc. Natl. Acad. Sci. 101, 15718–15723 (2004).

42. Norman, J. M. et al. Disease-specific alterations in the enteric virome in inflammatory bowel disease. Cell 160, 447–60 (2015).

43. Manrique, P. et al. Healthy human gut phageome. Proc. Natl. Acad. Sci. U. S. A. 113, 10400–10405 (2016).

44. Scanlan, P. D. Bacteria–Bacteriophage Coevolution in the Human Gut: Implications for Microbial Diversity and Functionality. Trends in Microbiology vol. 25 614–623 (2017).

45. Hsu, B. B. et al. Dynamic Modulation of the Gut Microbiota and Metabolome by Bacteriophages in a Mouse Model. Cell Host Microbe 25, 803-814.e5 (2019).

46. Hsu, B. B. et al. Dynamic Modulation of the Gut Microbiota and Metabolome by Bacteriophages in a Mouse Model. Cell Host Microbe 25, 803-814.e5 (2019).

47. Turnbaugh, P. J. et al. An obesity-associated gut microbiome with increased capacity for energy harvest. Nature 444, 1027–1031 (2006).

48. Ridaura, V. K. et al. Gut microbiota from twins discordant for obesity modulate metabolism in mice. Science 341, 1241214 (2013).

Chapter 3

Longitudinal Bacteriophage:Host Dynamics Following Diet-Induced Disruption of the Intestinal Microbiome

Abstract

The human microbiome has recently been estimated to contain roughly the same number of microbial cells as in the adult human body. The intestinal microbiome has the potential to benefit the host in many ways, such as metabolic cross-feeding and immune system priming, amongst others. Positive interactions between the host and bacterial symbionts have been linked to the maintenance and balance of microbial constituents. An imbalance or depletion of microbial components of the intestinal microbiome, termed dysbiosis, can be detrimental for both host and symbionts. With this in mind, it is important to determine the factors that influence composition of the microbiome and how can we use this knowledge to develop treatment for their manipulation. Here we explore the intestinal bacteriophage dynamics in parallel to their bacterial host during steady-state (chow) and following high-fat western diet (WD) feeding. To do this, microbial abundance estimates from microbiome samples of chow- and WD-fed mice were used in various statistical analyses to better define bacteriophage:host relationships during diet-induced variation. We found that WD feeding restructured the network community structure within the gut, with bacteriophage contributing more to overall community structure as compared to a chow diet. Furthermore, we found evidence that in many cases, bacteriophage shared similar abundance patterns to that of the host, regardless of diet. However, bacteriophage did not always follow the abundance patterns of their bacterial host. These findings suggest that bacteriophage can respond to environmental stimuli, such as host bacterial blooms, that allow for

some stability during steady-state conditions. These dynamics can potentially have consequences for the intestinal microbiome during dysbiosis and can predispose the mammalian host to disease.

Introduction

The human microbiome has recently been estimated to contain roughly the same number of cells as the adult human body, with an estimated 10^{14} in the colon alone [1]. The intestinal microbiome has the potential to benefit the host in many ways, such as metabolic cross-feeding and immune system priming, amongst others. Positive interactions between the mammalian host and bacterial symbionts has been linked to the maintenance and balance of microbial constituents as well as overall health of the host [2–4]. An imbalance or depletion of microbial components of the intestinal microbiome, termed dysbiosis, can be detrimental for both host and symbionts. Poor nutrient utilization, gastrointestinal disease, as well as disorders with the liver, heart, and neurological system have been linked to microbiome dysbiosis [5–9]. With this is mind, it is important to determine the factors that influence composition of the microbiome and determine how we can use this knowledge to develop treatments for their manipulation.

Regardless of the microbial environment, one of the most influential forces on microbial composition is the variety and amount of nutrients available. This is especially true of the intestinal environment. The intestinal microbiome composition typically reflects microbial organisms whose metabolic capabilities enhance utilization of the types of nutrients ingested by the host. For example, diets high in plant polysaccharides promote a colonic microbiome profile that is dominated by the class Bacteroides and Clostridia which specialize in digestion of these nutrients [10]. In contrast, Bacteroides and Clostridia have been reported as being reduced in relative abundance in the high-fat western diet (WD), as this diet is seen to support the growth of the class, Bacilli [11]. Furthermore, the microbiome associated with the low-fat, plant polysaccharide rich diet is enriched for pathways including N-glycan degradation, sphingolipid metabolism and glycosaminoglycan degradation [11]. Alternatively, gut microbiome following 1

day of western diet feeding revealed obvious shifts in the gene composition with enrichment of ATP-binding cassette transporters and phosphotransferase systems [5,11]. Maintaining microbial balance is of the upmost importance in optimal metabolic function and efficiency in the intestinal microbiome. Conversely, certain assemblages of bacteria have been linked to metabolic disorder. For example, WD-induced microbiome profiles have been reported to promote increased energy harvest from luminal content, induce production of adipocytes, and induce or exacerbate the obesogenic state of the host [5,12,13]. Studies evaluating diet on microbial composition have revealed a lot about bacterial dynamics in the intestinal microbiome. However, other microbial populations in the microbiome, such as bacteriophage, have been underrepresented in the literature and may hold insight into community structure in the intestinal microbial environment.

Bacteriophage are prokaryotic viruses that are among the most abundant members of the virome (viral component of the microbiome), yet, they are among the least understood [14]. Bacteriophage can infect specific host bacteria and replicate through a lytic or lysogenic program depending on their lifestyle [15]. Much remains to be determined about behavior of bacteriophage in microbial ecosystems, namely the intestinal microbiome. Investigating cause-and-effect relationships of bacteriophage and their bacterial host is extremely challenging due to incomplete bacteriophage annotation databases. Understanding the behavior of bacteriophages in the intestinal tract may have the potential to provide insights to the intestinal microenvironment during homeostasis and in times of dysbiosis. Recent interest in the phageome, the bacteriophage component of the intestinal microbiome, has allowed researchers to illuminate an association between elevated bacteriophage abundance and disease [16]. Understanding the behavior of bacteriophage in the intestinal microbiome may provide insights to microbial differences during dysbiosis and bring about therapeutic treatments to modulate the microbiome.

Although bacteriophage are thought to be antagonistic to bacteria, they have displayed more variability in their behavior as members of the intestinal microbiome. For example, Manrique, et al. have described the core intestinal phageome that is shared among more than one-half of all participants in the study [17]. However, the same study described disruption of this core phageome in patients with Chron's disease and Ulcerative Colitis [17]. Recent studies in dietary influences on viral community structure reported that individuals on the same diet had similar intestinal viral communities [18]. Most of the variation seen in the phageome has been attributed to bacteriophage reacting to host bacterial abundance patterns. In contrast, Hsu, et al. report bacteriophage can coexist over time with targeted bacteria in the intestinal environment, but their predation can induce cascading effects on microbial composition and, consequently, the gut metabolome [19]. This study addresses how bacteriophages impact bacterial communities in the intestinal microbiome of gnotobiotic mice. However, there is still more to be understood about bacteriophage dynamics in response to stimuli and if this is only due to host bacteria persistence in a natural model.

In this study, we monitored intestinal bacteriophage abundance following introduction of a high-fat western diet (WD) in parallel to their bacterial hosts. To do this, we administered the WD over the course of 72 days. Fecal samples were subjected to high throughput sequencing in order to quantify abundance of bacteriophage and their host. We found that WD feeding restructured community relationships within the gut, with bacteriophage contributing more to overall community structure as compared to a chow diet. Furthermore, we determined that in many cases, bacteriophage shared similar abundance patterns to that of the host, regardless of diet. However, bacteriophage did not always follow the abundance patterns of their bacterial host. In some instances, we describe the reduction of bacteria and an inverse bloom of

bacteriophage in WD-fed mice which may be due to the bacteriophage predator-prey relationship. Alternatively, certain bacteriophage genera displayed unique abundance patterns following WD feeding, not only from host, but also from bacteriophage who target the same host. These findings suggest that bacteriophage have the potential to respond to stimuli, such as diet, independently of their host.

Methods

Animals and Diets

Male C57BL/6J mice from Jackson Laboratories (Bar Harbor, ME) were singly housed in standard microisolator cages at the Veterinary Research Building, College of Veterinary Medicine, Auburn University. The room was maintained at an ambient temperature of 22°C ± 2°C on a 12:12 light:dark cycle with zeitgeber time (ZT) 0 representing lights on and ZT12 representing lights off. All experimental procedures were approved by the Auburn University Animal Care and Use Committee. Animals were fed standard rodent chow for 1-week during acclimation to the facility. After which, animals were split into groups receiving either the standard chow diet with tap water (Chow) or a High-Fat Western Diet with tap water (WD). The chow diet (Teklad Global Rodent Diet 2018) contained 24% of calories from protein, 18% from fat, and 58% from carbohydrate. The WD diet was based on the AIN-93G diet and consisted of 44% carbohydrate, 16% protein, and 40% fat, 30% of which was provided from lard, 30% from butterfat, 30% from Crisco, 7% from soybean oil and 3% from corn oil. All dietary groups were given food and water *ad libitum*.

Collection of fecal matter was performed at the initiation of diet change (Day 0) as well at four other time points following WD feeding: 2 days, 2-, 8-, and 12-weeks. Animals were

removed from their home cages and placed in sterile microisolator cages without bedding for 3 hours. Food and water were provided to the animals during this time. Mice were then returned to resident cages and feces were collected from the sterile cages for DNA extraction and shotgun metagenomic sequencing.

Shotgun metagenomic sequencing-based Microbiome Profiling

Intestinal microbial abundance was obtained from the Sugar_study_2015_Trimmed project on the MG-RAST repository (https://www.mg-rast.org/mgmain.html?mgpage=project&project=mgp81921). Materials and methods of this study are outlined in Chapter 2. To assess species-level bacteriophage dynamics, raw sequences from this study were aligned to annotated bacteriophage sequences and compared to the putative host genera. First, annotated fasta sequences were downloaded from the Sugar_study_2015_Trimmed project on the MG-RAST repository for each treatment sample at each timepoint. These sequences were filtered in order to create a database of Caudovirales sequences that were members of bacteriophage genera utilized in the k-mean analysis. The BWA-MEM algorithm was used to align raw reads of WD and Chow microbiome samples to the corresponding bacteriophage database [20]. Unmapped reads were removed using SAMtools [21] and mapped read hits were quantified. Bacteriophage database hit counts were normalized and converted to log2-fold change.

Microbiome statistical analysis

Interactions depicted within the co-occurrence networks were generated in R using SparCC within the SPIEC-EASI package [22]. SparCC calculates correlations values between

OTUs while accounting for sparse or missing data [22]. SparCC correlation values greater |0.3| were visualized in a network using igraph package [23]. Only nodes with at least 1 interaction that met the cutoff were included in the networks. Communities were detected using the multilevel community detection method within the igraph package.

Time-series log2-fold change was calculated from normalized microbial abundance hits from all bacteriophage genera and top 55 most abundant bacterial families at each time point. K-mean cluster analysis of the log2-fold change was generated using the Short Time-series Expression Miner (STEM) [24] with the parameters of 8 clusters and 25 random repeats. OTUs that did not display significant abundance changes over the course of the experiment were not able to be analyzed by STEM and were not included in the analysis. Two microbial taxa were not seen to match any other clusters from the chow samples which formed two clusters containing one cluster each. These two clusters were removed from this analysis.

Results

Microbiome Community Structure is Altered by the Western Diet

Before dissecting specific relationships between bacteriophage and their hosts, we wanted to determine how components of the gut microbiota interacted with each other in response to diet exposure. SparCC correlation coefficients were calculated for the top 55 most abundant bacterial families and all bacteriophage genera in each group. High-confidence coefficients were then plotted as a network to visually represent relationships. The chow network contained 3 communities that were parsed based on the multilevel cluster detection method. Based on this clustering method, the chow samples displayed a low modularity of 0.18. Specifically, 2 large communities were detected, containing multiple nodes that displayed a high

degree of connectivity, with a large majority of the nodes representing bacterial OTUs. Nodes with the highest degree of connectivity belong are representative of symbionts typically found in a healthy microbiota. These include Bacteroidaceae, Clostridaceae, Prevotellaceae, Enterococcaceae, Ruminococcaceae, amongst others. On the other hand, most nodes representing bacteriophage genera displayed a low degree of connectivity, pointing to bacteria contributing more to the overall community structure as compared to bacteriophage within the chow samples.

Similar to the chow samples, the WD samples contained 3 communities. However, the WD samples displayed a slightly higher degree of modularity of 0.20. Most notably, nodes representative of bacteriophage genera seemed to display a higher degree of connectivity, and overall contribute more to the community structure within the WD samples. For example, *TP21-, phiFL-, phiETA-, and P335-like viruses* displayed a high degree of connectivity within their communities. Some of these relationships are to be expected; for example, *TP21-like viruses* are temperate target bacteria within the family Enterococcaceae [25]. Nodes representing these bacteria and bacteriophage plot within the same community and share a similar degree of connectivity. Similarly, virulent bacteriophage genera are contained within the same community as their host bacterial family. This is exemplified in *P335-like* viruses and their relationship with the family Streptococcaceae, as well as *phiETA-like* viruses and the family Staphylococcaceae. On the other hand, some bacteriophage genera did not belong to the same community as their host. This was exemplified through *1706-* and *Sfi21-like* viruses and the family Streptococcaceae. In conclusion, bacteriophage seem to contribute more to overall community structure within the WD samples.

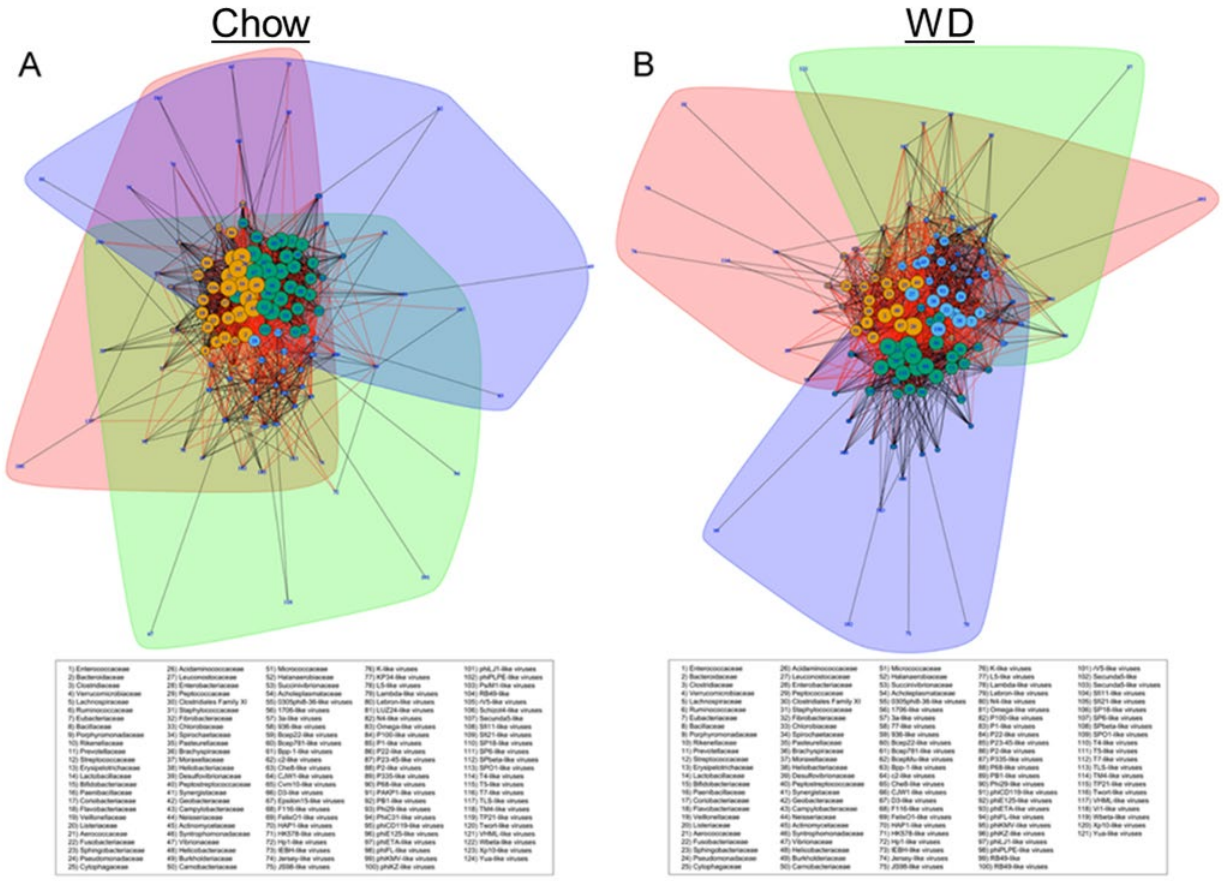

Figure 3.1. Co-occurrence network analysis of the gut microbiota from (A) Chow or (B) WD-treated mice. SparCC correlations were calculated from OTUs contained in samples taken 2, 14, 56, and 84 days post-dietary exposure in (A) Chow or (B) WD-fed mice. Nodes represent an individual OTU, and the color of the node denotes the particular module it belongs to. Sizes of the nodes are directly related to the number of connections it has within the network. Edges represent relationships between two nodes; green edges represent positive interactions, while red edges represent negative interactions. Different colored areas highlight boundaries of communities determined by multilevel community structuring. Only high-confidence interactions with a sparse correlation greater than |0.3| were included in the networks.

Differential Abundance Patterns following WD treatment

We next wanted to assess differential abundance patterns of the top 55 most abundant bacterial families and classified bacteriophage genera following during steady-state (chow) and WD feeding. Similar to the clustering of gene expression data, temporal microbial abundance clustering allows us to identify groups of organisms that behave similarly in an environment. Adaptation of this method allows for characterization of microbial constituents that are co-dependent and how these relationships may be disturbed by environmental stimuli. The fold-change patterns of microbial populations that did not fluctuate could not be analyzed by the STEM program and were therefore not assigned to a cluster. As expected, microbial abundance displayed modulation over time even within chow samples (Figure 3.2; clusters A-F). Two of the chow clusters contained only one microbial population and thus only six clusters were included in this discussion. Chow sample clusters showed mild fluctuations with most taxa of interest belonging to cluster C and cluster F (Figure 3.2). These clusters did not exceed a 2-fold difference from time 0 over the entirety of the experiment. Cluster C was the largest cluster of the chow samples which contained forty microbial taxa (Figure 3.2, Cluster C). These included commonly identified bacterial constituents of the intestinal microbiome (Bacteroidaceae, Burkholderiaceae, Clostridiaceae, Enterobacteriaceae, Pasteurellaceae, Prevotellaceae, Ruminococceae, Streptococcaceae) as well as bacteriophage genera that target members of these bacterial families (*936-like viruses*, *c2-like viruses, T4-like viruses,* and *T7-like viruses*). *phiFL-like viruses* and their host, Enterococcaceae, were found to have similar abundance dynamics in chow samples (Figure 3.2; cluster B). *phiETA-like viruses* also clustered with its putative host family, Staphylococcaceae in Cluster E, but the other 15 bacteriophage genera populations included in this analysis did not cluster with putative host families in chow microbiome samples.

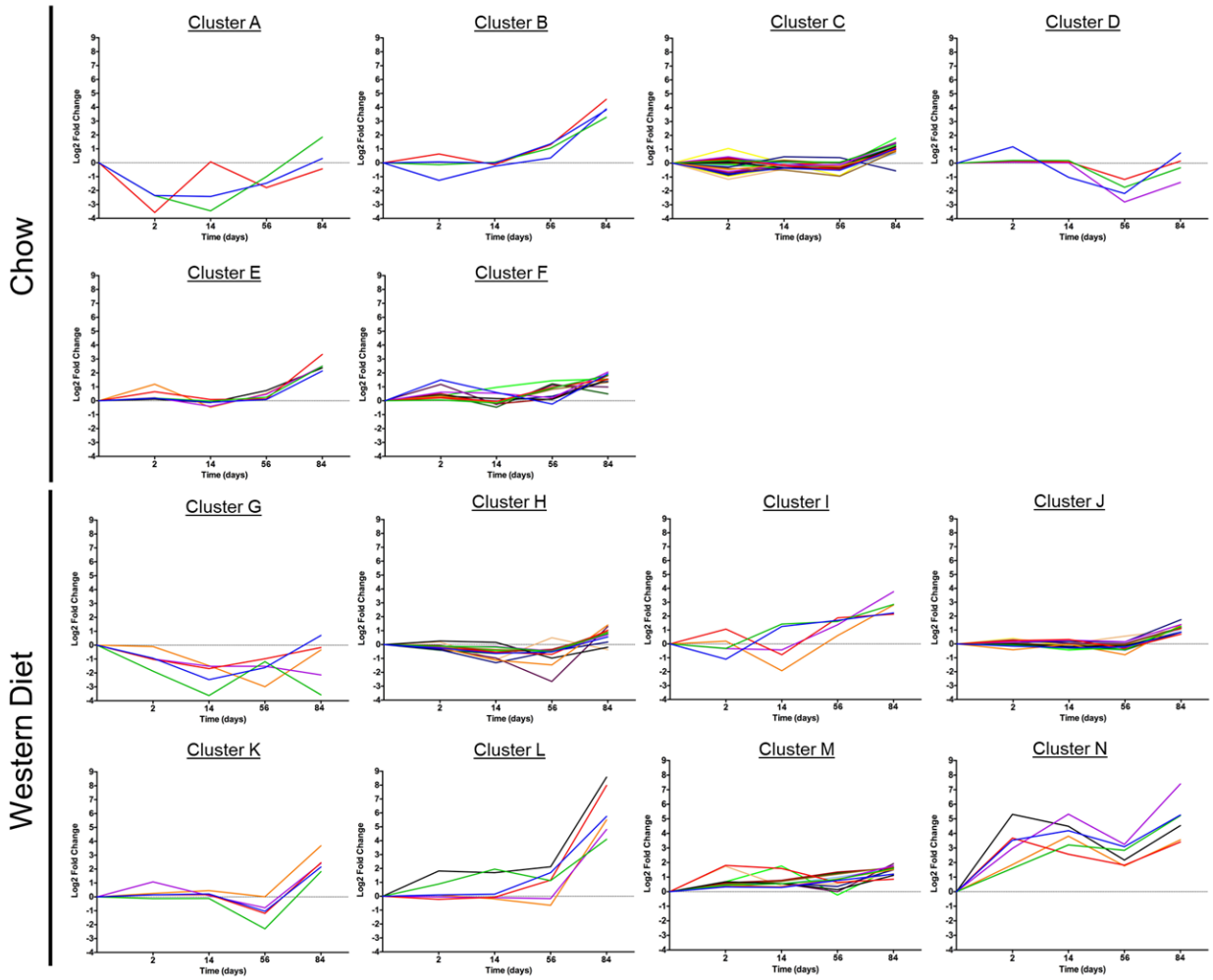

Figure 3.2. K-mean clustering of bacteria and bacteriophage differential abundance patterns following WD exposure. K-mean clusters of all bacteriophage genera and top 55 most abundant bacterial families in Chow or Western diet (WD) fed mice. Microbial taxa cluster of Chow diet are depicted in clusters A-F. WD microbial taxa clusters are shown in clusters G-N. Each colored line represents a different microbial taxa log2-fold change pattern. Differential log2-fold change and cluster designation is outlined in Table 2.

In conclusion, a majority of dominant taxa within the intestinal microbiota underwent only minor alterations in abundance over time when maintained on a consistent diet. During steady-state conditions, bacteriophage also experience marginal alteration, but their abundance patterns do not always statistically match that of the host.

In contrast to chow samples, WD samples displayed more organisms belonging to clusters that underwent significant and dynamic fluctuations (Figure 3.2; clusters G-N). For example, five taxa within chow samples displayed overt changes, 3-fold change or greater (Figure 32.; clusters A-F). In contrast, twelve taxa within WD samples exhibited an overt change in abundance (Figure 3.2; clusters G-N). Cluster J displayed similar dynamics to cluster C of the chow samples, but only contained 17 microbial taxa. Both cluster J and C contain Burkholderiaceae and Ruminococcaceae. Unlike cluster C of chow samples, cluster J of WD samples did not contain any bacteriophage genera as many of the bacteriophage studied displayed a greater magnitude of change following WD feeding. For example, Enterococcaceae and targeting bacteriophage genera, *phiFL-like viruses,* abundance dynamics still matched as they were both found in cluster L of WD samples, yet their abundance patterns were far different from that seen in chow samples (Figure 3.2; cluster B). Similarly, *936-like viruses* and Streptococcaceae were still found to cluster together although they both benefit from rapid blooms following WD feeding (Figure 3.2; cluster N). *P335-like viruses* target Streptococcaceae and were also found in cluster N with their host in WD samples, although this was not the case in chow samples. In conclusion, microbial communities experience more dynamic changes following alteration to environmental stimuli, such as nutrient availability. Following WD-feeding, less bacteriophage communities are statistically synchronous with host abundance pattern, but many appeared to share a similar overall abundance trend.

Table 3.1: Log2 Fold Change and K-mean Clusters
Data not shown for organisms that remain consistent throughout the experiment

	TREATMENT	AVERAGE LOG2 FOLD CHANGE				K-MEAN CLUSTER
		2D	14D	56D	84D	
1706-LIKE VIRUSES	CO	1.5	0.59	-0.24	1.95	5
	WD	-0.94	-2.48	-1.62	0.7	0
936-LIKE VIRUSES	CO	-0.77	-0.36	-0.51	1.03	2
	WD	3.53	4.19	3.09	5.26	7
ACHOLEPLASMATACEAE	CO	0.23	-0.04	0.97	1.56	5
	WD	-1.02	-1.69	-0.98	-0.17	0
ACIDAMINOCOCCACEAE	CO	0.29	-0.18	-0.46	1.09	2
	WD	-0.25	-0.64	-0.54	0.56	1
ACTINOMYCETACEAE	CO	0.19	0.1	0.07	1.34	2
	WD	-0.16	-0.27	-0.23	0.84	3
AEROCOCCACEAE	CO	0.46	-0.15	-0.12	1.42	2
	WD	-0.23	-0.55	-0.71	1.04	1
BACILLACEAE	CO	0.07	-0.02	1.36	3.81	1
	WD	0.1	0.15	1.7	5.75	5
BACTEROIDACEAE	CO	-0.46	-0.1	-0.23	0.9	2
	WD	0.33	0.29	0.77	1.2	6
BIFIDOBACTERIACEAE	CO	0.05	-0.16	0.91	1.84	5
	WD	1.8	1.59	0.64	0.86	6
BPP-1-LIKE VIRUSES	CO					NA
	WD	-1.1	1.26	1.7	2.23	2
BRACHYSPIRACEAE	CO	0.07	-0.32	-0.43	1.2	2
	WD	0.24	0.32	-0.32	0.71	3
BURKHOLDERIACEAE	CO	-0.38	-0.5	-0.94	0.85	2
	WD	-0.08	-0.31	-0.41	1.27	3
C2-LIKE VIRUSES	CO	-0.29	0.46	0.4	-0.55	2
	WD					NA
CAMPYLOBACTERACEAE	CO	-0.01	0.17	0.01	1.48	2
	WD	0.14	0.27	0.16	1.4	3
CARDIOBACTERIACEAE	CO	0.61	0.54	0.21	2.06	5
	WD	-0.42	-0.03	-0.78	1.38	3
CHE8-LIKE VIRUSES	CO	0.33	-0.15	0.98	1.52	5
	WD	-1.87	-3.63	-1.19	-3.58	0
CHLOROBIACEAE	CO	-0.7	-0.32	-0.32	0.99	2
	WD	0.45	0.55	0.84	1.59	6
CLOSTRIDIACEAE	CO	0.23	-0.18	-0.23	1.19	2
	WD	-0.11	-0.18	-0.5	0.8	1
CLOSTRIDIALES FAMILY XI	CO	0.35	0.15	0.1	1.54	5
	WD	0	-0.19	-0.12	0.85	3
CORIOBACTERIACEAE	CO	0.19	-0.19	0.82	1.33	5
	WD	0.33	0.3	0.83	1.78	6
CYTOPHAGACEAE	CO	-1.16	-0.43	-0.44	0.79	2
	WD	0.43	0.33	0.87	1.51	6
DESULFOVIBRIONACEAE	CO	-0.09	-0.37	-0.31	1.24	2
	WD	0.05	-0.07	-0.04	1.19	3
ENTEROBACTERIACEAE	CO	-0.21	0.01	-0.51	0.7	2
	WD	0.12	0.17	0.15	1.75	3
ENTEROCOCCACEAE	CO	0.64	-0.13	1.3	4.57	1
	WD	-0.22	-0.07	1.16	7.98	5
ERYSIPELOTRICHACEAE	CO	0.23	-0.02	0.32	1.41	5
	WD	0.68	0.56	0.14	1.12	6
EUBACTERIACEAE	CO	0.24	-0.26	-0.2	1.15	2
	WD	-0.14	-0.15	-0.46	0.71	1
FIBROBACTERACEAE	CO	-0.19	-0.21	-0.42	0.88	2
	WD					NA
FLAVOBACTERIACEAE	CO	-0.95	-0.29	-0.39	0.88	2
	WD	0.51	0.71	1.2	1.69	6
FUSOBACTERIACEAE	CO	0.04	-0.18	-0.27	1.21	2
	WD	0.28	0.04	0.03	1.21	3
GEOBACTERACEAE	CO	-0.2	-0.2	-0.05	1.3	2
	WD	0.44	0.56	0.36	1.5	6
HALANAEROBIACEAE	CO	-0.08	0.23	-0.03	1.41	2
	WD	-0.07	-0.25	-0.02	1.13	3
HELICOBACTERACEAE	CO	0.25	0.02	-0.39	1.35	2
	WD	-0.24	-1.13	-1.47	1.41	1
L5-LIKE VIRUSES	CO	0.08	-0.01	-0.15	1.09	2
	WD	-0.99	-1.52	-1.52	-2.14	0
LACHNOSPIRACEAE	CO	0.22	-0.23	-0.21	1.15	2
	WD	-0.08	-0.04	-0.43	0.84	3
LACTOBACILLACEAE	CO	1.18	-0.27	1.12	0.99	5
	WD	3.68	2.57	1.82	3.41	7
LAMBDA-LIKE VIRUSES	CO	1.18	-1.02	-2.19	0.73	3
	WD	1.07	-0.78	1.88	2.14	2
LEUCONOSTOCACEAE	CO	-0.13	0.04	1.05	3.28	1
	WD	1.6	3.21	2.84	5.22	7
LISTERIACEAE	CO	0.17	-0.11	0.09	2.14	4
	WD	0.88	1.95	1.13	4.1	5

	TREATMENT	AVERAGE LOG2 FOLD CHANGE				K-MEAN CLUSTER
		2D	14D	56D	84D	
MICROCOCCACEAE	CO	0.15	0.09	-1.17	0.15	3
	WD	0.15	0.21	-1.04	2.15	4
MORAXELLACEAE	CO	0.2	0.19	-1.74	-0.33	3
	WD	0.15	0.16	-1.19	2.46	4
NEISSERIACEAE	CO	-0.6	-0.18	-0.41	0.95	2
	WD	0.36	0.03	0.56	1.05	3
P2-LIKE VIRUSES	CO	2.24	2.21	1.1	2.82	7
	WD	0.25	0.16	-0.98	-0.19	1
P335-LIKE VIRUSES	CO	0.65	0.09	0.13	3.33	4
	WD	2.97	5.32	3.25	7.4	7
PAENIBACILLACEAE	CO	0.19	-0.02	0.25	2.48	4
	WD	-0.05	-0.1	-0.17	4.81	5
PASTEURELLACEAE	CO	0.03	-0.12	-0.32	1.25	2
	WD	0.4	0.56	0	1.92	6
PEPTOCOCCACEAE	CO	0.15	-0.3	-0.18	1.21	2
	WD	-0.03	-0.44	-0.24	1.16	3
PEPTOSTREPTOCOCCACEAE	CO	0.28	-0.05	0.05	1.39	2
	WD	-0.04	-0.17	-0.17	0.88	3
PHICD119-LIKE VIRUSES	CO	0.51	-0.23	0.14	1.81	5
	WD					NA
PHIE125-LIKE VIRUSES	CO	1	2.23	0.25	4.58	6
	WD	-0.1	-1.48	-2.99	-0.34	0
PHIETA-LIKE VIRUSES	CO	0.22	-0.4	0.46	2.49	4
	WD	0.1	-0.19	-0.65	5.5	5
PHIFL-LIKE VIRUSES	CO	-1.26	-0.24	0.35	3.88	1
	WD	1.82	1.7	2.12	8.58	5
PORPHYROMONADACEAE	CO	-0.88	-0.12	-0.18	0.79	2
	WD	0.61	0.78	1.35	1.6	6
PREVOTELLACEAE	CO	-0.73	-0.03	-0.12	0.97	2
	WD	0.56	0.7	1.27	1.66	6
PSEUDOMONADACEAE	CO	0.07	0.02	-2.8	-1.39	3
	WD	-0.12	-0.11	-2.3	1.82	4
RIKENELLACEAE	CO	-2.36	-2.43	-1.47	0.31	0
	WD	1.74	0.41	0.55	1.23	6
RUMINOCOCCACEAE	CO	0.37	-0.07	-0.15	1.19	2
	WD	-0.12	-0.12	-0.48	1.03	3
SFI11-LIKE VIRUSES	CO					NA
	WD	-0.32	1.43	1.62	2.84	2
SFI21-LIKE VIRUSES	CO	0.41	-0.46	1.22	0.49	5
	WD	0.68	1.76	-0.23	1.64	6
SP18-LIKE VIRUSES	CO	-3.58	0.07	-1.79	-0.44	0
	WD	-0.33	-0.43	1.38	3.76	2
SPBETA-LIKE VIRUSES	CO	1.19	-0.47	0.51	2.48	4
	WD	1.08	0.09	-0.79	2.41	4
SPHINGOBACTERIACEAE	CO	-0.86	-0.2	-0.18	1.03	2
	WD	0.57	0.54	0.99	1.57	6
SPIROCHAETACEAE	CO	0.03	0	-0.35	1.28	2
	WD	0.19	-0.32	-0.38	0.88	3
SPO1-LIKE VIRUSES	CO					NA
	WD	0.2	-1.93	0.6	2.8	2
STAPHYLOCOCCACEAE	CO	0.11	-0.13	0.73	2.36	4
	WD	0.25	0.45	0.01	3.68	4
STREPTOCOCCACEAE	CO	0.36	-0.38	-0.25	1.79	2
	WD	1.85	3.81	1.77	3.56	7
SUCCINIVIBRIONACEAE	CO	0.23	0.17	0.1	1.55	5
	WD	0.4	-0.15	-0.06	1.19	3
SYNERGISTACEAE	CO	0.31	0.2	-0.07	1.12	2
	WD	-0.13	-0.36	-0.43	0.93	1
SYNTROPHOMONADACEAE	CO	0.09	0.14	-0.05	1.4	2
	WD					NA
T4-LIKE VIRUSES	CO	-0.05	-0.24	-0.24	1.26	2
	WD	-0.38	-1.31	-0.48	0.18	1
T7-LIKE VIRUSES	CO	1.06	0.01	-0.91	1.45	2
	WD	-0.31	-0.97	-2.66	1.3	1
THERMOANAEROBACTERACEAE	CO	0.17	0.16	-0.06	1.29	2
	WD	-0.07	-0.54	-0.35	0.79	1
THERMOANAEROBACTERALES FAMILY III	CO	0.32	0.18	0.04	1.22	2
	WD	-0.41	-0.65	-0.51	0.55	1
TWORT-LIKE VIRUSES	CO	0.34	0.96	1.44	1.57	5
	WD	0.18	-1.09	0.49	-0.37	1
VEILLONELLACEAE	CO	0.23	-0.13	-0.28	1.27	2
	WD	-0.23	-0.43	-0.46	0.9	1
VERRUCOMICROBIACEAE	CO	-2.37	-3.46	-1	1.84	0
	WD	5.31	4.49	2.17	4.54	7

Bacteria:Bacteriophage time-series dynamics are not always synchronous

We sought to compare the temporal differential abundance of host bacterial family and the bacteriophage genera that target them following WD administration. As previously mentioned, similar abundance patterns are exhibited by many of the bacteria:bacteriophage relationships regardless of designated lifestyle (Figure 3.3). This is especially true for families Bacillaceae, Enterococcaceae, and Staphylococcaceae where bacteriophage that target them tended to follow the abundance pattern of their host regardless of diet. Likely, *SPbeta-, phiFL-* and *phiETA-like viruses* abundance patterns are directly related to host abundance as they are classified as temperate and could be present as prophage. *SPO1-like viruses,* on the other hand, is classified as virulent and likely increases in abundance as Bacillaceae increases consistent with a "kill-the-winner" pattern [26]. In the classic predator-prey model of kill-the-winner, fast-growing bacteria are infected by virulent bacteriophage that benefit from the bloom of their bacterial host [26,27]. In this way, lytic bacteriophage are thought to play a role in bacterial community control and structure.

Surprisingly, some bacteriophage acted in a different manner than that of their bacterial host family. Bacterial families Enterbacteriaceae and Burkholderiaceae showed minimal change in abundance over the course of the experiment regardless of diet. However, many of the bacteriophage that target these families displayed a decline in abundance following administration of the WD, namely *CHE8-, T7-* and *phiE125-like viruses* (Figure 3.3). Burkholderiaceae-targeting *phiE125-like viruses* were classified as temperate but exhibited a 3-fold decrease in abundance after 56 days on the WD. This was followed by a return to initial levels in line with a slight increase in abundance of its host. Thus, this was a predictable pattern, as host population abundance increases, the bacteriophage abundance would also increase.

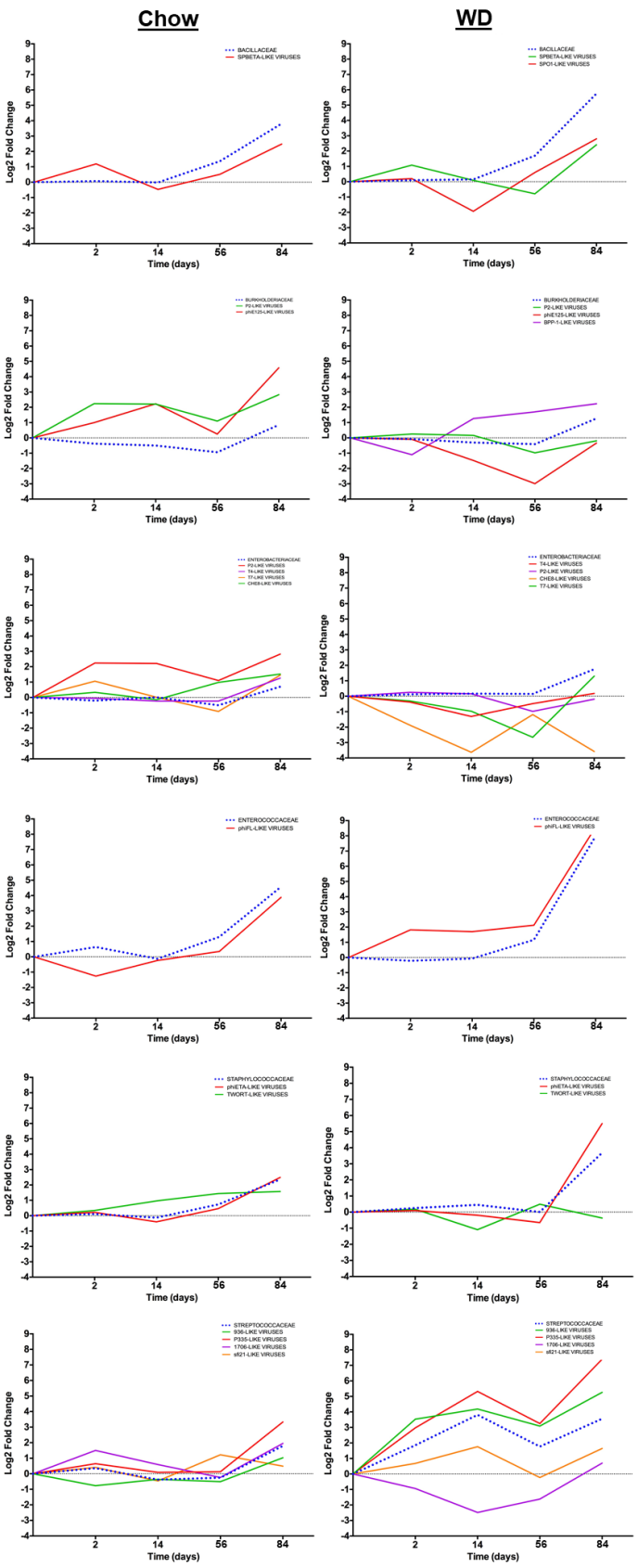

Figure 3.3. Temporal bacteriophage genus dynamics in perspective of putative host family's abundance following WD exposure. K-mean data was reconstructed to show mean log_2-fold change of bacterial host families (Bacillaceae, Burkholderiaceae, Enterobacteriaceae, Enterococcaceae, Staphylococcaceae Streptococcaceae) and bacteriophage genera that target them in Chow or Western diet (WD) microbiome samples. Figures on the left show bacterial families and bacteriophage genera abundance dynamics from Chow microbiome samples over time. Figures on the right side are the matching bacteria:bacteriophage relationship follow WD feeding. Dotted lines represent the bacterial host family and solid, colored lines represent different bacteriophage genera that target the designated bacterial host family. Putative host family and lifestyle characterization is outlined in Table 1. Differential log2-fold change and cluster designation is outlined in Table 2.

The dynamics of Streptococcaceae and related bacteriophage genera are not as predictable as those previously discussed. The Streptococcaceae and targeting bacteriophage genera had similar abundance patterns overtime in the chow samples (Figure 3.3). Following administration of the WD, larger fluctuations in abundance were observed for Streptococcaceae and the bacteriophage genera who target them (Figure 3.3). Namely, virulent bacteriophage genera *1706-* and *P335-like viruses* did not reach above a 1-fold difference until 84 days in chow samples indicating a relatively stable abundance profile (Figure 3.3). In WD-treated animals, abundance patterns for *1706-* and *P335-like viruses* began to diverge 2 days following dietary exposure regardless of shared host and lifestyle. *1706-like viruses* decreased 4-fold by 14 days in treatment groups before beginning to recover to base levels by 84 days (Figure 3.3). *P335-like viruses'* abundance profile for WD-treated mice quickly rose 5-fold by 14 days. It was reduced 3-fold at 56 days but recovered by 84 days to above a 5-fold increase as compared to time 0 (Figure 3.3). This fold change progression is similar to that of its host, Streptococcaceae. This is likely due to two factors: 1) "kill-the-winner" dynamics of virulent bacteriophage species that comprised approximately half of the *P335-like viruses* abundance and 2) potential lysogenic bacteriophage present as prophage in host genomes. Interestingly, dissimilar abundance patterns were observed for Streptococcaceae-targeting bacteriophage genera *1706-* and *Sfi21-like viruses* following dietary exposure which indicates either an antagonistic relationship with their host or that these viruses were negatively affected by bacterial host response to the WD. In summary, bacteriophage do not always fluctuate in the same manner as their putative host following diet change, indicating that bacteriophage population can be affected by diet change independently of their host.

Diversity in abundance modulation among enteric bacteriophage species following WD feeding

We quantified log fold-change in bacteriophage species abundance over time in WD and Chow microbiome samples in an attempt to better define individual bacteriophage species dynamics following WD feeding. Temperate bacteriophage (designated by black titles; Figure 3.4) typically followed the same abundance patterns of their host (represented by dashed lines; Figure 3.4) regardless of dietary conditions (Chow in blue, WD in red; Figure 3.4). Most of the bacteriophage species followed similar abundance modulation throughout the experiment regardless of diet, which agrees with findings previously discussed. For example, *Staphylococcus phage Sfi19, Burkholderia phage phiE202* and *phi1026b* experienced synchronous abundance patterns in both dietary conditions. This could be due to the low variability in bacterial host abundance over the course of the experiment. Interestingly, *Lactococcus* and *Staphylococcus* also experienced relatively low variability in Chow-fed samples, yet, *Lactococcus phage Tuc2009* of *P335-like viruses* and *Staphylococcus phage EW* of *phiETA-like viruses* under these conditions underwent a large bloom at the final time point, following a slight elevation in host bacterial abundance. This confirms reports of the bacteriophage genera and their host dynamics previously discussed (Figure 3.3 and 3.4). *Lactococcus phage Tuc2009* exhibited a 10-fold increase from initial abundance levels, and *Staphylococcus phage EW* displayed an 8-fold increase at the final timepoint following a slight increase of host bacteria (< 2-fold increase on average). Under WD conditions, *Lactococcus phage Tuc2009* showed a significant bloom (6-fold increase) that exceeded that of its host (3-fold increase) as early as 2 days following WD feeding (Figure 3.4). This was even more distinct for WD samples at 84 days, where *Lactococcus phage Tuc2009* experienced an abundance increase 12-fold greater than the initial levels and *Lactococcus* displayed 4-fold increase at the same timepoint. Taken together,

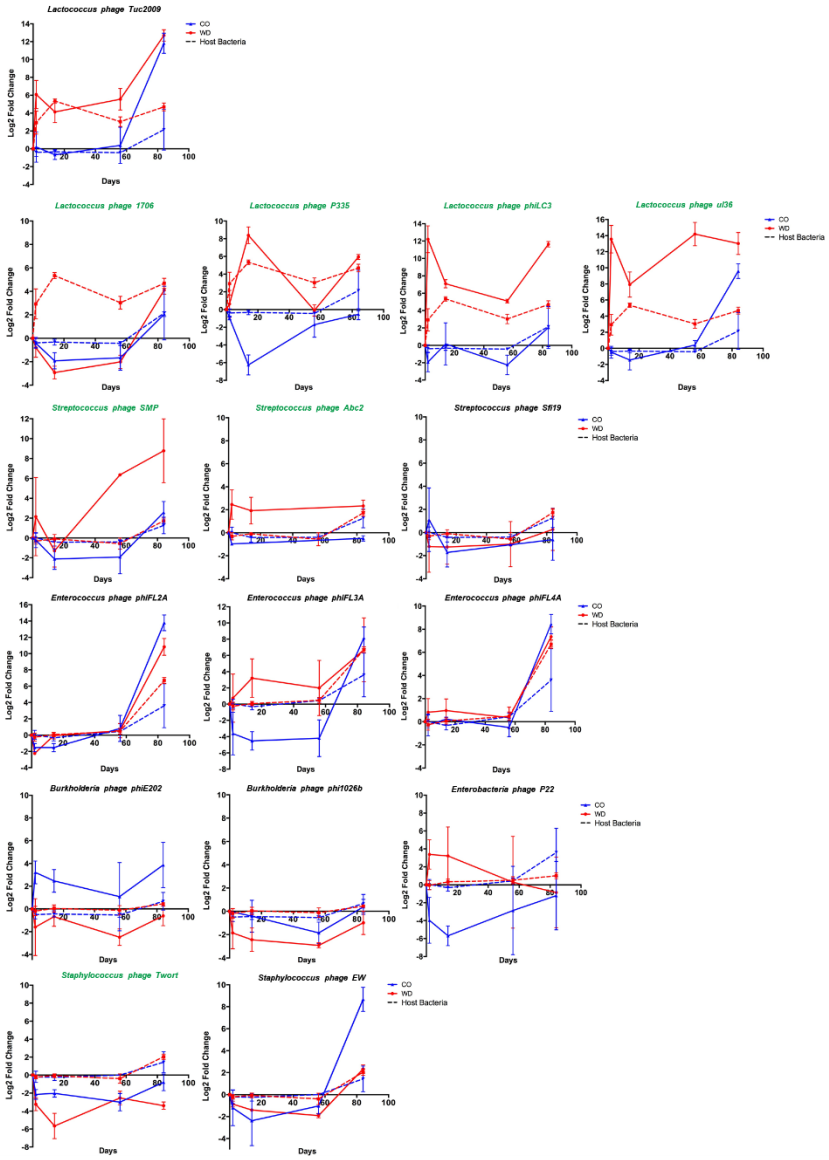

Figure 3.4. Differential log2-fold change patterns of bacteriophage species and their putative host following WD feeding. Differential log2-fold change of bacteriophage species following WD feeding in perspective of their bacterial host genera. Solid lines represent the bacteriophage species while dashed lines represent host bacterial genera. WD (red) and Chow diet (blue) are depicted within one figure for each bacteriophage species:bacterial host pair. Bacteriophage species with green lettering are identified as virulent bacteriophage and those in black are described as temperate bacteriophage.

temperate bacteriophage typically followed the abundance patterns of the bacterial host genera regardless of diet. However, temperate bacteriophage did show examples of significant blooms even following seemingly low abundance increases of the host.

Virulent bacteriophage (designated by red titles; Figure 3.4) dynamics were much more variable than previous models have described. Classic models of virulent bacteriophage in microbial communities, namely the kill-the-winner model, describe how any bacteria increasing beyond a certain threshold in abundance will trigger a positive net production of bacteriophage, based on viral host-specificity [26]. Virulent bacteriophage species in our study followed this model, and this was exemplified in the bacteriophage:host relationships of *Lactococcus phage P335, Lactococcus phage phiLC3, Lactococcus phage ul36, Streptococcus phage SMP, Streptococcus phage SMP* and *Streptococcus phage Abc2,* especially in WD samples. In Chow samples, these bacteriophage species showed some decline in abundance, but recovered to or exceed that of initial levels with an increase in host genera populations. WD samples showed rapid elevation in abundance of these bacteriophage species following WD feeding, even with minimal abundance changes of the host genera. Bacteriophage species responses were not uniform, even among members of the same bacteriophage genera. For example, *Lactococcus phage P335, phiLC3* and *ul36* are all members of *P335-like viruses*. *Lactococcus phage phiLC3* and *ul36* experienced rapid and significant blooms (12-fold and 14-fold increase by day 2) in WD samples and remained elevated throughout the duration of the experiment. Although *Lactococcus phage P335* did exhibit an early bloom in WD samples (8-fold increase by 14 days), this bacteriophage species did not reach equivalent elevation in log fold change patterns as other members of *P335-like viruses*. Dissimilarity between *Streptococcus phage SMP* and *Abc2* were also observed in WD samples, even with low variation of bacterial host genera. Of interest, we

did see virulent bacteriophage that did not follow classic models of lytic behavior. *Lactococcus phage 1706* revealed similar abundance fluctuations to that of the host in Chow samples but had contrasting dynamics in WD samples. *Lactococcus phage 1706* experience a 3-fold decline in abundance when their host *Lactococcus* reached a 5-fold increase in abundance. By the final time point, we did see a net positive abundance increase in this bacteriophage species. Similarly, *Staphylococcus phage Twort* had an early decline in abundance even when *Staphylococcus* experiences elevations in abundance at the final timepoint. Virulent bacteriophage tended to follow the kill-the-winner model, but we report that they do not always act according to this model of behavior in a dynamic microbial community.

Discussion

In this study, we demonstrated that bacteriophage communities are sensitive to WD feeding. The community network revealed that bacteriophage genera play integral roles in the microbiome samples of WD-fed mice. The bacteriophage genera in the WD sample networks also displayed a higher degree of connectivity, indicating they impact many more bacterial families than those they target as hosts. Clustering strategies also highlighted the dynamic nature of both bacteriophage genera and bacterial families following WD feeding. Overall, abundance of bacterial families and bacteriophage genera did not greatly vary from baseline levels in control samples and bacteria: bacteriophage dynamics were mostly synchronous. Within WD samples, many temperate bacteriophages followed the abundance patterns of their putative host family following WD feeding. However, virulent bacteriophage behavior was not as predictable. Some Streptococcaceae-targeting bacteriophage underwent divergent abundance patterns from Streptococcaceae. Taken together, WD feeding disrupted baseline levels of bacteriophage genera

and altered bacteriophage community's contribution to have more of an impact on the microbiome as a whole.

Here we show that compositional shifts in the microbiota following WD feeding result in shift in the overall network of microbial community structure. I discussed in Chapter 1 that WD microbiome samples depicted dissimilarity from chow counterparts in nMDS plots (Figure 2.4). This is in line with previous reports of dissimilarity in intestinal microbiome composition between opposing diets, where individuals on the same diet cluster closely together within various ordination plots [13,28,29]. Virus-like particle (VLP) of bacteriophage communities on a low-fat diet have displayed dissimilarity from VLP communities of individuals fed a high-fat diet [28]. Furthermore, others investigations characterizing both prokaryotic and eukaryotic viral populations in the intestinal microbiome (virome) report divergence of the virome communities in human samples following low-fat or high-fat feeding [29]. Individuals on the same diet had more similar communities of virus-like particles in the intestinal microbiome than those on the alternative diet [29]. Our findings support and expand upon the understanding of these divergent communities through evaluation of the community structure of the intestinal microbiome. Community structure on the chow diet shows high connectivity between many bacterial constituents. Bacteriophage genera were shown to have few connections and were more peripheral in relation to the central network in the chow samples. WD samples showed a higher modularity of communities than the basal diet. These modules may indicate a loss in microbial community collaboration and proficiency. Bacteriophage genera in our WD samples had more connections and were found to potentially play a more integral part in community structure as compared to chow samples. Our findings support previous studies, and show bacteriophage

potentially contribute more to overall community structure in these communities as microbial composition changes following WD feeding.

Recently, there has been a rise in appreciation of the enteric virome due to metagenomic sequencing, which has given us a reliable method to study the complexity within this community [15]. In the present study, we utilized whole shotgun metagenomic samples annotated by MG-RAST to track abundance patterns of bacteriophage and their host. Of note, we were selectively targeting the bacteriophage community, namely those belonging to the order Caudovirales. This study did not use methods to speak to prokaryotic enveloped, prokaryotic RNA, or eukaryotic viral abundance and how these viral components contribute to community structure in the intestinal microbiome. To date, many studies report bacteriophage communities in terms of VLPs [29–32]. This is useful for evaluating the overall community but is not descriptive enough to infer implications of these communities on the microbiome as a whole. The challenge facing investigation of resident viral communities is that viral taxonomy identification databases are severely incomplete. In this study, we attempted to establish defined populations of bacteriophage in the intestinal microbiome in order to describe the dynamics of both the bacteriophage and its putative host. To do this, we cross-annotated species annotations (70% identity threshold), within the order Caudovirales, from the RefSeq database with the International Committee on Taxonomy of Viruses taxonomic database or other documentation detailing classification of the bacteriophage into respective genera. Descriptions of bacteriophage genera present are outlined in Appendix 1. One limitation of our study pertained to bacteriophage who were not specifically classified to a genus. We did see some change in the relative abundance of those who fell in the unclassified components of our sample but were unable to delve into these relationships. This limitation can only be overcome by significant

expansion of bacteriophage annotations within available databases. Another limitation of our study lies in determining whether a viral annotation was due to prophage integration in host genome, or if it was free living. To accommodate for this, we attempted to identify the lifestyle characterization of the viral species used to better define the mechanism of abundance change. This limitation of mis-annotation could still exist even in the event that bacterial and viral components are separated prior to DNA extraction. To distinguish bacterial components from integrated prophage will require development of new tools and significant improvement of viral databases.

Recent studies have described the bacteriophage community's potential to induce a cascading effect in the intestinal microbiome [19,27,33]. This study characterized bacteria:bacteriophage dynamics following colonization of human gut commensal bacteria and administration of lytic bacteriophage in gnotobiotic mice [19]. First, the results established that bacteriophage can coexist over time with targeted gut bacteria, which follows theoretical models of bacteriophage biology [19,26,27,33]. This idea is supported in our chow samples, as a steady prevalence of bacteriophage genera and their bacterial host was described for a vast majority of microbial constituents. Following administration of bacteriophage, the researchers described alterations of not only target bacterial communities, but also cascading effects that resulted in modulation of the microbiota and metabolites they produced [19]. The network analysis in the present study supports this idea, as bacteriophage within the WD samples contributed more to the central network with more interconnectivity. Hsu, *et al.* described a gnotobiotic model reminiscent of intestinal microbiome alteration following bacteriophage therapy [19]. In our study, we describe the modulation potential of resident bacteriophage communities within the intestinal microbiome

following WD feeding. This allows for a better assessment the susceptibility of bacteriophage populations to modulation following WD feeding.

The present study also characterized the variations of multiple bacteria:bacteriophage relationships occurring in tandem with the entire microbiome following WD-induced community changes. Bacteriophage genera dominated with temperate bacteriophage typically followed the abundance patterns of their putative host. This was confirmed in bacteriophage species dynamics with host bacterial genera. This behavior was attributed to the fact that they may be present as prophage within the host genome. Temperate bacteriophage are thought to prefer lysogeny within rapidly dividing host bacterial cells [27,33]. As the host genome is replicated, so too is the prophage genome replicated; this is known as 'piggyback-the-winner' [27,33]. Temperate bacteriophage do have the possibility of existing as free bacteriophage particles, similar to virulent bacteriophage, and therefore the possibility of ambient temperate bacteriophage in our samples cannot be overlooked. Spontaneous induction of prophage can occur in a range of conditions such as following host induction of the SOS response [34–37], extrinsic factors like altered gene expression of the host [38], coordination using communication molecules [39], molecular cues [40] and phage-phage interactions [41,42]. Spontaneous induction of prophage in these microbial environments can serve to increase the pool of prophage being replicated, as well as kill off related bacterial competitors [27]. A more recent investigation also describes communication among bacteriophage that act to coordinate lytic-lysogenic decisions [39]. Models such as these may provide explanation for bacteriophage lifestyle decisions in microbial communities, and potential mechanisms of a bacteriophage's ability to control bacterial communities. We also described rapid abundance increases of *Staphylococcus phage EW* and *Streptococcus phage Tuc2009* in response to marginal host abundance blooms. In these bacteriophage species, there

may be a combination of piggyback-the-winner and prophage induction in response to some host abundance threshold being reached. In contrast, *Enterococcus phage phiFL4A* showed close correlations with host abundance patterns which likely explained solely by piggyback-the-winner dynamics.

One possible explanation for elevation of free bacteriophage, such as virulent bacteriophage, abundance following diet change could be due to the fact that viruses replicate at a much faster rate than bacteria. One bacteriophage particle can give rise to hundreds of new virions within one host cell per replication cycle as compared to host binary fission. Additionally, bacteriophage require less resources and time to produce progeny than bacteria. When the opportunity arises, such as a bloom in target bacteria in response to variation in nutrient availability, bacteriophage can benefit from the increase in viable host bacteria. In this way, a small bloom of bacteria could give rise to a larger production of bacteriophage that target this host. Bacterial abundance levels could appear reduced or stagnant as bacteriophage progeny are infecting new daughter bacterial cells. In this way, bacteriophage could curb potential unwanted blooms of organisms, such as opportunistic pathogens and those who promote disease states and contribute to overall stability of the microbiome. This has been outlined in the classic theoretical bacterial control model of kill-the-winner [26]. In this model, there is not much predation in steady states, and this preserves the diversity of bacteriophages and bacteria. In the event that bacterial species bloom to a particular threshold, bacteriophage can prevent any single bacterial species from over-taking the whole community [26]. This is exemplified in abundance patterns of virulent bacteriophage species and their host in Chow samples. At the final timepoint for many of the bacteria genera studied, we saw an increase in bacteria and virulent bacteriophage. Future investigations could extend the duration of the experiment to see if these results point cyclical ebb-and-flow described in these

bacteriophage behavioral models. Similarly, in line with these models, we described significant elevations of virulent bacteriophage species targeting *Lactococcus* following elevations in host abundance in WD microbiome samples. In the context of our fold-change results, it appears that bacteriophage experience more rapid and elevated abundance increases in response to WD feeding. More sensitive sampling strategies will be needed to provide the necessary evidence of the mechanisms and timeline of predator-prey dynamics in response to environmental stimuli.

We have demonstrated that bacteriophage abundance dynamics do not always follow that of the host and this is exacerbated following WD feeding. As compared to control counterpart dynamics, Streptococcaceae-targeting bacteriophage genera showed a wide range of sensitivities to the WD. *P335-like* and *936-like viruses* showed similar responses to the WD, which were parallel to that of their host. More detailed investigations of bacteriophage species belonging to *P335-like viruses* supported the possibility of this arising from the combination of both temperate and virulent bacteriophage species propagation strategies. Previous theories of bacteriophage ecology and abundance predict that bacteriophage populations would follow that of their putative host - either due to lysogeny or kill-the-winner dynamics [26,33,43]. In addition, we also noted bacteriophage populations that were affected by diet *inversely* as compared to their bacterial host. Similar to *P335-like* and *936-like viruses*, *1706-like viruses* are virulent bacteriophage who target Streptococcaceae but showed a reduction in abundance as compared to its bacterial host and control counterparts. I do not have a definitive explanation of why this occurred, but it could be due to a decrease in additional unclassified bacterial host populations or sensitivities of these bacteriophage to components, such as metabolites, within the microbiome following dietary exposure. Nutrient have shown to influence the behavior of bacteriophage [44,45]. For example, adsorption efficiency of *E. coli* bacteriophage is influenced by temperature and the

presence of L-tryptophan in media [44]. Other investigations of bacteriophage biology state that nutrient poor conditions do not restrict bacteriophage reproduction as much as concentration of bacteriophage where the lowest concentration of bacteriophage resulted in the highest progeny yield [45]. Our study demonstrates that relative abundance fluctuations tend to match that of their host, but this study also demonstrates that bacteriophage communities can respond to environmental stimuli independently of their host overtime. Future investigations into bacteria:bacteriophage dynamics will hopefully reveal if alteration to bacteriophage abundance precedes that of their bacterial host or if rapid replication of bacteriophage genera is disguising blooms of the bacterial host.

With the surge of antibiotic resistance within recent years, researchers are embracing the idea of utilizing bacteriophage as therapy for bacterial infections. Many have pointed to the specificity of bacteriophage therapy being a major advantage of this treatment over broad-spectrum antibiotics. However, Hsu, *et al.* showed the potent cascading effects of bacteriophage administration on the microbiota species that are not directly targeted and the resulting modulation to the metabolome [19]. Rippling effects of bacteriophage prevalence could bring about homeostasis or perpetuate disease states of the enteric microbiome. Potential therapies could be developed by understanding the role bacteriophage play during microbiome compositional alteration and applying these lessons to modulate microbial symbionts. Furthermore, bacteriophage communities could act as an indicator population to help proactively diagnose disruption of community structure in the intestinal microbiome. Our work provides initial evidence of these bacteria:bacteriophage relationships within the intestinal microbiome following WD feeding.

References

1. Sender, R., Fuchs, S. & Milo, R. Revised Estimates for the Number of Human and Bacteria Cells in the Body. PLOS Biol. 14, e1002533 (2016).

2. Obata, Y. & Pachnis, V. The Effect of Microbiota and the Immune System on the Development and Organization of the Enteric Nervous System. Gastroenterology vol. 151 836–844 (2016).

3. Cani, P. D. Human gut microbiome: hopes, threats and promises. Gut gutjnl-2018-316723 (2018) doi:10.1136/gutjnl-2018-316723.

4. Zuo, T. et al. Gut mucosal virome alterations in ulcerative colitis. Gut gutjnl-2018-318131 (2019) doi:10.1136/gutjnl-2018-318131.

5. Turnbaugh, P. J. et al. An obesity-associated gut microbiome with increased capacity for energy harvest. Nature 444, 1027–1031 (2006).

6. Chang, J. Y. et al. Decreased Diversity of the Fecal Microbiome in Recurrent Clostridium difficile –Associated Diarrhea. J. Infect. Dis. 197, 435–438 (2008).

7. Le Roy, T. et al. Intestinal microbiota determines development of non-alcoholic fatty liver disease in mice. Gut 62, 1787–1794 (2013).

8. Zhu, W. et al. Gut Microbial Metabolite TMAO Enhances Platelet Hyperreactivity and Thrombosis Risk. Cell 165, 111–124 (2016).

9. Hsiao, E. Y. et al. Microbiota modulate behavioral and physiological abnormalities associated with neurodevelopmental disorders. Cell 155, 1451–1463 (2013).

10. Huttenhower, C. et al. Structure, function and diversity of the healthy human microbiome. Nature 486, 207–214 (2012).

11. Turnbaugh, P. J. et al. The effect of diet on the human gut microbiome: a metagenomic analysis in humanized gnotobiotic mice. Sci. Transl. Med. 1, 6ra14 (2009).

12. Backhed, F. et al. The gut microbiota as an environmental factor that regulates fat storage. Proc. Natl. Acad. Sci. 101, 15718–15723 (2004).

13. Ridaura, V. K. et al. Gut microbiota from twins discordant for obesity modulate metabolism in mice. Science 341, 1241214 (2013).

14. Lopetuso, L. R., Ianiro, G., Scaldaferri, F., Cammarota, G. & Gasbarrini, A. Gut Virome and Inflammatory Bowel Disease. Inflamm. Bowel Dis. 22, 1708–1712 (2016).

15. Ofir, G. & Sorek, R. Contemporary Phage Biology: From Classic Models to New Insights. Cell (2018) doi:10.1016/j.cell.2017.10.045.

16. Norman, J. M. et al. Disease-specific alterations in the enteric virome in inflammatory bowel disease. Cell 160, 447–60 (2015).

17. Manrique, P. et al. Healthy human gut phageome. Proc. Natl. Acad. Sci. U. S. A. 113, 10400–10405 (2016).

18. Minot, S. et al. The human gut virome: inter-individual variation and dynamic response to diet. Genome Res. 21, 1616–1625 (2011).

19. Hsu, B. B. et al. Dynamic Modulation of the Gut Microbiota and Metabolome by Bacteriophages in a Mouse Model. Cell Host Microbe 25, 803-814.e5 (2019).

20. Li, H. & Durbin, R. Fast and accurate short read alignment with Burrows-Wheeler transform. Bioinformatics 25, 1754–1760 (2009).

21. Li, H. et al. The Sequence Alignment/Map format and SAMtools. Bioinformatics 25, 2078–2079 (2009).

22. Kurtz, Z. D. et al. Sparse and Compositionally Robust Inference of Microbial Ecological Networks. PLoS Comput. Biol. 11, (2015).

23. Csardi, G., & Nepusz, T. The Igraph Software Package for Complex Network Research. InterJournal 2006, Complex Systems, 1695. - References - Scientific Research Publishing. https://www.scirp.org/(S(vtj3fa45qm1ean45vvffcz55))/reference/ReferencesPapers.aspx?ReferenceID=1426710 (2006).

24. Ernst, J. & Bar-Joseph, Z. STEM: a tool for the analysis of short time series gene expression data. BMC Bioinformatics 7, 191 (2006).

25. Klumpp, J., Calendar, R. & Loessner, M. J. Complete Nucleotide Sequence and Molecular Characterization of Bacillus Phage TP21 and its Relatedness to Other Phages with the Same Name. Viruses 2, 961–71 (2010).

26. Thingstad, T. & Lignell, R. Theoretical models for the control of bacterial growth rate, abundance, diversity and carbon demand. Aquat. Microb. Ecol. 13, 19–27 (1997).

27. Silveira, C. B. & Rohwer, F. L. Piggyback-the-Winner in host-associated microbial communities. npj Biofilms Microbiomes 2, 16010 (2016).

28. Howe, A. et al. Divergent responses of viral and bacterial communities in the gut microbiome to dietary disturbances in mice. ISME J. 10, 1217–1227 (2016).

29. Minot, S. et al. The human gut virome: inter-individual variation and dynamic response to diet. Genome Res. 21, 1616–25 (2011).

30. Dutilh, B. E. et al. A highly abundant bacteriophage discovered in the unknown sequences of human faecal metagenomes. Nat. Commun. (2014) doi:10.1038/ncomms5498.

31. Reyes, A., Wu, M., McNulty, N. P., Rohwer, F. L. & Gordon, J. I. Gnotobiotic mouse model of phage-bacterial host dynamics in the human gut. Proc. Natl. Acad. Sci. U. S. A. 110, 20236–41 (2013).

32. Mobberley, J. M., Authement, R. N., Segall, A. M. & Paul, J. H. The temperate marine phage PhiHAP-1 of Halomonas aquamarina possesses a linear plasmid-like prophage genome. J. Virol. 82, 6618–30 (2008).

33. Knowles, B. et al. Lytic to temperate switching of viral communities. Nature (2016) doi:10.1038/nature17193.

34. Little, J. W. Chance phenotypic variation. Trends Biochem. Sci. 15, 138 (1990).

35. Miyazaki, R. et al. Cellular Variability of RpoS Expression Underlies Subpopulation Activation of an Integrative and Conjugative Element. PLoS Genet. 8, e1002818 (2012).

36. Nanda, A. M. et al. Analysis of SOS-induced spontaneous prophage induction in Corynebacterium glutamicum at the single-cell level. J. Bacteriol. 196, 180–188 (2014).

37. Smith, C. L. & Oishi, M. Early events and mechanisms in the induction of bacterial SOS functions: Analysis of the phage repressor inactivation process in vivo. Proc. Natl. Acad. Sci. U. S. A. 75, 1657–1661 (1978).

38. Broussard, G. W. et al. Integration-Dependent Bacteriophage Immunity Provides Insights into the Evolution of Genetic Switches. Mol. Cell 49, 237–248 (2013).

39. Erez, Z. et al. Communication between viruses guides lysis-lysogeny decisions. Nature 541, (2017).

40. Casjens, S. et al. The Chromosome of Shigella flexneri Bacteriophage Sf6: Complete Nucleotide Sequence, Genetic Mosaicism, and DNA Packaging. J. Mol. Biol. 339, 379–394 (2004).

41. Lemire, S., Figueroa-Bossi, N. & Bossi, L. Bacteriophage crosstalk: Coordination of prophage induction by Trans-Acting antirepressors. PLoS Genet. 7, e1002149 (2011).

42. Campoy, S. et al. Induction of the SOS response by bacteriophage lytic development in Salmonella enterica. Virology 351, 360–367 (2006).

43. Virgin, H. W. The virome in mammalian physiology and disease. Cell vol. 157 142–150 (2014).

44. Anderson, T. F. The Influence of Temperature and Nutrients on Plaque Formation by Bacteriophages Active on Escherichia coli Strain B. J. Bacteriol. 55, 659 (1948).

45. Moebus, K. Marine bacteriophage reproduction under nutrient-limited growth of host bacteria. II. Investigations with phage-host system [H3:H3/1]. Mar. Ecol. Prog. Ser. 144, 13–22 (1996).

Chapter 4

In vitro Analysis of Intestinal Inflammations Effect on Bacteriophage Infectivity Rates.

Abstract

The intestinal immune system must maintain a delicate balance between tolerance of enteric commensals and defense against pathogens. The enteric microbiota is composed of a variety of microorganisms, including bacteria, bacteriophage, and several others. During periods of intestinal inflammation, the enteric microbiota can be subjected inadvertently to damage by immune-derived antimicrobial agents, such as reactive oxygen and chlorine species. While we have some knowledge of how inflammation affects bacteria, we understand significantly less about how inflammatory products impact the dynamics of bacteria:bacteriophage interactions. The primary objective of this study was to determine how immune system products, namely hydrogen peroxide and hypochlorous acid, impact bacteriophage infectivity rates of a virulent bacteriophage. The effect of hydrogen peroxide and hypochlorous acid on the infectivity rate of bacteriophage was measured using a modified one-step growth curve, which determined the timeline of the growth cycle and burst size of an *Escherichia coli*-specific bacteriophage, *PF-2*. Adsorption kinetics allowed for quantification of adsorption efficiency during exposure to hydrogen peroxide and hypochlorous acid. We observed a delay in adsorption rate in a dose-dependent manner in the presence of either hydrogen peroxide or hypochlorous acid. Additionally, hydrogen peroxide treated PF-2 samples were delayed in replication, presumably due to inefficiency of adsorption, but this did not reduce overall progeny production at low concentrations. Though adsorption kinetics were also modified in a dose-dependent manner by

hypochlorous acid, the replication cycle of *PF-2* was not changed at doses of 0.6mg/L or 1mg/L hypochlorous acid. Hypochlorous acid treatment did result in a slightly longer latent period, but this did not result in significant change in the overall timeline or progeny produced. In conclusion, we demonstrated the negative effects of reactive oxygen and chlorine species on the adsorption efficiency of *PF-2.* For reactive oxygen, this translates into downstream effects of delayed and reduced replication cycles especially at higher concentrations. Regardless of delay in adsorption, hypochlorous acid treatment did not affect the overall infectivity rate of *PF-2* even at the highest dose.

Introduction

Bacteriophage have recently gained much attention in the field of microbial ecology, especially among those who investigate the intestinal microbiome. These prokaryote-targeting viruses are dominant members of the viral community in many microbial environments, including the intestinal microbiome [1,2]. It is well established that bacteria play a role in the mammalian health and physiology. Recent investigations of bacteriophage communities have displayed evidence that they too are contributing members of microbial communities, namely the healthy gut microbiome [1,3]. Bacteriophage, namely those belonging to the order Caudovirales, are tailed, double-stranded DNA viruses as seen in Figure 4.1B. Caudovirales is further divided into Podoviridae, Siphoviridae, and Myoviridae families [2]. In Chapters 1 and 2, we discussed the impact of environmental stimuli, namely WD feeding, on the composition of the bacteriophage community in the intestinal microbiome. Similar findings of bacteriophage modulation have been reported in the context of nutrient availability [4] and intestinal inflammation [3,5]. However, detailed mechanism for the plasticity seen in the bacteriophage communities has yet to be determined, especially in the setting of intestinal inflammation.

The mammalian intestine can be home to both commensal and opportunistic pathogenic bacteria, among other microorganisms [6]. The intestinal immune system has a unique challenge in maintaining homeostasis while providing protection from invading pathogens [7]. In times of pathogenic invasion or a breach in the intestinal barrier, the immune system becomes activated and intestinal inflammation initiates with signaling of proinflammatory cytokines and recruitment of granulocytes [8]. Among the first innate immune cells to arrive at the scene of inflammation is neutrophils [9]. These innate granulocytes are equipped with machinery that aids in destruction of pathogenic threats - including phagocytosis, granules filled with antimicrobial

agents, and respiratory burst caused by NADPH oxidase [10–12]. Many of these antimicrobial tactics are used in tandem to maximize clearing of infectious agents. For example, neutrophils can maximize the potency of NADPH oxidase action by the additional release of myeloperoxidase during degranulation [12]. Reactive oxygen intermediates are released into the extracellular space following oxidative burst by neutrophils. One of these intermediates, hydrogen peroxide, acts as the substrate in the myeloperoxidase-catalyzed peroxidation of chloride ions to form reactive chlorine intermediates, namely hypochlorous acid [10,12]. It is well established that these antimicrobial substances aid the immune system in clearing bacterial threats [12]. In response, bacteria have evolved global regulatory systems for adaptation to both environmental and/or inflammatory stress. These regulatory systems aid in detecting and initiating responses to stressors including pH, nutrient depletion, and oxidation that could destroy necessary proteins and nucleic acids [13]. Genes within these systems are usually autoregulating, and increase or decrease expression based on the level of the stress applied to the system [13–15]. Activation of lytic-lysogenic switches have been reported in the temperate lambda bacteriophage following damage response system (the SOS response) activation [16]. However, it is unclear how these environmental conditions affect free bacteriophage particles, virulent bacteriophage or newly released temperate bacteriophage, and their ability to efficiently and effectively infect.

Recent publications show evidence that bacteriophage communities display modulation within the enteric microbiome during intestinal inflammation[3,5,17]. For example, members of the defined core phageome were significantly depleted or absent in IBD patients as compared to healthy counterparts [3]. Additionally, Norman, et al. reported elevations in bacteriophage richness with reciprocal decline in bacterial diversity in fecal microbiome samples of IBD patients [5]. Elevated bacteriophage abundance could be connected with bacterial dysbiosis and could lead to

replication of prophage within rapidly dividing host or release of temperate bacteriophage following induction [16]. Higher concentrations of bacteriophage could perpetuate inflammation via lysis of host bacteria and subsequent release of pathogen-associated molecular patterns or by triggering of the immune response directly [5,18]. Early studies in bacteriophage therapy have defined the immunogenic nature of bacteriophage and how the immune system responds to systemic bacteriophage prevalence [5,14-16]. For example, bacteriophage are rapidly detectable in multiple organ systems, including the central nervous system, following systemic administration and are cleared within 30 minutes by the liver if their host is not located [19]. The bacteriophage particles are immunogenic enough to promote proliferation of neutrophils *in vivo* [20] and elicit immunoglobulin production in infants which has now been potentially linked to a TLR9-dependent mechanism [5,18]. A recent publication showed that activation of the host immune responses via TLR9 of germ-free mice was observed after bacteriophage administration which resulted in immune cell proliferation, IFN-ɣ production and exacerbation of colitis [18]. Unlike bacteria, bacteriophage share purely a mutualistic relationship to the mammalian host. Bacteriophage have been shown to provide microbial regulation and/or provide a type of resistance to bacterial infection by populating the mucin layer over mucosal surfaces [21]. Yet, knowledge of how the immune system affects bacteriophage infectivity during intestinal inflammation is lacking in the literature.

Bacteriophage can be classified as either virulent or temperate based on how they infect and replicate. Virulent bacteriophage do not contain the genes for lysogeny and proceed directly to lytic infection cycle (Figure 4.1A). On the other hand, temperate bacteriophage with the genes for lysogeny and can undergo either lysogenic or lytic infection cycles (Figure 4.1A). At the

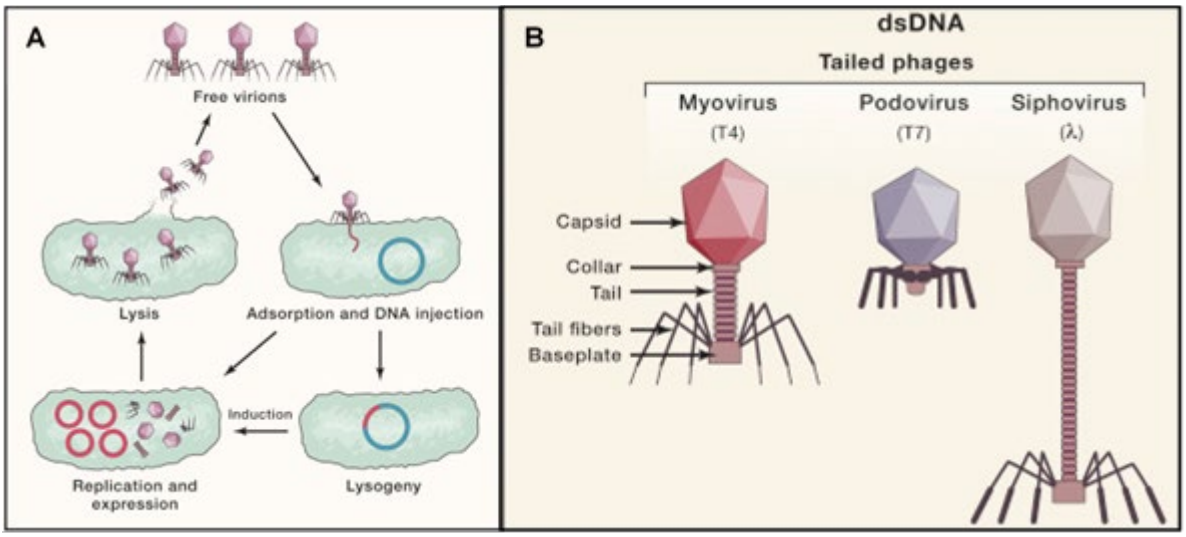

Figure 4.1. Bacteriophage life cycles and morphology. (a) Bacteriophage life cycles. (b) Bacteriophage taxonomy within the order Caudovirales is based on morphology. A representative type of bacteriophage is present for each taxonomical group within this order. Both images from Ofir and Sorek, 2017 [1].

conclusion of infection, all bacteriophage undergo the lytic infection cycle, where progeny phage particles are released from the host cell in a process that most often involves host cell lysis via bacteriophage-derived proteins (Figure 4.1A) [1]. Infection begins with adsorption of the phage particle or virion to its host cell through specific receptor recognition. The eclipse phase of the phage infection cycle describes the time taken to adsorb and deliver nucleic acid into host cells (Figure 4.2). The following stage is termed the synthetic period where new bacteriophage particles are being produced intracellularly. The collective term for the eclipse and synthetic period is the latent period, otherwise described as the time period in which attachment, entry, replication, transcription, translation and assembly of progeny occur (Figure 4.2) [22]. Following the latent period comes the rise period where bacteriophage progeny are emerging from host bacterial cells, described as the burst [22]. Many investigations of bacteria:bacteriophage relationships utilize temperate bacteriophage to explain bacteriophage behavior following host response to environmental stimuli. Yet, virulent bacteriophage can also be affected by decisions of the host. Virulent bacteriophage are potent modulators of bacterial composition as they have been sought after as the anti-bacterial agents in bacteriophage therapy [1]. Understanding bacteriophage behavior during bacterial stress may give insight to the resilience of bacteriophage therapies during inflammation as well as elucidate potential mechanisms of bacteriophage modulation during intestinal inflammation.

In this study, we examined known antimicrobial agents of the immune system and their potential effects on virulent bacteriophage infectivity rates during inflammation. We performed a series of assays to determine efficiency of adsorption and progeny production in an intestinal bacteriophage isolate. Reactive oxygen and chlorine species had deleterious effects on

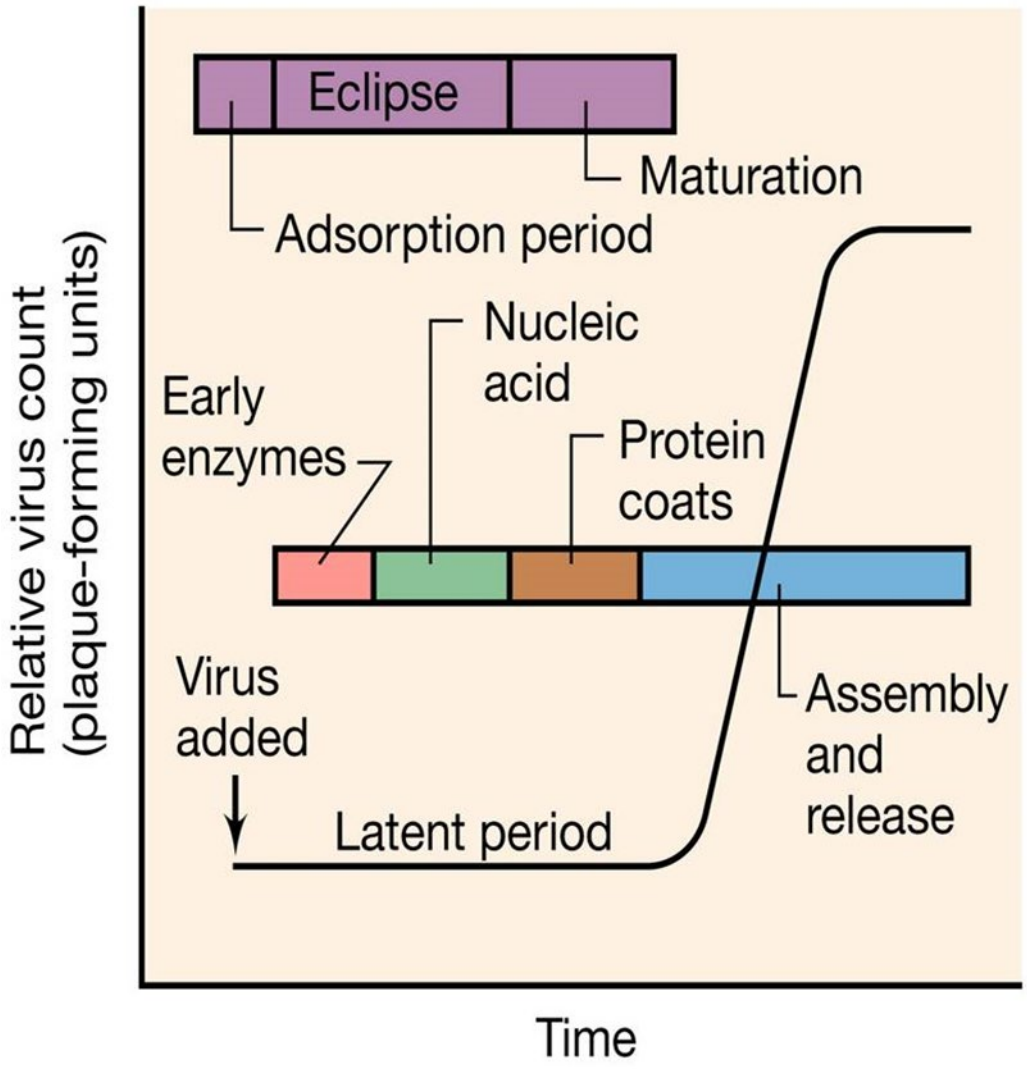

Figure 4.2. Diagram of Bacteriophage Replication Timeline. (Image from One step multiplication curve for bacteriophages – Biotech Khan) [23].

bacteriophage adsorption efficiency with increasing concentrations. We found that delays in adsorption were followed by delayed and reduced progeny production in hydrogen peroxide treatments. However, this was not the case for hypochlorous acid samples where bacteriophage infectivity rates were seemingly unaffected regardless of treatment and dosing timing. Our study highlights effects of reactive oxygen and chlorine species on the reproduction efficiency of enteric virulent bacteriophage. Characterization of such a process will allow more insight into how bacteriophage are affected by inflammation.

Materials and Methods

Bacteriophage isolation and bacterial isolation

Microbial isolates were harvested from fecal samples of a Mangalica Pig housed at the Auburn University Swine Facility. We were able to isolate a Gram-negative bacterium that was identified as *Escherichia coli* based on the following criteria: negative Gram-stain; motile rods; positive growth on EMB plates with metallic green colonies; catalase positive; negative for growth on MSA plates, positive mannitol, lactose, and nitrate metabolism, among other biochemical tests. This *E. coli* isolate was utilized as the indicator strain in bacteriophage isolation of *PF-2* and in subsequent bacteriophage infectivity experiments.

To isolate bacteriophage, fecal samples were diluted 1:10 in salt-magnesium buffer with 10% beef extract. Homogenized samples were filtered through a 0.45 μm filter. Sample filtrate was administered to a double agar overlay plate as part of the spot test as described by Clokie and Kropinski [24]. In short, a double agar overlay is a plating strategy where 200 μL of *E. coli* culture, or the indicator strain, is added to 3 mL of a soft agar (0.7% agar) containing 0.1% of 2,3,5-Triphenyltetrazolium chloride (TTC) (Supplier: Millipore Sigma). TTC acts as a dye to

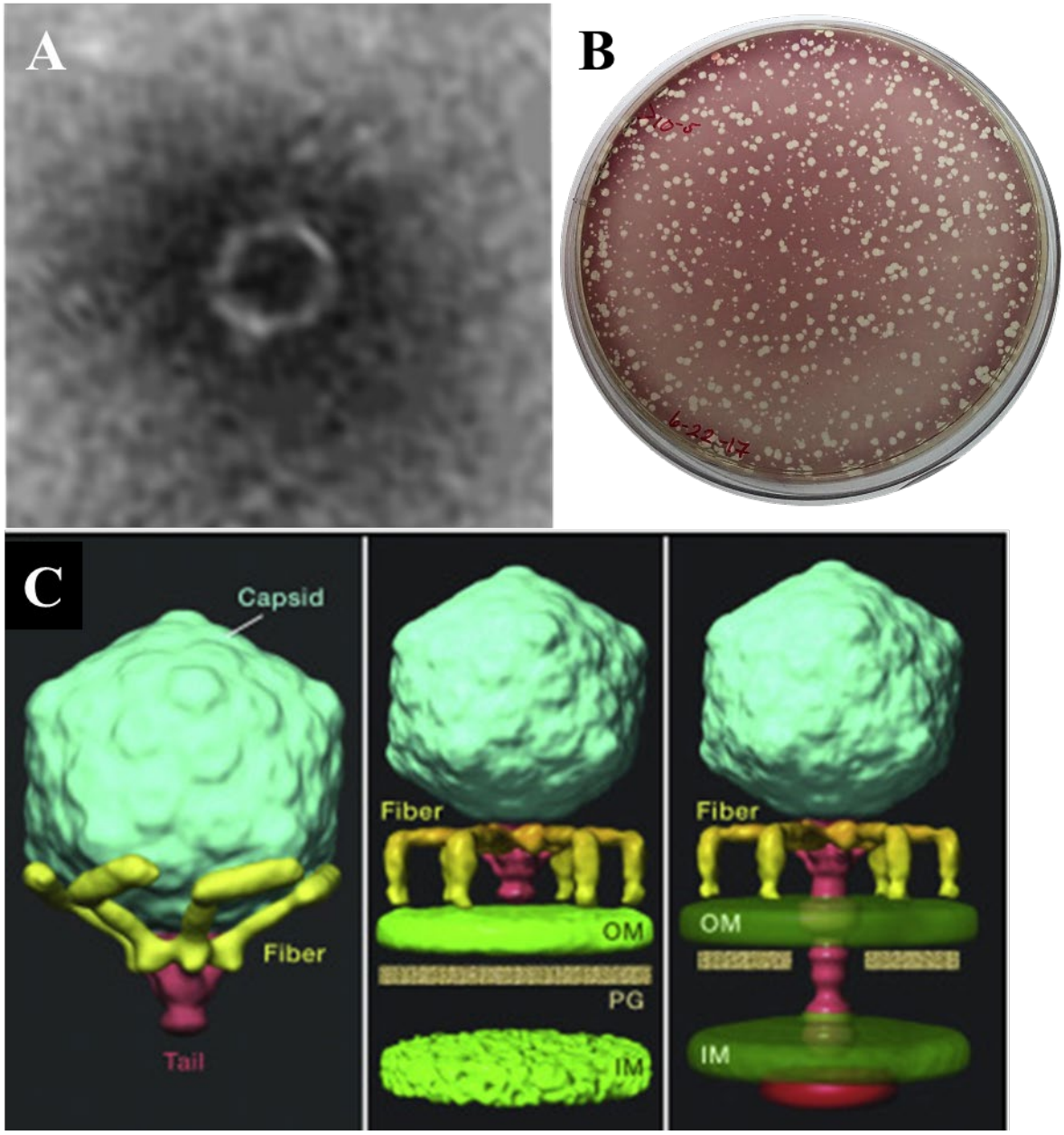

Figure 4.3. Characterization of *PF-2.* (a) Transmission electron microscopy of *PF-2* particle isolated from the Mangalica pig enteric microbiome. (b) Double agar overlay plate 24hrs after plating with 10^6 PFU/mL. (c) Cryo-EM structural reconstruction of T7 virions prior to and during adsorption from (Image from Hu, et al., 2013) [25]. The final panel of this figure shows penetration of the tail through the outer membrane (OM), peptidoglycan (PG) and inner membrane (IM) in order to facilitate transfer of the bacteriophage genome [25].

provide a colored backdrop of the bacterial lawn. This allowed bacteriophage plaques to be easily identified following addition of bacteriophage as shown in Figure 4.3B. Positive spot tests were cored, and cores were allowed to diffuse in 500 µL of SM buffer with 10% chloroform 4 hours at room temperature. The upper phase of the solutions containing cores were removed and used in bacteriophage isolation procedures. Multiple rounds of bacteriophage isolation were conducted in which single plaques were cored, processed, and utilized in the following isolation assay. Following this series of isolation passes, one bacteriophage was isolated and amplified. This bacteriophage was given the designation of *PF-2*. *PF-2* has been characterized as a virulent, *E. coli*-targeting bacteriophage. Transmission electron microscopy revealed that *PF-2* had a short, non-contractile tail, morphology consistent with the family Podoviridae (Figure 4.3A). Recent advancements in microscopy have allowed for a 3D rendering of a similar Podoviridae bacteriophage, *Escherichia bacteriophage T7*, to better characterize its morphology and mechanics (Figure 4.3C; From Hu, et al., 2013) [25]. We speculate that *PF-2* could share morphological and behavioral similarities to what was described by Hu, et al., 2013 [25]. Morphological and behavior characteristics of *PF-2* have been characterized but sequencing of the *PF-2* genome has not been performed to date to either classify or identify this bacteriophage. Plaque morphology of *PF-2* showed clear plaques with finite size and distinct edges (Figure 4.3B). Plaque characteristics, such as selective growth on log-phase bacteria and ability to lyse a significant portion of bacterial cell culture, were indications that *PF-2* is a virulent bacteriophage. Cell surface receptors of *E. coli* utilized in adsorption have not been characterized for *PF-2*. *PF-2* did not display cross reactivity on *Samonella enteria*. All together, these characteristics made the bacteriophage isolate *PF-2* an ideal candidate for further experimentation.

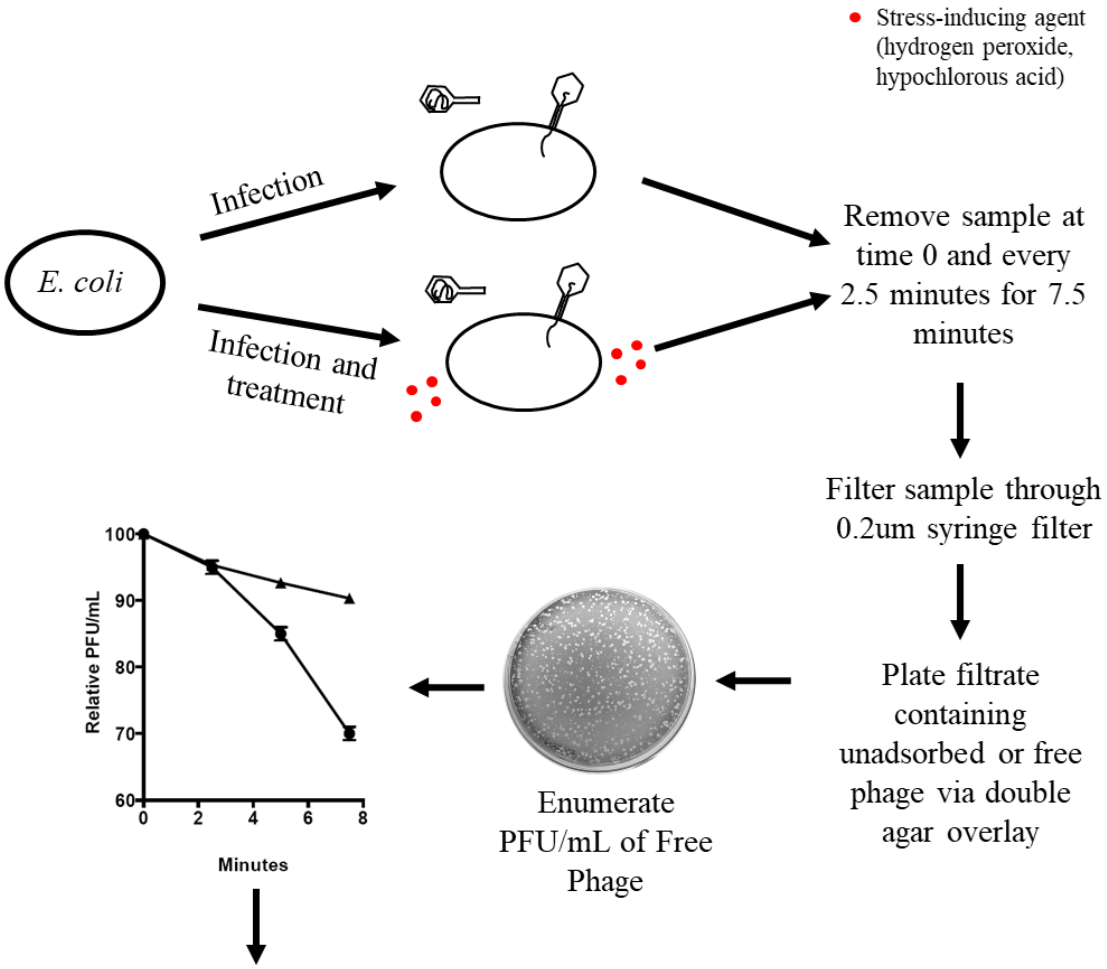

Figure 4.4. Diagram of adsorption constant methods and description of analysis.

Reagents

We selected hydrogen peroxide and hypochlorous acid as representative inflammatory products of neutrophils. 3% hydrogen peroxide stock was diluted to either a 0.5mM, 1mM, 2mM or 3mM concentration in dH_2O and incubated with bacteriophage in adsorption kinetics assays and one-step growth curve assays. We also exposed *PF-2* samples to sodium hypochlorite which is a commonly used reagent that has shown to simulate the effects of HOCl [12,26]. Phage samples in adsorption kinetics experiments were challenged with hypochlorous acid at a concentration of 0.2 mg/L, 0.4 mg/L, 0.6 mg/L or 1 mg/L. Treatment samples in the one-step growth curve were administered hypochlorous acid at either a concentration of 0.6 mg/L or 1 mg/L. Reagents were prepared daily for use by diluting in dH_2O prior to diluting to the final concentration in treatment culture flask.

Quantification of stress-induced alteration to bacteriophage infectivity rates

Adsorption kinetics assay and one-step growth curves were performed in order to quantify changes in *PF-2* infectivity rates following a similar protocol to those described previously [24,27]. Adsorption kinetics were obtained by filtering samples of co-cultured of *E. coli* and *PF-2* (MOI 0.1) through a 0.2 µm filter every 2.5 minutes for 7.5 minutes. The filtrate is then used to enumerate non-adsorbed or free bacteriophage via double agar overlay (Figure 4.4). The free plaque forming unit concentrations (PFU/mL) over time were used to calculate the adsorption slopes and *k* (adsorption constant) via linear regression. Determination of slope differences was performed using an ANCOVA

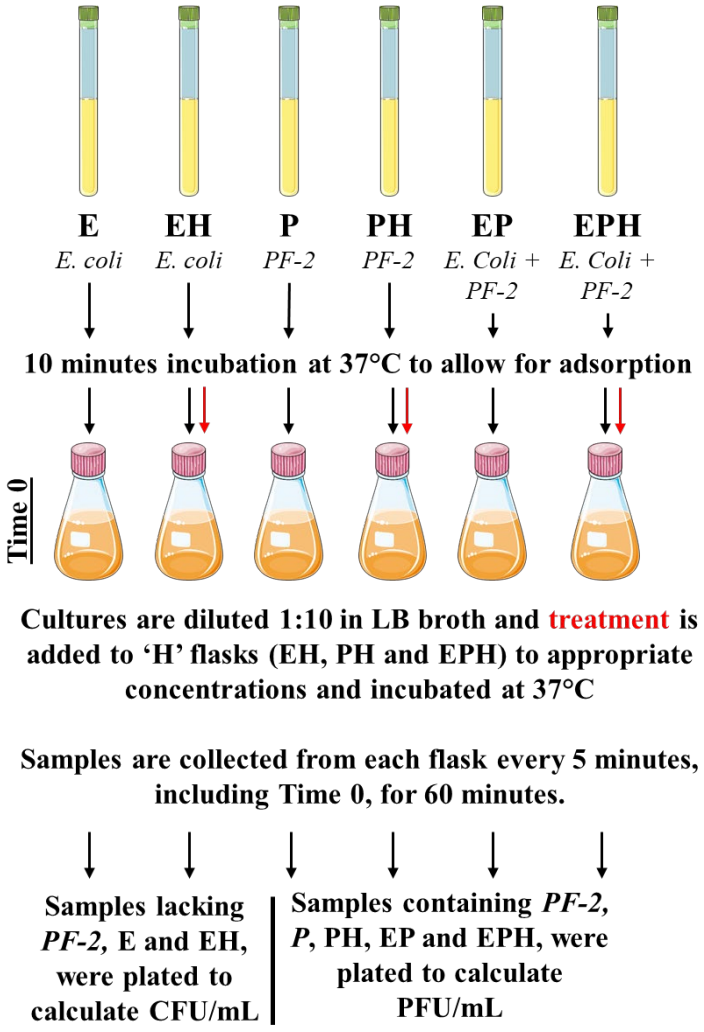

Figure 4.5. Description of modified one-step growth curve protocol.

Dose-dependent effects on burst were determined by the one-step growth curve as described previously [24,28]. To do this, mono- and co-cultures *of E. coli* and *PF-2* were treated following the strategy outlined in Figure 4.5 at a MOI of 0.1. Cultures were incubated at 37° C for 10 minutes to allow for adsorption. Following the adsorption period, cultures were diluted in treatment flasks and stress-inducing products were added at the appropriate concentration. We sampled mono- and co-cultures of bacteria and bacteriophage every 5 minutes to determine PFU/mL and every 10 minutes to determine bacterial colony forming units (CFU/mL) for a total of 60 min (Figure 4.5). One step growth curve experiment using HOCl treatments had additional treatments of $HOCl_{initial}$ and $HOCl_{initial+}$. $HOCl_{initial}$ samples received a dose of HOCl at the start of the 10-minute allotment time for adsorption and were not treated with HOCl again upon initiation of growth curve sampling. $HOCl_{initial+}$ samples were treated in a similar fashion to $HOCl_{initial}$ samples with the addition of a secondary dosing at the initiation of the growth curve (diagram of methods can be found in Appendix 3). Burst estimates were determined by subtracting free PFU/mL prior to burst (5 minutes post-adsorption) from total PFU/mL follow burst plateau (~30 minutes post-adsorption; variable). Free PFU/mL were estimated by filtering EP and EPH samples at 5 minutes post-adsorption through a 0.2 μm filter. The filtrate was then used to enumerate plaques via double agar overlay. Significance differences of treatment samples from control samples were determined using the students t-test.

Results

Reactive oxygen species do not directly damage PF-2

We first established a dose range suitable to induce stress in *E. coli* without killing either phage or bacteria. These experiments were conducted in tandem with the one-step growth curve.

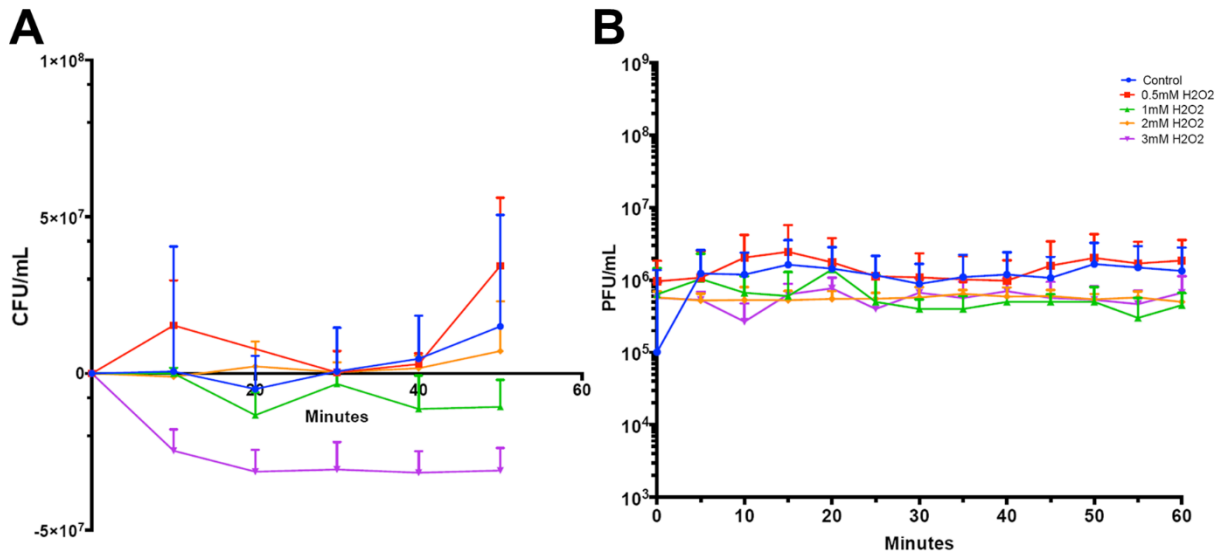

Figure 4.6. Effect of hydrogen peroxide on microbial growth over time. (a) Impact of hydrogen peroxide (H_2O_2) concentrations on *E. coli* growth rate in LB broth media containing a concentration of 0.12320 % Magnesium Sulfate (LBM). Starting inoculum (time zero), $1x10^7$ CFU/ml.; (b) Impact of hydrogen peroxide (H_2O_2) concentrations of ambient *PF-2* in LB broth media containing a concentration of 0.12320 % Magnesium Sulfate (LBM). Starting inoculum was $1x10^6$ PFU/ml.

We did see a dose-dependent effect of H_2O_2 on bacterial cultures (Figure 4.6A). Bacterial cell loss was detected in samples treated with 3mM H_2O_2, thus, this treatment was not utilized in downstream experiments (Figure 4.6A). *PF-2,* an *E. coli*-targeting virulent bacteriophage, did not display any sensitivity to H_2O_2 as determined by consistent PFU/mL over the course of the experiment regardless of H_2O_2 concentration (Figure 4.6B). These findings lead us to conclude that *PF-2* bacteriophage particles were less sensitive to hydrogen peroxide-induced oxidative stress than their bacterial hosts and were still able to infect host cells after H_2O_2 exposure.

Reactive oxygen species negatively impacts PF-2's adsorption efficiency

To assess the effects of reactive oxygen species on *PF-2*'s ability to adsorb, we performed a series of adsorption constant determination assays in the presence of varying concentrations of H_2O_2. In control samples, *PF-2* displayed an average adsorption slope of -4.456 over the course of 7.5 minutes (Table 4.1). This describes the acceleration of the loss of free bacteriophage in the culture as they undergo reversible and irreversible adsorption to bacterial host. From this, we were able to determine that the adsorption constant (*k)* of *PF-2* is 1.7290×10^{-7} mL/min (Table 4.1). The adsorption constant describes the likelihood of a single bacteriophage adsorbing to a single bacterium within a defined volume and time. A higher adsorption constant relates to a faster overall adsorption rate. *PF-2* displayed relatively rapid adsorption speed with approximately 30% of the bacteriophage adsorbing within 7.5 minutes (Figure 4.7).

Low concentrations of H_2O_2 caused a significant delay in adsorption as indicated by a significant slope incline following 0.5mM H_2O_2 treatment (Figure 4.7A; Table 4.1). Though not significant, 1mM H_2O_2 treatment was similar to 0.5mM treatment in having an adsorption slope

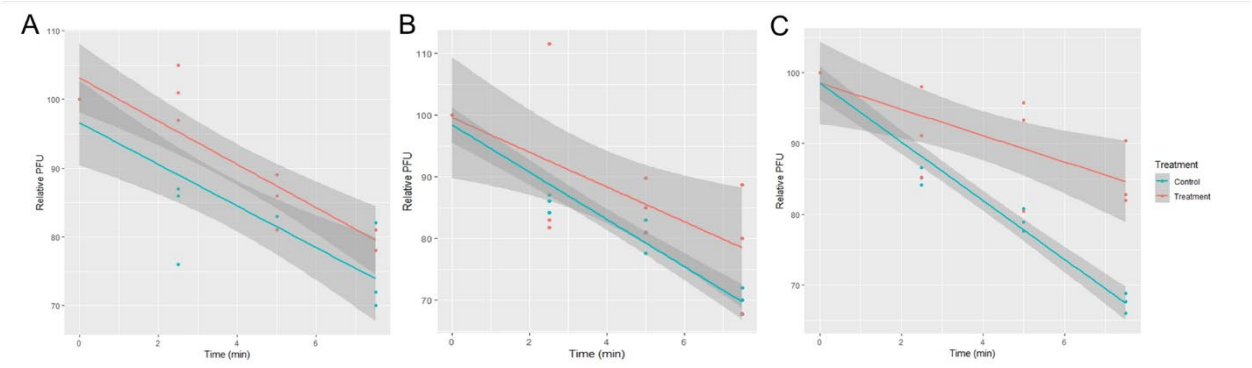

Figure 4.7. Dose-dependent effect of hydrogen peroxide on adsorption kinetics over time. Free bacteriophage estimate following hydrogen peroxide (H_2O_2) treatment at a concentration of (a) 0.5mM, (b) 1mM and (c) 2mM on cultures of bacteria:bacteriophage. Detailed quantification of slope, *k* and p-value are outlined in Table 4.1. * $p < 0.05$; ** $p < 0.01$; *** $p < 0.001$.

Table 4.1. Adsorption Efficiency following Hydrogen Peroxide Treatment

Treatment	Difference in Slopes	*k*	p-value
Control	Mean slope: - 4.456	1.7290×10^{-7} mL/min	
0.5mM H_2O_2	+ 1.175	1.2588×10^{-7} mL/min	0.022*
1mM H_2O_2	+ 1.007	1.1401×10^{-7} mL/min	0.154
2mM H_2O_2	+ 2.464	7.4320×10^{-8} mL/min	0.004**

that was approximately elevated by 1 (Figure 4.7B; Table 4.1). The adsorption constant, or *k,* of 0.5mM and 1mM treatment samples did not differ greatly from those seen in control samples. Higher concentrations of H_2O_2 significantly delayed the adsorption of *PF-2.* Adsorption slopes of 2mM H_2O_2 treatments showed a significant incline in the slope as compared to control samples (Figure 4.7C; Table 4.1). Additionally, the *k* was 10-fold less than control adsorption constant results. Taken together, these results indicate H_2O_2 induces a delay in adsorption of *PF-2* in a dose-dependent manner.

Hydrogen peroxide disrupts the overall infectivity cycle of PF-2

To assess the effects of reactive oxygen species on *PF-2*'s overall infectivity cycle, we performed a modified one-step growth curve in the presence of varying concentrations of H_2O_2. *PF-2* displayed a rapid replication cycle as seen in control samples of the one-step growth curve (Figure 4.8A). The primary burst of the control samples was seen starting at the 10-minute post-adsorption. This, combined with the time allotted for adsorption, indicated it took a total of 20 minutes to reach the burst. The latent phase duration of *PF-2* was 14 minutes on average, with the first detectable burst at approximately 20 minutes (Figure 4.8C). Burst estimates were calculated by subtracting free phage estimates prior to the primary burst, from the PFU/mL concentration at the plateau following the primary rise period (~25 minutes post adsorption in controls). This plateau is distinguished from the secondary burst at the following timepoint (~30-minute time point in controls). The mean burst estimates, or the average yield of infectious particles per host cell, of *PF-2* was $1x10^8$ (Figure 4.8B). Similar behavioral traits have been displayed by the *Escherichia* bacteriophage T7 [27]. This supports the idea that *PF-2* is a potent infectious agent of *E. coli.*

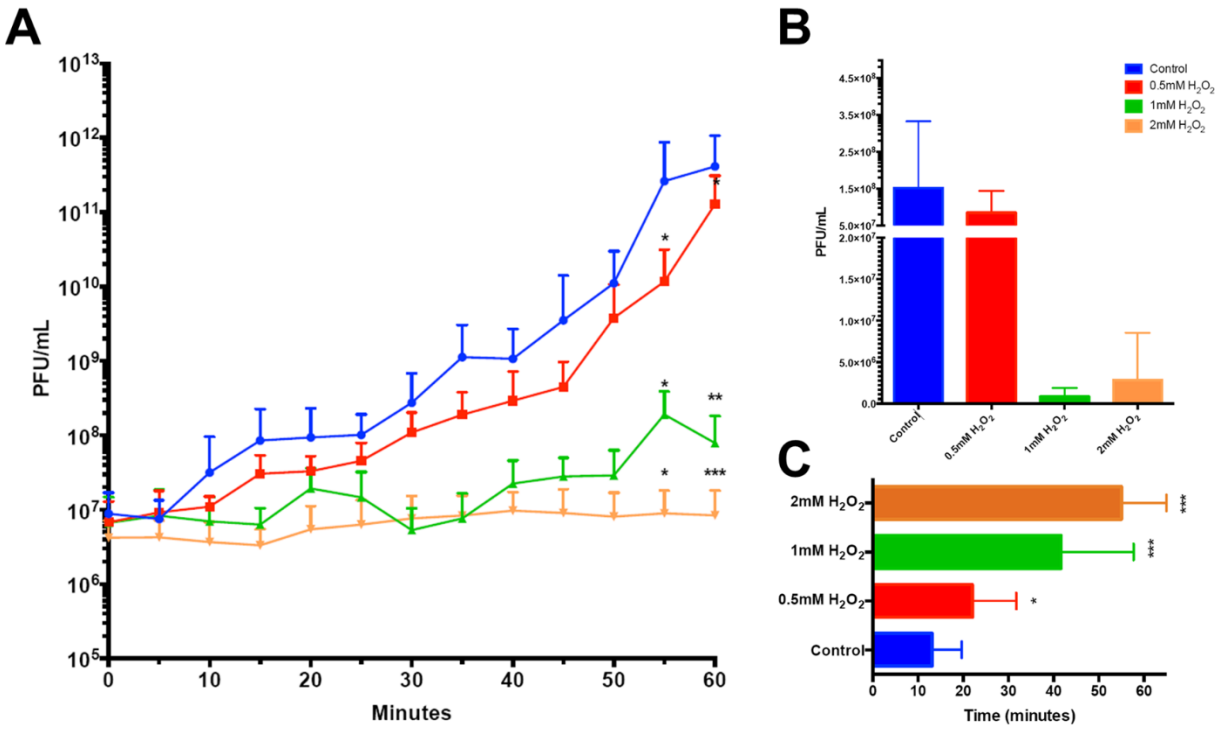

Figure 4.8. Effects of hydrogen peroxide on *PF-2* infectivity rates over time. (a) Impact of hydrogen peroxide (H_2O_2) concentrations on *PF-2* infectivity rates. Starting inoculum was $1x10^6$ PFU/ml; (b) Impact of hydrogen peroxide (H_2O_2) concentrations on burst estimates of *PF-2*; (c) Impact of H_2O_2 concentrations on duration of latent period of *PF-2*. * $p < 0.05$; ** $p < 0.01$; *** $p < 0.001$.

Similar to the adsorption kinetic results, we observed a dose-dependent effect on *PF-2* infectivity rates (Figure 4.8). Low concentrations of H_2O_2 (0.5mM) did not greatly disrupt the ability of *PF-2* to replicate. While the latent period duration was significantly increased to an average of 20 minutes by H_2O_2, this was not enough to significantly reduce burst estimates or delay further progeny production (Figure 4.8A and B). Significant differences in PFU/mL concentrations were not detected until 55 minutes post-adsorption. *PF-2* displayed a significant reduction in their overall infectivity cycle in the presence of 1mM and 2mM H_2O_2 concentrations. Both 1mM and 2mM H_2O_2 concentrations significantly impaired latent period duration of *PF-2* (Figure 4.8C) ($p \leq 0.001$). In fact, some replicates of the 2mM treatment did not demonstrate a primary burst during 60-minute experiment. Strikingly, these treatments induced a prolonged latent period duration (Figure 4.8C), and the estimated burst were 10-fold less than estimates of control and 0.5mM samples (Figure 4.8B). Reduction of progeny production, as measured by PFU/mL concentrations, was detectable over the course of the experiment for 1mM and 2mM H_2O_2 treated samples, even though significant differences were not detectable until the 55-minute post-adsorption (Figure 4.8A). Taken together, hydrogen peroxide does not seem to damage or kill PF-2 directly, but increased dosage of hydrogen peroxide delays progeny production. At high doses of hydrogen peroxide, progeny production is likely delayed due to damage of its host, *E. coli.*

Reactive chlorine delays adsorption but does not interrupt the progeny production of PF-2

Neutrophils not only produce reactive oxygen species as a result of oxidative burst, but they also produce reactive chlorine species following release of myeloperoxidase. With this in mind, we also sought to describe effects the of hypochlorous acid (HOCl) on the infection

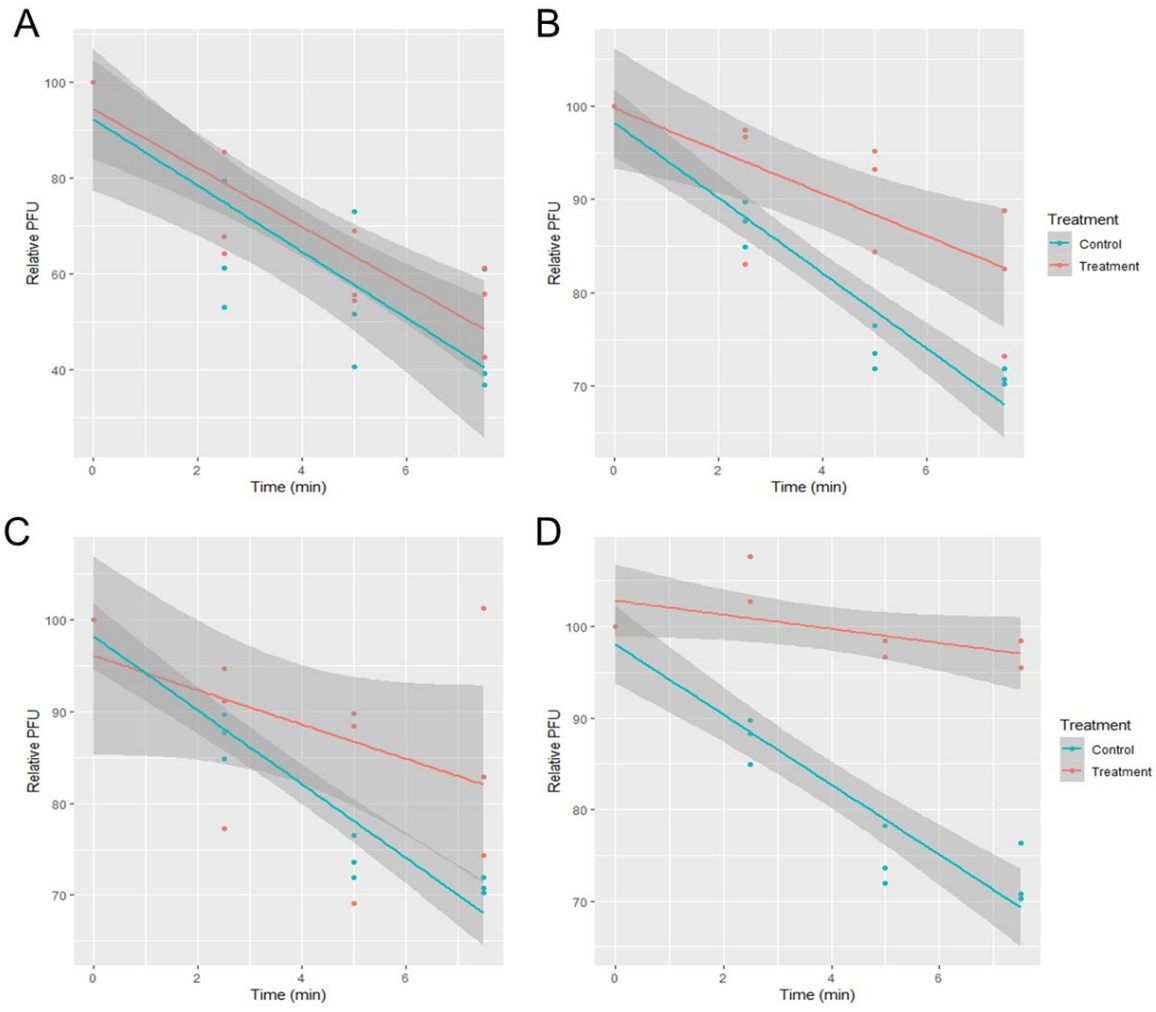

Figure 4.9. Dose-dependent effect of hypochlorous acid on adsorption kinetics over time. Free bacteriophage estimate following hypochlorous acid (HOCl) treatment at a concentration of (a) 0.2mg/L, (b) 0.4mg/L, (c) 0.6gm/L and (d) 1mg/L on cultures of bacteria:bacteriophage. Detailed quantification of slope, *k* and p-value are outlined in Table 4.2. * $p < 0.05$; ** $p < 0.01$; *** $p < 0.001$.

Table 4.2. Adsorption Efficiency following Hypochlorous Acid Treatment

Treatment	Difference in Slopes	*k*	p-value
Control	Mean slope: - 4.456	1.8053×10^{-7} mL/min	
0.2mg/L HOCl	+ 0.772	2.4850×10^{-7} mL/min	0.377
0.4mg/L HOCl	+ 1.742	9.2222×10^{-8} mL/min	0.007 **
0.6mg/L HOCl	+ 2.147	7.5810×10^{-8} mL/min	0.204
1mg/L HOCl	+ 3.053	3.1297×10^{-8} mL/min	0.001 **

efficiency of *PF-2*. Similar to reports of H_2O_2, HOCl did not appear to destroy or damage *PF-2* bacteriophage particles directly, as there was not a detectable reduction of viable *PF-2* particles over the course of the experiment regardless of treatment. Additionally, bacteriophage were able to infect host bacteria following treatment regardless of duration in specified concentration (data not shown). Though not directly damaged by HOCl, *PF-2* did prove to be less efficient in its ability to adsorb in increasing concentrations of HOCl (Figure 4.9). 0.2 mg/L HOCl treatment did not result in significant differences in *k* or slope (Figure 4.9A; Table 4.2). For other concentrations of HOCl, we observed a dose-dependent increase in the adsorption slope by approximately 1 between each treatment as compared to the control, with significant differences for 0.4 mg/L and 1 mg/L HOCl treatment (Figure 4.9B, C, D; Table 4.2). Elevation in slope resulted in a lower *k* for 0.4 mg/L, 0.6 mg/L and 1 mg/L HOCl treatment groups (Table 4.2). These results lead us to conclude that HOCl treatment reduces the adsorption efficiency of *PF-2* in a dose-dependent manner.

Although HOCl negatively impacted *PF-2's* ability to adsorb, this did not translate into negative effects on downstream progeny production. Control samples displayed similar trends consistent with the characterized infectivity cycle of *PF-2*. Surprisingly, 0.6mg/L did not prove to have a major effect on *PF-2's* ability to produce progeny (Figure 4.10). Over the course of the 60 minutes, we did not detect any significant difference between 0.6 mg/L HOCl treatment and control samples (Figure 4.10A), nor were there detectable differences in burst estimates (Figure 4.10B) or the latent period duration (Figure 4.10C). The one-step growth curve in these experiments aimed to evaluate the infectivity cycle following adsorption. This would simulate bacterial stress occurring after adsorption. With the understanding that HOCl treatment

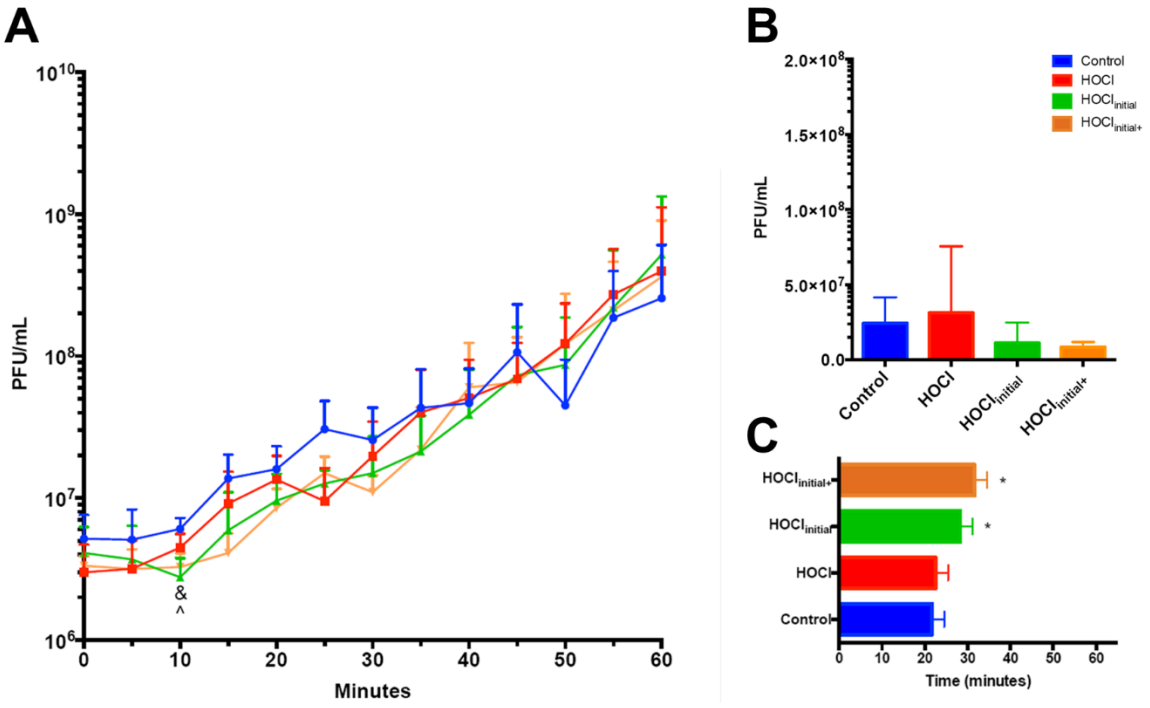

Figure 4.10. Effects of 0.6mg/L hypochlorous acid treatment on *PF-2* infectivity rates over time. (a) Impact of HOCl concentrations on *PF-2* infectivity rates including two treatments that receive dosing prior at the start of the adsorption period. Starting inoculum was $1x10^6$ PFU/ml; (b) Impact of 0.6mg/L HOCl on burst estimates of *PF-2*; (c) Impact of 0.6mg/L HOCl treatment on the duration of latent period of *PF-2*. * describes statistical difference between the control and HOCl treatments while & and ^ describe statistical difference of $HOCl_{initial}$ and $HOCl_{initial+}$, respectively, from control samples. *$p < 0.05$; ** $p < 0.01$; *** $p < 0.001$.

negatively affected adsorption efficiency (Figure 4.9C), we added two additional treatment groups to describe the effect of HOCl treatment during adsorption on progeny production. We detected a significant difference at the 10-minute time point for $HOCl_{initial}$ and $HOCl_{initial+}$ treatments (Figure 4.10A). This is likely explained by the significant, 5-minute delay in the latent period of the $HOCl_{initial}$ or $HOCl_{initial+}$ samples, followed by a burst at the 20-minute time point that is comparable control samples (Figure 4.10C). There was also a slight reduction in estimated burst size following $HOCl_{initial}$ or $HOCl_{initial+}$ treatments, however, these were not significantly different from the control (Figure 4.10B). At 25 minutes, $HOCl_{initial}$ and $HOCl_{initial+}$ treatments showed a reduction in PFU/mL estimates, but this again is likely due to the slight delay of the primary burst, as the following time points for these samples were comparable to bacteriophage abundances seen in control samples (Figure 4.10A). Under 0.6mg/L treatment conditions, *PF-2* was able to undergo normal replication regardless of dosing during adsorption ($HOCl_{initial}$), after adsorption (HOCl), or throughout both events ($HOCl_{initial+}$).

For the1mg/L HOCl treatment, we again did not see major deviations of *PF-2's* characterized growth cycle (Figure 4.11A). A significant reduction was observed for HOCl treatments at the final two timepoints regardless of dosing strategy (Figure 4.11A). This may indicate that progeny produced following the primary burst period have a delayed secondary rise due to inefficient adsorption. Significant differences in burst estimates and latent period duration were not observed for any treatment of 1mg/L HOCl (Figure 4.11B and C) as compared to control samples. Under 1.0mg/L treatment conditions, *PF-2* is able to undergo normal replication rates regardless of dosing strategy, but residual effects of HOCl may inhibit replication potential of newly synthesized progeny.

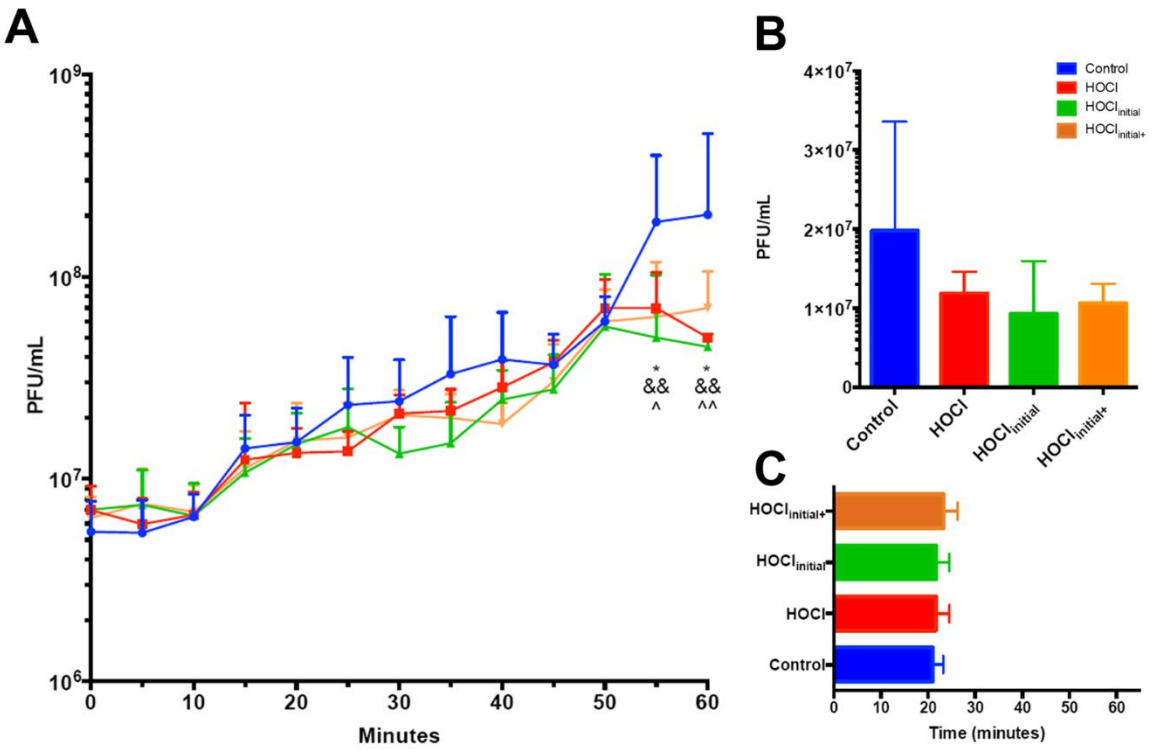

Figure 4.11. Effects of 1mg/L hypochlorous acid treatment on *PF-2* infectivity rates over time. (a) Impact of HOCl concentrations on *PF-2* infectivity rates including two treatments that receive dosing prior at the start of the adsorption period. Starting inoculum was $1x10^6$ PFU; (b) Impact of 1mg/L HOCl on burst estimates of *PF-2*; (c) Impact of 1mg/L HOCl treatment on the duration of latent period of *PF-2*. * describes statistical difference between the control and HOCl treatments while & and ^ describe statistical difference of $HOCl_{initial}$ and $HOCl_{initial+}$, respectively, from control samples. * $p < 0.05$; ** $p < 0.01$; *** $p < 0.001$.

Discussion

Here we describe the infectivity rates of an enteric virulent bacteriophage, *PF-2,* and characterize the effects of reactive chlorine and oxygen species on the efficiency of virulent bacteriophage infection. Although *PF-2* was not damaged directly, both reactants elicited elevations in slopes of adsorption indicating delayed and inefficient adsorption. For hydrogen peroxide, delayed adsorption coincides with reductions in progeny production and increased latent period duration. Hypochlorous acid did not prove to greatly alter the infectivity potential of *PF-2* regardless of inefficient adsorption indicated by a lower *k* in comparable concentrations. When HOCl treatment was administered pre-adsorption, we did see a significant delay in the latent period, but this did not appear to alter progeny production. Taken together, reactive oxygen and chlorine species have shown to reduce adsorption efficiency of *PF-2*. Hydrogen peroxide treatment also greatly reduces replication rates of this virulent bacteriophage in elevated concentrations. Overall, immune-derived antimicrobial agents have the potential to alter infectivity efficiency of virulent bacteriophage.

We undertook the task of addressing these questions with a use of a bacteriophage isolate from porcine fecal samples. We felt that using an intestinal isolate may give better descriptions of mammalian host effects during intestinal inflammation on bacteria:bacteriophage dynamics within the intestinal microbiome than a lab strain. This particular isolate, *PF-2,* proved to be resilient in the presence of hydrogen peroxide and hypochlorous acid exclusively. However, contrasting responses in downstream reproduction efficiency speaks to the dependency on the bacterial host. These studies were performed on one bacteriophage:host relationship and may not explain events that occur within the dynamic environment of the intestinal microbiome. Future investigations could explore these responses in co-cultures of multiple bacterial isolates and

bacteriophage to simulate the nature of community involvement in bacteriophage efficiency during events of stress, similar to the microbiome environment during intestinal inflammation.

Bacterial adaptability to the presence of hydrogen peroxide has been extensively studied [12,29,30]. From this, we know exposure of low concentrations of hydrogen peroxide lead to the induction of cellular defense mechanisms in exponentially growing cells under the control of transcriptional activator, OxyR [12]. These strategies aim to protect against the most common effects of hydrogen peroxide. Hydrogen peroxide resistance is also one of the many functions encoded under the control of *rpoS,* which enables bacteria to survive starvation [12]. *PF-2* did not prove to have adequate replication efficiency using static bacterial host cultures in stationary phase. Therefore, we utilized exponentially growing cells which would allow us to assess the full effects of similar mechanisms on bacteriophage infectivity following oxidative burst. Quantification of bacterial stress response induction was not measured in these experiments. Future experimentation will benefit from the correlation between induction of stress response genes with bacteriophage reproduction efficiency during inflammation-induced stress.

In bacteria, stress responses to external stressors, such as those triggered by DNA damage, lead to activation of the lytic-lysogenic switch, such as in the case of *Escherichia bacteriophage Lambda* [16,29,31]. In this study, we describe the adverse effect of hydrogen peroxide on *PF-2* progeny production [16]. The effects of high concentrations of H_2O_2 were apparent as early as the eclipse phase of the growth cycle. It is possible the elevation of bacteriophage diversity seen in microbiome samples of IBD patients [3,5] could be due to a combination of free phage particles released following induction of prophage, and free virulent bacteriophage that are unable to infect their host shortly after hydrogen peroxide exposure.

Similar mechanisms that confer resistance to hydrogen peroxide are utilized in protection against hypochlorous acid stress [12]. Resistance to hypochlorous acid damage in *E. coli* is largely mediated by genes that are upregulated during oxidative conditions [30]. Myeloperoxidase-catalyzed peroxidation of chloride ions during inflammatory responses induces *rpoS*- and *oxyR*-governed adaptive responses to protect against hypochlorous acid stress [12]. This is likely due to the fact that hypochlorous acid and hydrogen peroxide can generate common deleterious reactive oxygen species, such as hydroxyl radicals, that act to damage DNA [12]. However, hypochlorous acid does not readily diffuse across bacterial cell membranes like hydrogen peroxide [12]. Regardless, hypochlorous acid is considered a nonselective oxidant that reacts avidly with a variety of cellular components, and negatively affects metabolic processes of bacterial cells [12]. At low concentrations, hypochlorous acid has a more bacteriostatic effect, as it rapidly acts to inhibit cell division [12]. The low concentrations used in our study did seem to negatively affect efficiency of adsorption. Interestingly, hypochlorous acid treatment following adsorption had essentially no effect on ability of *PF-2* to produce viable progeny. It is possible that hypochlorous acid induces oxidative damage of cell surface receptors needed for adsorption. With the additional understanding that hypochlorous acid does not readily diffuse across the membrane, bacteriophage are likely not exposed to oxidative conditions at low concentrations of hypochlorous acid following adsorption. The mechanism behind reduced growth levels in higher doses of HOCl will require further investigation. Additionally, more descriptive investigations of receptor damage and bacteriophage adsorption efficiency could give insight as to what cell surface receptors may be responsible for less efficient adsorption of *PF-2*.

Understanding bacteriophage biology in the context of the inflammatory environment can enhance our understanding of bacteriophage therapy efficiency, as well as provide mechanistic

explanations to elevation in bacteriophage abundance during intestinal inflammation [5]. The varying responses of these two reactants that induce similar bacterial responses calls for more investigations into the mechanistic characterization of bacteriophage infection in the context of inflammation. In this same context, bacteriophage therapy may be less efficient during early onset inflammation due to the high influx of neutrophils and their products, namely reactive oxygen species. Alternatively, other immune compounds, like hypochlorous acid, can act in conjunction with bacteriophage to stagnate bacterial abundance while bacteriophage lyse host cells following completion of infection. With the surge of antibiotic resistance within recent years, researchers are embracing the idea of utilizing bacteriophage as therapy for bacterial infections. Our work provides context to virulent bacteriophage infection potential during inflammation-induced bacterial stress. Future work in bacteriophage therapy could look at effect of other immune-derived products and their effects on bacteriophage therapy efficiency to further elucidate bacteriophage behavior in inflammatory environments.

References

1. Ofir, G. & Sorek, R. Contemporary Phage Biology: From Classic Models to New Insights. Cell (2018) doi:10.1016/j.cell.2017.10.045.

2. Lopetuso, L. R., Ianiro, G., Scaldaferri, F., Cammarota, G. & Gasbarrini, A. Gut Virome and Inflammatory Bowel Disease. Inflamm. Bowel Dis. 22, 1708–1712 (2016).

3. Manrique, P. et al. Healthy human gut phageome. Proc. Natl. Acad. Sci. U. S. A. 113, 10400–10405 (2016).

4. Howe, A. et al. Divergent responses of viral and bacterial communities in the gut microbiome to dietary disturbances in mice. ISME J. 10, 1217–1227 (2016).

5. Norman, J. M. et al. Disease-specific alterations in the enteric virome in inflammatory bowel disease. Cell 160, 447–60 (2015).

6. Chang, J. Y. et al. Decreased Diversity of the Fecal Microbiome in Recurrent Clostridium difficile –Associated Diarrhea. J. Infect. Dis. 197, 435–438 (2008).

7. Barr, J. J., Youle, M. & Rohwer, F. Innate and acquired bacteriophage-mediated immunity. Bacteriophage 3, e25857 (2013).

8. Ryan, G. B. & Majno, G. Acute inflammation. A review. Am. J. Pathol. 86, 183–276 (1977).

9. Knowles, B. et al. Lytic to temperate switching of viral communities. Nature (2016) doi:10.1038/nature17193.

10. Hurst, J. K., Barrette, W. C., Michel, B. R. & Rosen, H. Hypochlorous acid and myeloperoxidase-catalyzed oxidation of iron-sulfur clusters in bacterial respiratory dehydrogenases. Eur. J. Biochem. 202, 1275–82 (1991).

11. De Oliveira, S., Rosowski, E. E. & Huttenlocher, A. Neutrophil migration in infection and wound repair: Going forward in reverse. Nature Reviews Immunology vol. 16 378–391 (2016).

12. Dukan, S., Danie`, D. & Touati, D. Hypochlorous Acid Stress in Escherichia coli: Resistance, DNA Damage, and Comparison with Hydrogen Peroxide Stress. JOURNAL OF BACTERIOLOGY vol. 178 http://jb.asm.org/ (1996).

13. Ron, E. Z. Bacterial Stress Response. in The Prokaryotes 1012–1027 (Springer New York, 2006). doi:10.1007/0-387-30742-7_32.

14. Wilson, B. A., Salyers, A. A., Whitt, D. D. & Winkler, M. E. Bacterial Pathogenesis. Bacterial Pathogenesis (American Society of Microbiology, 2011). doi:10.1128/9781555816162.

15. Bacterial Stress Responses, Second Edition. Bacterial Stress Responses, Second Edition (American Society of Microbiology, 2011). doi:10.1128/9781555816841.

16. Howard-Varona, C., Hargreaves, K. R., Abedon, S. T. & Sullivan, M. B. Lysogeny in nature: Mechanisms, impact and ecology of temperate phages. ISME Journal (2017) doi:10.1038/ismej.2017.16.

17. Hsu, B. B. et al. Dynamic Modulation of the Gut Microbiota and Metabolome by Bacteriophages in a Mouse Model. Cell Host Microbe 25, 803-814.e5 (2019).

18. Gogokhia, L. et al. Expansion of Bacteriophages Is Linked to Aggravated Intestinal Inflammation and Colitis. Cell Host Microbe 25, 285-299.e8 (2019).

19. Appelmans, R. Le dosage du bactériophage. Compt Rend Soc Biol 85, 701 (1921).

20. Weber-Dabrowska, B., Zimecki, M., Mulczyk, M. & Górski, A. Effect of phage therapy on the turnover and function of peripheral neutrophils. FEMS Immunol. Med. Microbiol. 34, 135–8 (2002).

21. Barr, J. J. et al. Bacteriophage adhering to mucus provide a non–host-derived immunity. Proc. Natl. Acad. Sci. 110, 10771–10776 (2013).

22. One step multiplication curve for bacteriophages. – Biotech Khan. https://biotechkhan.wordpress.com/2014/07/01/one-step-multiplication-curve-for-bacteriophages/.

23. One step multiplication curve for bacteriophages. – Biotech Khan. https://biotechkhan.wordpress.com/2014/07/01/one-step-multiplication-curve-for-bacteriophages/.

24. Clokie, M. R. J., Kropinski, A. M. (Andrew M. B. & Lavigne, R. Bacteriophages : methods and protocols.

25. Hu, B., Margolin, W., Molineux, I. J. & Liu, J. The bacteriophage T7 virion undergoes extensive structural remodeling during infection. Science (80-.). 339, 576–579 (2013).

26. McKenna, S. M. & Davies, K. J. A. The inhibition of bacterial growth by hypochlorous acid. Possible role in the bactericidal activity of phagocytes. Biochem. J. 254, 685–692 (1988).

27. Storms, Z. J., Smith, L., Sauvageau, D. & Cooper, D. G. Modeling bacteriophage attachment using adsorption efficiency. Biochem. Eng. J. 64, 22–29 (2012).

28. Jun, J. W. et al. Bacteriophage application to control the contaminated water with Shigella. Sci. Rep. 6, 22636 (2016).

29. Selva, L. et al. Killing niche competitors by remote-control bacteriophage induction. Proc. Natl. Acad. Sci. U. S. A. 106, 1234–1238 (2009).

30. Yamamoto, N. Damage, repair, and recombination. II. Effect of hydrogen peroxide on the bacteriophage genome. Virology 38, 457–463 (1969).

31. Nanda, A. M. et al. Analysis of SOS-induced spontaneous prophage induction in Corynebacterium glutamicum at the single-cell level. J. Bacteriol. 196, 180–188 (2014).

Chapter 5

Discussion and Conclusion

Summary of Work

In this dissertation, I have described the dynamics of enteric bacteriophage interactions with their hosts and their ability to adapt to environmental stimuli. We demonstrated that WD-feeding adversely effects the systemic metabolic profile and the intestinal microbiome. We also described dynamic alterations to the composition of the intestinal microbiota as early as 2 days post WD-feeding. Furthermore, fluctuations in the phageome occurred rapidly post WD-feeding, often preceding changes in abundance of their bacterial host. After 12-weeks of WD-feeding, constituents of the enteric microbiome, namely bacteria and bacteriophages, showed distinct correlation patterns between microbiome constituents and the metabolic phenotype, which allowed us to distinguish between a healthy microbiome and one more typical of obesity. We also noted significant differences in the composition of microbial communities within the intestinal microbiome, which is consistent with previous reports [1–4].

The western diet induces alterations of the intestinal microbiome that coincides with metabolic dysregulation of the mammalian host.

It has well been established that bacterial components of the intestinal microbiome undergo alterations in community composition following diet change [1,2,5]. Recent reports have also implicated diet change in inducing bacteriophage community modulation [3,4]. One such previous study demonstrated contrasting viral communities between individuals on a low-fat

versus a milk-fat diet [3]. In this study, mice microbiome samples were characterized in a 6-week diet perturbation study in response to low-fat and milk-fat diet. The researcher utilized a milk-fat diet, due to the high-refined sugar content which made it a close approximation of western diet consumption [3]. They characterized dissimilarity in community composition of virus-like particles using an nMDS ordination plot. Similar to this study, our findings support the notion that the host's diet can induce modulation of the microbiome, including both bacteria and bacteriophage populations. Many analytical strategies used throughout this dissertation have provided evidence that alterations in bacteriophage community structure tends to coincide with abundance changes of the putative host. For example, as Streptococcaceae began to bloom following WD feeding, we also saw a reciprocal increase in the abundance of *P335-like viruses'* a phage known to prey on this group of bacteria [6–8]. Alterations of bacteriophage abundance in the microbiome following diet change could be attributed to bacteriophage replication rates being much faster than that of host bacteria [9]. One bacteriophage can give rise to hundreds of new virions within one host cell where bacteria typically produce one daughter cell per replication cycle [9,10]. Not only do bacteriophage produce a larger fraction of progeny per replication cycle, but they also require far less resources for reproduction than bacteria as many of these are supplied by the host [11]. Should an opportunity arise, bacteriophage are thought to exploit blooms of viable host bacteria, such as those that occur following nutrient oscillations [11–14]. Thus, a modest increase in abundance of host bacteria could result in rapid bacteriophage progeny production. In this way, bacteriophage could curb potential unwanted blooms of opportunistic pathogens or organisms implicated in inflammatory disease, potentially stabilizing the overall microbiome.

Unique dynamics of bacteriophage during microbiome modulation

In a more in-depth analysis of this relationship (Chapter 3), we further explore the influence of WD-feeding on the modulation of bacteriophage communities in relation to host bacteria populations. Community structure of the gut microbiota within our chow diet animals revealed a high connectivity between many bacterial constituents. The bacterial communities within the chow diet were more closely associated with other community clusters and appeared to dominate the central community as depicted by Figure 3.1. WD microbiome network structure had a higher modularity, denoted by more distance between community clusters, than the chow diet. Distances observed between community modules on the WD suggest that the WD may lead to a loss in microbial community collaboration and metabolic proficiency of the intestinal microbiome. Additionally, bacteriophage genera in WD samples appeared to play a more integral role in the intestinal microbiome as compared to chow samples. Many bacteriophage genera were shown to locate more centrally on the network analysis plots of WD samples and displayed a higher degree of connectivity within the WD microbiome. These results indicate that bacteriophage communities impact more components of the intestinal microbiome than just their host, results consistent with similar finding in the literature [11,15–17]. Hsu, *et al.* conducted experiments using gnotobiotic mice (germ-free mice that are colonized with a defined set of microorganisms) to monitor the influence of bacteriophage predation on bacterial community stability within the intestinal microbiome. The results showed that bacteriophage can coexist overtime with targeted gut bacteria, which aligns with bacteriophage predation models [12–15] as well as results from the chow microbiome samples in our study. Many investigations have established that bacteriophage have the potential to modulate host bacterial abundance [11,18–20], but recent findings also suggest that bacteriophage predation on one particular host bacteria can

induce a cascade of alterations in microbial communities, namely the intestinal microbiome [15]. The bacteriophage-induced community modulation was also accompanied with significant alteration to the metabolite profile of the intestinal microbiome [15]. Our findings support these ideas and describe how bacteriophage populations can contribute to the overall community structure. Complementary results from chapters 2 and 3 support the idea that the WD induces dissimilarity in microbiome composition from their chow counterparts. Furthermore, the alterations of microbial populations are accompanied by bacteriophage occupying a more central role in the in the overall community structure of the gut microbiome in the WD as compared to the chow diet.

The relative abundance of bacterial families and bacteriophage genera in our study did not greatly vary from baseline levels in chow samples and bacteria:bacteriophage dynamics were generally synchronized. Temperate bacteriophage, regardless of diet, tended to correlate closely with the abundance patterns of their putative host family. This makes sense, as temperate bacteriophage are said to prefer to be integrated as prophage during the exponential growth phase of their host bacteria, also known as piggyback-the-winner [13,14,21]. Under steady state conditions, some spontaneous induction does occur in microbial environments which serves to perpetuate bacteriophage replication, provide genetic information transfer among bacteria within the microbiome, or to kill off related bacterial competitors [11,14,21–25]. Under stress-inducing conditions, temperate bacteriophage have demonstrated the ability to switch from lysogenic to lytic cycles in response to the bacterial host stress-induced SOS response [23,26,27]. It has been proposed that temperate bacteriophage have developed this mechanism in an effort to allow for their survival in the event of host cell death [26,27]. More recent investigations also described communication among bacteriophage that act to coordinate these lytic-lysogenic decision [28]. In

this study, the authors report that the temperate *Bacillus bacteriophage phi3T* relies on a small communication molecule, termed *arbitrium* molecule, to unanimously execute lysis-lysogeny [28]. Models such as these may provide explanation for bacteriophage lifestyle decisions in microbial communities, and potential mechanisms of a bacteriophage's ability to control bacterial communities. In the current study, we described rapid increases in *Staphylococcus phage EW* and *Streptococcus phage Tuc2009* abundance in response to comparably marginal host blooms. In these bacteriophage species, there is potentially a combination of piggyback-the-winner and lytic switching in response to some abundance threshold being reached in the host. In contrast, *Enterococcus phage phiFL4A* showed close correlations with host replication and abundance patterns, which is likely explained solely by piggyback-the-winner dynamics.

Virulent bacteriophage behavior was not as dynamic in the Chow samples as compared to WD microbiome samples. Similarly, the kill-the-winner model describes that there is not much predation during steady-state conditions, and this preserves the diversity of bacteriophages and bacteria [12]. In Chapter 2, we found microbiome samples of mice on the basal chow diet had consistent bacterial and bacteriophage diversity and evenness rankings, while WD samples revealed a temporal decline in these metrics over the course of 12-week experiment. Furthermore, virulent bacteriophage behavior did not always follow the classic bacteriophage models following WD feeding [12,29,30]. Traditional models of virulent behavior, such as the kill-the-winner dynamic, would predict an increase in bacteriophage abundance alongside or following a bloom in targeted bacterial host populations [12,29,30]. A seemingly small bloom of bacteria could give rise to an exponentially larger production of bacteriophage for reasons described previously [11,20]. In the event that bacterial species bloom to a particular threshold, bacteriophage can prevent any single bacterial species from overtaking the whole microbial

community [12]. In this way, bacteriophage could curve potential unwanted blooms of organisms, such as opportunistic pathogens and those who promote disease states, as to contribute to overall stability of the microbiome. Our studies support the kill-the-winner model of virulent bacteriophage species in chow microbiome samples. We did note an increase in many bacteria and the virulent bacteriophage that target them in the chow samples at the final timepoint of the study. Future investigations could extend the duration of the experiment to see if these results point to a cyclical ebb and flow as is described in previously mentioned bacteriophage behavioral models [12,14,29,30]. Similarly, in line with these models, we described significant elevations of virulent bacteriophage species targeting *Lactococcus* following elevations in host abundance in WD microbiome samples. In the context of log-fold change, it appears that bacteriophage experienced more rapid and elevated abundance increases in response to WD feeding. Development of more sensitive sampling strategies will be needed to provide the necessary evidence of the mechanisms and timeline of predator-prey dynamics in response to environmental stimuli. Where these interactions are expected based on information outlined in the literature [12,14,29,30], some *Lactococcus*-targeting bacteriophage demonstrated divergent abundance patterns from *Lactococcus* following WD feeding, namely *Lactococcus phage 1706.* Investigative procedures used in our studies did not explain why this phenomenon occurred. It is possible that *Lactococcus phage 1706* did not benefit from the bloom in *Lactococcus* following WD feeding because either it targeted another unclassified bacterial host, it was unable to successfully infect *Lactococcus* under these environmental conditions, or *Lactococcus* was not susceptible to this bacteriophage due to bacterial evolution or gene upregulation following nutrient availability [31,32]. Taken together, these findings provide evidence that bacteriophage do

not always follow patterns of their host, and this may be exacerbated during microbial adaptation to environmental stimuli.

The impact of the bacterial stress response on reproduction efficiency of virulent bacteriophage

One stimulus that could greatly affect microbial prevalence is the inflammatory environment created by immune cell activation. In Chapter 4, I described the infectivity rates of an enteric bacteriophage isolate, *PF-2,* and demonstrated the effects of reactive chlorine and oxygen species on its infectivity potential. Although *PF-2* was not damaged directly, both reactants elicited delayed or inefficient adsorption to its host, *Escherichia coli*. In the case of hydrogen peroxide treatment, not only was adsorption delayed, but there was also a prolonged latent period with a reduction in overall progeny produced. Bacteria utilize similar resistance mechanisms to survive hydrogen peroxide and hypochlorous acid exposure [33,34]. During exponential phase, the adaptive response to H_2O_2 in bacteria is mediated by the induction of the oxyR regulon [33,35]. Protection against HOCl exposure has also linked to induction of oxyR regulon [33]. Although the specific genes involved in the oxyR-dependent resistance have not be identified, differential gene expression of *katG, ahp*, and *dps* were experienced between H_2O_2 and HOCl samples [33]. Yet, hypochlorous acid did not prove to greatly alter the infectivity potential of *PF-2*, regardless of lower *k* in comparable dose concentrations. Both hydrogen peroxide and hypochlorous acid have been implicated in facilitating production of harmful oxidative species which can act to damage DNA [33,35,36]. At low concentrations, hypochlorous acid is more of a bacteriostatic agent, as it rapidly acts to inhibit cell division [33,36]. Interestingly, hypochlorous acid treatment following adsorption had essentially no effect on ability of *PF-2* to produce viable progeny. It is possible that hypochlorous acid induces oxidative damage of cell

surface receptors needed for adsorption which results in delayed adsorption efficiency, but this does not appear to negatively affect downstream progeny production at these concentrations. With the additional understanding that hypochlorous acid does not readily diffuse across the membrane [33,36], bacteriophage are likely not exposed to oxidative damage within the host following administration of a low dose of hypochlorous acid. Overall, immune-derived antimicrobial agents have the potential to alter infectivity efficiency in virulent bacteriophage which could result in ineffective bacteriophage treatment during initiation of inflammation.

Implications of these findings

These studies explore bacteriophage dynamics under various environmental stimuli and provide evidence that bacteriophage are integral members of microbial environments, especially in the context of dysbiosis. Recent publications have discussed the contribution of bacteriophage in microbial environments, such as the intestinal microbiome [3,15,17]. Temperate bacteriophage, in particular, have been studied in this setting as they have been proven to have an effect on bacterial communities via mediation of horizontal gene transfer, alteration of host gene expression, and providing protection against infection from other bacteriophages [11,13,14]. Thorough investigations of the temperate *Escherichia bacteriophage Lambda* have characterized the lysis-lysogeny decision as a complex, intricate network of transcriptional repressors and activators, as well as other components [11,27,28,37,38]. The prophage monitors the metabolic state of the host, as well as the bacteriophage multiplicity of infection in order to make decisions of when to implement the switch to lytic cycle [11,13,27,28,37]. A recent study examined lysogeny dynamics of *Bacillus* phage phi3T and found that a quorum sensing like mechanisms of small-molecule communication between bacteriophages is used to coordinate lysis-lysogeny decision of

temperate bacteriophage [28]. Media with high concentrations of the communication molecule influenced bacteriophage induction providing evidence that a density threshold of the molecule should be reached to induce lytic cycle activation [28]. Unlike temperate bacteriophage, virulent bacteriophage were not thought to be capable of altering infection cycles in response to environmental stimuli. Virulent bacteriophage are thought to following kill-the-winner dynamics, where virulent bacteriophage benefit from blooming host bacteria [13,20]. In line with these models, we described low variability of temperate and virulent bacteriophage abundance under steady-state conditions and the abundance patterns of bacteriophage populations were in parallel to the temporal dynamics of the bacterial host. Following diet change, we characterized rapid and exaggerated fluctuations of temperate and virulent bacteriophage. In WD samples, virulent bacteriophage typically matched the abundance patterns of the bacterial host, although they experienced greater abundance increases as compared to the host. However, some bacteriophage did not experience this rapid expansion, and were seen to decline in abundance following WD feeding. These findings align with well characterized bacteriophage behavior [11,13,14,29], as well as contradict them such as in the case of *Lactococcus phage 1706.* Furthermore, the integration and interconnectivity of bacteriophage genera in the intestinal microbiome community networks of WD-fed mice provided further evidence of their ability to not only affect host prevalence, but also a vast multitude of mutualistic relationships within the microbiome. This idea has been demonstrated by Hsu, *et al.* where the authors demonstrate the potent cascading effects of bacteriophage administration on the microbiome community structure, and the resulting modulation to the metabolome [20]. In relation to modulation during WD feeding, we demonstrated novel relationships between specific microbiome constituents and pathophysiological metabolic parameters associated with obesity.

The intestinal microbiome has gained much attention in respect to its contributions to mammalian host health. Many studies of the gut microbiome have been focused primarily on bacterial constituents, utilizing16S amplicon sequencing, as these do account for the majority of metabolically relevant organisms in the gut microbiota [1,5,32,39]. 16S amplicon sequencing, although sound technology, is lacking in comparison to shotgun metagenomics due to its limited taxonomic and functional resolution [40]. Primers used in 16S amplicon sequencing can also lead to discordant annotation results [40,41]. Our studies utilized shotgun metagenomic sequencing which allowed for identification other organisms within the microbiome, namely bacteriophage, as well as enhanced resolution of both functional and taxonomic annotations. The intestinal microbiome data was then compared with the metabolic phenotype analysis which allowed us to connect several important aspects of host-microbiome interaction in the context of WD-induced obesity. Not only did we observe changes that are consistent with existing studies of the bacteriome in obesity [1,2,42–44], but also we bring into context changes in the phageome in concert with host metabolic changes. For our study, the distinct advantage of shotgun metagenomics was the ability to characterize bacteriophage population alongside putative bacterial host. However, this does not speak to the vast amount of information that can be obtained from these types of big data sets so long as you have the time and programs to investigate them.

With the surge of antibiotic resistance within recent years, researchers are embracing the idea of utilizing bacteriophage as therapy for bacterial infections. One noted advantage of bacteriophage therapy to traditional antibiotics is their high degree of specificity, reducing off-target impacts on the host's commensal microbiome [18,45,46]. In a similar fashion, bacteriophage could be utilized to cause depletions of certain bacterial constituents in the intestinal microbiome in order to bring about homeostasis during diseases such as colitis or obesity. However, recent

publications discussed here describe the rippling effects of bacteriophage administration that could bring about homeostasis or perpetuate disease states of the enteric microbiome [20]. Potential therapies could be developed by understanding the role bacteriophage play during dysbiosis and applying these lessons to modulate microbial symbionts. Furthermore, bacteriophage communities could act as an indicator population to help proactively diagnose disruption of community structure in the intestinal microbiome.

Bacteriophage therapy can also benefit from characterization of bacteriophage behavior in the context of inflammation. In bacteria, stress responses, such as those triggered by cell DNA damage, lead to activation of the lytic-lysogenic switch that occurs for temperate bacteriophage [35,47,48]. We characterized an enteric bacteriophage isolate's response to immune-derived oxidizing reagents to assess the infectivity potential in the presence of immune stressors. Our work provides context to bacteriophage infection potential during inflammation-induced bacterial stress. Where these findings may have implications for bacteriophage therapy efficiency, we think this investigation also expands the understanding of virulent enteric bacteriophage behavior in an inflammatory environment. Rather than use a lab strain, we used a bacteriophage isolate from a porcine fecal sample to better describe the potential effects of mammalian host-derived inflammatory products on bacteria:bacteriophage dynamics within the intestinal microbiome. This particular isolate, *PF-2*, proved to be resistant to damage from hydrogen peroxide and hypochlorous acid when unaccompanied by their host. However, when bacteriophage were in the presence of their host and immune stressors, differences in replication efficiencies illustrate the potential for differential responses of bacteriophage. We described the damaging effects of hydrogen peroxide and hypochlorous acid on adsorption potential of bacteriophage. However, this did not relate to downstream bacteriophage replication efficiency

for all inflammatory products. Similar studies found that hydrogen peroxide was responsible for inactivation of bacteriophage via damage of nucleic acids, but there was a range of responses among nucleic acid types [34]. In similar concentrations of H_2O_2, inactivation of RNA phage MS2 occurred rapidly, while this phenomenon occurred more slowly for the double-stranded DNA phage P22 [34]. Yet, hydrogen peroxide has been implicated in prophage induction [11,34,48,49]. This may explain the elevated bacteriophage abundance following initiation of inflammation, but it does not speak to the infectivity potential of the progeny. In the context of the intestinal environment, microbiome samples of patients suffering from IBD have been reported as having increase diversity and richness of bacteriophages populations, and this was correlated with a decline in bacterial diversity [16,17]. These results may be due to induction of prophage, but, again, it may not appropriately illustrate the infectivity potential of free bacteriophage. Additionally, bacteriophage administration has shown to induce proliferation of neutrophils which could further perpetuate the phenotype in IBD patients [50]. Taken together, bacteriophage therapy may prove to be less efficient during early onset inflammation due to the accumulation of granulocytes and their products. Alternatively, other immune-derived antimicrobial agents, such as hypochlorous acid, can complement actions of bacteriophage. It is intriguing to think that the action of one enzyme could make a significant difference in the infectivity potential of bacteriophage in an oxidative environment.

Short-comings, Limitations, and Future work

In recent years, there has been a rise in appreciation of the enteric virome. This is due to technological advances in metagenomic sequencing, which has given us a reliable method to examine the complexity within this community. The experimental design of our study allowed us

to follow the abundance patterns of a subset of organisms within the virome, the order Caudovirales, which contains bacteriophage. Of note, our study did not use methods to quantify enveloped viruses or RNA viruses, and there may be much more to learn about these components of the enteric virome, especially in the setting of obesity. We targeted bacteriophages in order to describe the longitudinal shifts in their abundance following diet change as compared to their bacterial host. To do this, we cross-annotated species annotations (70% identity threshold), within the order Caudovirales, from the RefSeq database with the International Committee on Taxonomy of Viruses taxonomic database or other documentation detailing classification of the bacteriophage into respective genera (descriptions of genera present are outlined in Appendix 1).

One limitation of our study pertained to bacteriophage who were not specifically classified to a genus. We did see some change in the relative abundance of those who fell in the unclassified components of our samples but were unable to delve into these relationships. This limitation is consistent among many enteric bacteriophage investigations and can only be overcome by significant expansion of bacteriophage annotations within available databases. Another limitation of our study lies in determining whether a viral annotation was integrated into the genome of the host, or if it was free living, as bacteriophage were not filtered from fecal microbiome samples. To accommodate for this, we attempted to identify the lifestyle characterization of the viral species used to better define the mechanism of abundance change. This limitation of mis-annotation could still exist even in the event that bacterial and viral components are separated prior to DNA extraction. To distinguish bacterial components from integrated prophage will require development of new tools and significant improvement of viral databases.

Limitations in experimental methods or platforms direct the scientific community to develop improved strategies to answer the deeper questions around them. One such strategy could aim to characterize bacteria:bacteriophage dynamics and determine which population, bacteriophage or host, expands first. Different stimuli and development of more sensitive sampling techniques can help reveal the full range of bacteriophage dynamics. More questions remain unanswered in the final study, as this was a newly established model of virulent bacteriophage dynamics. First, we studied a limited range of immune-derived antimicrobial compounds. Effects of a wider range of antimicrobial agents are necessary for more thorough descriptions of bacteriophage behavior and infectivity potential in inflammatory environments. The two reactants, hydrogen peroxide and hypochlorous acid, both resulted in negative effects on adsorption efficiency. Yet, hypochlorous acid did not display many of the negative effects in downstream progeny production. Along these lines, more descriptive investigations of receptor damage and bacteriophage efficiency could give insight as to what cell surface receptors may be responsible for less efficient adsorption of enteric bacteriophage. The varying responses of bacteriophage to two reactants that reportedly induce similar bacterial responses calls for more investigations into the mechanistic characterization of bacteriophage infection during bacterial stress. These studies could also benefit from parallel quantification of bacterial gene expression in order to establish correlations between virulent bacteriophage activity and induction of host stress response in the context of intestinal inflammation. Finally, these studies were performed on one bacteriophage:host relationship, and may not explain events that occur within the dynamic environment of the intestinal microbiome. Future investigations could explore these responses in co-cultures of multiple bacterial isolates and bacteriophage to simulate the nature of

community involvement in bacteriophage efficiency during events of stress, similar to the microbiome environment during intestinal inflammation.

Conclusion

Throughout this collective work, we have characterized the responsive nature of bacteriophage. In early investigations (Chapters 2 and 3), we discussed the responsive nature of bacteriophage to WD-feeding, and their role as integral components of the microbiome. Monitoring abundance patterns of bacteriophage in relation to their host supports the idea that bacteriophage do not solely react to the abundance functions of their host. In the final portion of this work, we expand on these ideas and demonstrate that individual bacteriophage can respond differently to oxidative treatments, even though similar adaptation strategies are utilized by the host. Collectively, these studies provide evidence that bacteriophage are integral members of microbial environments that can respond to environmental stimuli regardless of host effects. The responses of bacteriophage could prove to have greater implications for microbiome modulation and efficiency of bacteriophage therapy.

References

1. Hakkak, R., Korourian, S., Foley, S. L. & Erickson, B. D. Assessment of gut microbiota populations in lean and obese Zucker rats. PLoS One 12, e0181451 (2017).

2. Turnbaugh, P. J. et al. An obesity-associated gut microbiome with increased capacity for energy harvest. Nature 444, 1027–1031 (2006).

3. Howe, A. et al. Divergent responses of viral and bacterial communities in the gut microbiome to dietary disturbances in mice. ISME J. 10, 1217–1227 (2016).

4. Minot, S. et al. The human gut virome: inter-individual variation and dynamic response to diet. Genome Res. 21, 1616–1625 (2011).

5. Turnbaugh, P. J. et al. The effect of diet on the human gut microbiome: a metagenomic analysis in humanized gnotobiotic mice. Sci. Transl. Med. 1, 6ra14 (2009).

6. Samson, J. E. & Moineau, S. Characterization of Lactococcus lactis phage 949 and comparison with other lactococcal phages. Appl. Environ. Microbiol. 76, 6843–52 (2010).

7. Blatny, J. M., Godager, L., Lunde, M. & Nes, I. F. Complete genome sequence of the Lactococcus lactis temperate phage φLC3: comparative analysis of φLC3 and its relatives in lactococci and streptococci. Virology 318, 231–244 (2004).

8. Christiansen, B., Johnsen, M. G., Stenby, E., Vogensen, F. K. & Hammer, K. Characterization of the lactococcal temperate phage TP901-1 and its site-specific integration. J. Bacteriol. 176, 1069–76 (1994).

9. Abedon, S. T. Kinetics of phage-mediated biocontrol of bacteria. Foodborne Pathogens and Disease vol. 6 807–815 (2009).

10. Hyman, P. Bacteriophages and Nanostructured Materials. in Advances in Applied Microbiology vol. 78 55–73 (Academic Press Inc., 2012).

11. Ofir, G. & Sorek, R. Contemporary Phage Biology: From Classic Models to New Insights. Cell (2018) doi:10.1016/j.cell.2017.10.045.

12. Thingstad, T. & Lignell, R. Theoretical models for the control of bacterial growth rate, abundance, diversity and carbon demand. Aquat. Microb. Ecol. 13, 19–27 (1997).

13. Knowles, B. et al. Lytic to temperate switching of viral communities. Nature (2016) doi:10.1038/nature17193.

14. Silveira, C. B. & Rohwer, F. L. Piggyback-the-Winner in host-associated microbial communities. npj Biofilms Microbiomes 2, 16010 (2016).

15. Hsu, B. B. et al. Dynamic Modulation of the Gut Microbiota and Metabolome by Bacteriophages in a Mouse Model. Cell Host Microbe 25, 803-814.e5 (2019).

16. Norman, J. M. et al. Disease-specific alterations in the enteric virome in inflammatory bowel disease. Cell 160, 447–60 (2015).

17. Manrique, P. et al. Healthy human gut phageome. Proc. Natl. Acad. Sci. U. S. A. 113, 10400–10405 (2016).

18. Sybesma, W. et al. Bacteriophages as potential treatment for urinary tract infections. Front. Microbiol. 7, (2016).

19. Ul Haq, I., Chaudhry, W. N., Akhtar, M. N., Andleeb, S. & Qadri, I. Bacteriophages and their implications on future biotechnology: A review. Virology Journal vol. 9 (2012).

20. Hsu, B. B. et al. Dynamic Modulation of the Gut Microbiota and Metabolome by Bacteriophages in a Mouse Model. Cell Host Microbe 25, 803-814.e5 (2019).

21. Lemire, S., Figueroa-Bossi, N. & Bossi, L. Bacteriophage crosstalk: Coordination of prophage induction by Trans-Acting antirepressors. PLoS Genet. 7, e1002149 (2011).

22. Campoy, S. et al. Induction of the SOS response by bacteriophage lytic development in Salmonella enterica. Virology 351, 360–367 (2006).

23. Little, J. W. Chance phenotypic variation. Trends Biochem. Sci. 15, 138 (1990).

24. Miyazaki, R. et al. Cellular Variability of RpoS Expression Underlies Subpopulation Activation of an Integrative and Conjugative Element. PLoS Genet. 8, e1002818 (2012).

25. Broussard, G. W. et al. Integration-Dependent Bacteriophage Immunity Provides Insights into the Evolution of Genetic Switches. Mol. Cell 49, 237–248 (2013).

26. Nanda, A. M. et al. Analysis of SOS-induced spontaneous prophage induction in Corynebacterium glutamicum at the single-cell level. J. Bacteriol. 196, 180–188 (2014).

27. Smith, C. L. & Oishi, M. Early events and mechanisms in the induction of bacterial SOS functions: Analysis of the phage repressor inactivation process in vivo. Proc. Natl. Acad. Sci. U. S. A. 75, 1657–1661 (1978).

28. Erez, Z. et al. Communication between viruses guides lysis-lysogeny decisions. Nature 541, (2017).

29. Guenther, S., Huwyler, D., Richard, S. & Loessner, M. J. Virulent bacteriophage for efficient biocontrol of Listeria monocytogenes in ready-to-eat foods. Appl. Environ. Microbiol. 75, 93–100 (2009).

30. Rodriguez-Valera, F. et al. Explaining microbial population genomics through phage predation. Nat. Rev. Microbiol. 7, 828–836 (2009).

31. Scanlan, P. D. Bacteria–Bacteriophage Coevolution in the Human Gut: Implications for Microbial Diversity and Functionality. Trends in Microbiology vol. 25 614–623 (2017).

32. Muegge, B. D. et al. Diet Drives Convergence in Gut Microbiome Functions Across Mammalian Phylogeny and Within Humans. Science (80-.). 332, 970–974 (2011).

33. Dukan, S., Danie`, D. & Touati, D. Hypochlorous Acid Stress in Escherichia coli: Resistance, DNA Damage, and Comparison with Hydrogen Peroxide Stress. JOURNAL OF BACTERIOLOGY vol. 178 http://jb.asm.org/ (1996).

34. Yamamoto, N. Damage, repair, and recombination. II. Effect of hydrogen peroxide on the bacteriophage genome. Virology 38, 457–463 (1969).

35. Bacterial Stress Responses, Second Edition. Bacterial Stress Responses, Second Edition (American Society of Microbiology, 2011). doi:10.1128/9781555816841.

36. McKenna, S. M. & Davies, K. J. The inhibition of bacterial growth by hypochlorous acid. Possible role in the bactericidal activity of phagocytes. Biochem. J. 254, 685–92 (1988).

37. Houk, V. S. & DeMarini, D. M. Induction of prophage lambda by chlorinated pesticides. Mutat. Res. Mutagen. Relat. Subj. 182, 193–201 (1987).

38. Casjens, S. et al. The Chromosome of Shigella flexneri Bacteriophage Sf6: Complete Nucleotide Sequence, Genetic Mosaicism, and DNA Packaging. J. Mol. Biol. 339, 379–394 (2004).

39. Trosvik, P., Stenseth, N. C. & Rudi, K. Convergent temporal dynamics of the human infant gut microbiota. ISME J. 4, 151–158 (2010).

40. Jovel, J. et al. Characterization of the Gut Microbiome Using 16S or Shotgun Metagenomics. Front. Microbiol. 7, 459 (2016).

41. Frank, J. A. et al. Critical evaluation of two primers commonly used for amplification of bacterial 16S rRNA genes. Appl. Environ. Microbiol. 74, 2461–2470 (2008).

42. Backhed, F. et al. The gut microbiota as an environmental factor that regulates fat storage. Proc. Natl. Acad. Sci. 101, 15718–15723 (2004).

43. David, L. A. et al. Diet rapidly and reproducibly alters the human gut microbiome. Nature 505, 559–563 (2014).

44. Ley, R. E., Turnbaugh, P. J., Klein, S. & Gordon, J. I. Microbial ecology: Human gut microbes associated with obesity. Nature 444, 1022–1023 (2006).

45. Mai, V., Ukhanova, M., Reinhard, M. K., Li, M. & Sulakvelidze, A. Bacteriophage administration significantly reduces shigella colonization and shedding by shigella-challenged mice without deleterious side effects and distortions in the gut microbiota. Bacteriophage (2015) doi:10.1080/21597081.2015.1088124.

46. Danis-Wlodarczyk, K. et al. A proposed integrated approach for the preclinical evaluation of phage therapy in Pseudomonas infections. Sci. Rep. 6, 28115 (2016).

47. Howard-Varona, C., Hargreaves, K. R., Abedon, S. T. & Sullivan, M. B. Lysogeny in nature: Mechanisms, impact and ecology of temperate phages. ISME Journal (2017) doi:10.1038/ismej.2017.16.

48. Selva, L. et al. Killing niche competitors by remote-control bacteriophage induction. Proc. Natl. Acad. Sci. U. S. A. 106, 1234–1238 (2009).

49. Role of catalase in SOS induction by H2O2. (A) Survival of S. aureus... | Download Scientific Diagram. https://www.researchgate.net/figure/Role-of-catalase-in-SOS-induction-by-H2O2-A-Survival-of-S-aureus-strains-in-media_fig2_23785136.

50. Weber-Dabrowska, B., Zimecki, M., Mulczyk, M. & Górski, A. Effect of phage therapy on the turnover and function of peripheral neutrophils. FEMS Immunol. Med. Microbiol. 34, 135–8 (2002).

Appendix 1. Bacteriophage Genera Characteristics Database

Information collected from ICTV[144] and other literature in order to annotate species within the order Caudovirales

Family	Subfamily	Genera	Lifestyle Present Within Sample	Host Family	Reference
Myoviridae		0305phi8-36-like viruses	Virulent	Bacillaceae	145
Siphoviridae		1706-like viruses	Virulent	Streptococcaceae	146
Siphoviridae		3a-like viruses	Virulent and Temperate	Staphylococcus	76,147
Siphoviridae		77-like viruses	Temperate	Staphylococcus	148
Siphoviridae		936-like viruses	Virulent	Streptococcaceae	149,150
Podoviridae		Bcep22-like viruses	Virulent	Burkholderiaceae	151
Myoviridae		Bcep781-like viruses	Virulent	Burkholderiaceae	76,152,153
Myoviridae		BcepMu-like viruses	Temperate	Burkholderiaceae	154
Podoviridae		Bpp-1-like viruses	Temperate	Alcaligenaceae, Burkholderia	76,155
Siphoviridae		c2-like viruses	Virulent	Streptococcaceae	77,149,156,157
Siphoviridae		Che8-like viruses	Mostly Temperate (1 Unknown)	Enterobacteriaceae	158
Siphoviridae		CJW1-like viruses	Virulent	Mycobacteriaceae	158,159
unclassified		Cvm10-like viruses	Virulent	Enterobacteriaceae	160
Siphoviridae		D3112-like viruses	Unknown	Pseudomonadaceae	161,162
Siphoviridae		D3-like viruses	Temperate	Pseudomonadaceae	163
Podoviridae		Epsilon15-like viruses	Temperate	Enterobacteriaceae	164,165
Podoviridae		F116-like viruses	Temperate	Pseudomonadaceae	166
Myoviridae		FelixO1-like viruses	Virulent	Enterobacteriaceae	167
Myoviridae		HAP1-like viruses	Temperate	Halomonadaceae	103,168
Siphoviridae		HK578-like viruses	Virulent	Enterobacteriaceae	169
Myoviridae	Peduovirinae	HP1-like viruses	Temperate	Pasteurellaceae	76,170,171
Siphoviridae		IEBH-like viruses	Temperate	Bacillaceae	172
Siphoviridae	Guernseyvirinae	Jersey-like viruses	Virulent	Enterobacteriaceae	173,174
Myoviridae	Tevenvirinae	JS98-like viruses	Unknown	Enterobacteriaceae	
Myoviridae	Spounavirinae	K-like viruses	Virulent	Staphylococcus	76
Podoviridae	Autogrphivirinae	KP34-like viruses	Virulent	Enterobacteriaceae	175,176
Siphoviridae		L5-like viruses	Virulent and Temperate	Mycobacteriaceae	158,159,177
Siphoviridae		Lambda-like viruses	Temperate	Multiple	178–183
Siphoviridae		Lebron-like viruses	Temperate	Mycobacteriaceae	158
Podoviridae		LUZ24-like viruses	Temperate	Pseudomonadaceae	184
Podoviridae		N4-like viruses	Virulent	Enterobacteriaceae	185
Siphoviridae		Omega-like viruses	Temperate	Mycobacteriaceae	158
Myoviridae	Spounavirinae	P100-like viruses	Virulent	Listeriaceae	134
Myoviridae		P1-like viruses	Temperate	Enterobacteriaceae	64,186
Podoviridae		P22-like viruses	Temperate	Enterobacteriaceae	76,110,181,187–189
Siphoviridae		P23-45-like viruses	Virulent	Thermaceae	190
Myoviridae	Peduovirinae	P2-like viruses	Temperate	Burkholderiaceae, Enterobacteraceae	75,181,187,191,192
Siphoviridae		P335-like viruses	Virulent and Temperate	Streptococcaceae	64,76,77,79
Podoviridae	Picovirinae	P68-like viruses	Virulent	Staphylococcus, Streptococcus	193,194
Myoviridae		PAKP1-like viruses	Unknown	Vibrionaceae	
Myoviridae		PB1-like viruses	Virulent	Burkholderiaceae	75,195
Podoviridae	Picovirinae	Phi29-like viruses	Virulent	Bacillaceae, Streptococcaceae	196
Siphoviridae		PhiC31-like viruses	Temperate	Streptomycetaceae	197
Myoviridae		phiCD119-like viruses	Temperate	Clostridaceae	74,198–200
Siphoviridae		phiE125-like viruses	Temperate	Burkholderia	152
Siphoviridae		phiETA-like viruses	Temperate	Staphylococcus	64,76,147,185,201,202
Siphoviridae		phiFL-like viruses	Temperate	Enterococcaceae	203
Podoviridae	Autogrphivirinae	phiKMV-like viruses	Virulent	Pseudomonadaceae	176
Myoviridae		phiKZ-like viruses	Virulent	Pseudomonadaceae	142
Siphoviridae		phiLJ1-like viruses	Virulent	Lactobacillaceae	204
Myoviridae		phiPLPE-like viruses	Virulent and Temperate	Pateurellaceae	205,206
Siphoviridae		PsiM1-like viruses	Unknown	Methanobacteriaceae	
Myoviridae	Tevenvirinae	RB49-like viruses	Virulent	Enterobacteriaceae	207
Myoviridae		rV5-like viruses	Virulent	Enterobacteriaceae	164,208
Myoviridae	Tevenvirinae	Schizot4-like viruses	Virulent	Vibrionaceae	207
Myoviridae		Secunda5-like viruses	Virulent	Aeromonadaceae	207
Siphoviridae		Sfi11-like viruses	Virulent and Temperate	Streptococcaceae	76,209–211
Siphoviridae		Sfi21-like viruses	Virulent and Temperate	Clostridium, Streptococcaceae	76,199,210,212
Myoviridae	Tevenvirinae	SP18-like viruses	Virulent	Enterobacteriaceae	127,213,214
Podoviridae	Autogrphivirinae	SP6-like viruses	Virulent	Enterobacteriaceae	76,181,187
Siphoviridae		SPbeta-like viruses	Temperate	Bacillaceae	215
Myoviridae	Spounavirinae	SPO1-like viruses	Virulent	Bacillaceae	76,187
Myoviridae	Tevenvirinae	T4-like viruses	Virulent	Multiple	64,76,207,216–218
Siphoviridae		T5-like viruses	Virulent	Enterobacteriaceae	76,219
Podoviridae	Autogrphivirinae	T7-like viruses	Virulent	Enterobacteriaceae	64,76,181,185,187,220–222
Siphoviridae		TM4-like viruses	Virulent	Mycobacteriaceae	177,223
Siphoviridae		TP21-like viruses	Temperate	Bacillaceae	99
Myoviridae	Spounavirinae	Twort-like viruses	Virulent	Staphylococcus	76
Myoviridae		VHML-like viruses	Temperate	Vibrionaceae	76
Myoviridae		Vi1-like viruses	Virulent	Comamonadeceae	224
Siphoviridae		Wbeta-like viruses	Temperate	Bacillaceae	99
Siphoviridae		Xp10-like viruses	Virulent	Xanthomonadaceae	76,225
Siphoviridae		Yua-like viruses	Temperate	Alphaproteobacteria	226

References

1. Chassaing, B., Aitken, J. D., Gewirtz, A. T. & Vijay-Kumar, M. Gut Microbiota Drives Metabolic Disease in Immunologically Altered Mice. in *Advances in Immunology* vol. 116 93–112 (Academic Press Inc., 2012).
2. Turnbaugh, P. J. *et al.* The effect of diet on the human gut microbiome: a metagenomic analysis in humanized gnotobiotic mice. *Sci. Transl. Med.* **1**, 6ra14 (2009).
3. Lander, E. S. *et al.* Initial sequencing and analysis of the human genome. *Nature* **409**, 860–921 (2001).
4. A review of 10 years of human microbiome research activities at the US National Institutes of Health, Fiscal Years 2007-2016. *Microbiome* vol. 7 31 (2019).
5. Muller, P. A. *et al.* Crosstalk between muscularis macrophages and enteric neurons regulates gastrointestinal motility. *Cell* **158**, 300–313 (2014).
6. Weinstock, G. M. Genomic approaches to studying the human microbiota. *Nature* vol. 489 250–256 (2012).
7. Wagatsuma, K. *et al.* Diversity of Gut Microbiota Affecting Serum Level of Undercarboxylated Osteocalcin in Patients with Crohn's Disease. *Nutrients* **11**, (2019).
8. HAMER, H. M. *et al.* Review article: the role of butyrate on colonic function. *Aliment. Pharmacol. Ther.* **27**, 104–119 (2007).
9. Cani, P. D. Human gut microbiome: hopes, threats and promises. *Gut* gutjnl-2018-316723 (2018) doi:10.1136/gutjnl-2018-316723.
10. HOSHI, H. *et al.* Lymph Follicles and Germinal Centers in Popliteal lymph Nodes and Other Lymphoid Tissues of Germ-Free and Conventional Rats. *Tohoku J. Exp. Med.* **166**, 297–307 (1992).
11. Hapfelmeier, S. *et al.* Reversible microbial colonization of germ-free mice reveals the dynamics of IgA immune responses. *Science (80-.).* **328**, 1705–1709 (2010).
12. Lopetuso, L. R., Ianiro, G., Scaldaferri, F., Cammarota, G. & Gasbarrini, A. Gut Virome and Inflammatory Bowel Disease. *Inflamm. Bowel Dis.* **22**, 1708–1712 (2016).
13. Obata, Y. & Pachnis, V. The Effect of Microbiota and the Immune System on the Development and Organization of the Enteric Nervous System. *Gastroenterology* vol. 151 836–844 (2016).
14. Trosvik, P., Stenseth, N. C. & Rudi, K. Convergent temporal dynamics of the human infant gut microbiota. *ISME J.* **4**, 151–158 (2010).
15. Hepworth, M. R. *et al.* Group 3 innate lymphoid cells mediate intestinal selection of commensal bacteria-specific CD4+ T cells. *Science (80-.).* **348**, 1031–1035 (2015).
16. Virgin, H. W. The virome in mammalian physiology and disease. *Cell* vol. 157 142–150 (2014).
17. Human Microbiome Project Consortium. Structure, function and diversity of the healthy human microbiome. *Nature* **486**, 207–214 (2012).
18. Edwards, L. A. *et al.* Aberrant response to commensal Bacteroides thetaiotaomicron in Crohn's disease: An ex vivo human organ culture study. *Inflamm. Bowel Dis.* **17**, 1201–1208 (2011).
19. Duncan, S. H. *et al.* Reduced dietary intake of carbohydrates by obese subjects results in decreased concentrations of butyrate and butyrate-producing bacteria in feces. *Appl. Environ. Microbiol.* **73**, 1073–8 (2007).
20. Ridaura, V. K. *et al.* Gut microbiota from twins discordant for obesity modulate metabolism in mice. *Science* **341**, 1241214 (2013).

21. Ley, R. E., Turnbaugh, P. J., Klein, S. & Gordon, J. I. Microbial ecology: Human gut microbes associated with obesity. *Nature* **444**, 1022–1023 (2006).
22. Turnbaugh, P. J. *et al.* An obesity-associated gut microbiome with increased capacity for energy harvest. *Nature* **444**, 1027–1031 (2006).
23. Ofir, G. & Sorek, R. Contemporary Phage Biology: From Classic Models to New Insights. *Cell* (2018) doi:10.1016/j.cell.2017.10.045.
24. Manrique, P. *et al.* Healthy human gut phageome. *Proc. Natl. Acad. Sci. U. S. A.* **113**, 10400–10405 (2016).
25. Norman, J. M. *et al.* Disease-specific alterations in the enteric virome in inflammatory bowel disease. *Cell* **160**, 447–60 (2015).
26. Minot, S. *et al.* The human gut virome: inter-individual variation and dynamic response to diet. *Genome Res.* **21**, 1616–25 (2011).
27. Reyes, A. *et al.* Viruses in the faecal microbiota of monozygotic twins and their mothers. *Nature* **466**, 334–338 (2010).
28. Huttenhower, C. *et al.* Structure, function and diversity of the healthy human microbiome. *Nature* **486**, 207–214 (2012).
29. Kobyliak, N., Virchenko, O. & Falalyeyeva, T. Pathophysiological role of host microbiota in the development of obesity. *Nutr. J.* **15**, 43 (2016).
30. Parekh, P. J., Arusi, E., Vinik, A. I. & Johnson, D. A. The role and influence of gut microbiota in pathogenesis and management of obesity and metabolic syndrome. *Frontiers in Endocrinology* vol. 5 (2014).
31. Thaiss, C. A. *et al.* Hyperglycemia drives intestinal barrier dysfunction and risk for enteric infection. *Science (80-.).* **359**, (2018).
32. Howe, A. *et al.* Divergent responses of viral and bacterial communities in the gut microbiome to dietary disturbances in mice. *ISME J.* **10**, 1217–1227 (2016).
33. Vernocchi, P., Del Chierico, F. & Putignani, L. Gut microbiota profiling: Metabolomics based approach to unravel compounds affecting human health. *Frontiers in Microbiology* vol. 7 (2016).
34. Sun, L. *et al.* Insights into the role of gut microbiota in obesity: pathogenesis, mechanisms, and therapeutic perspectives. *Protein Cell* **9**, 397 (2018).
35. Duncan, S. H. *et al.* Human colonic microbiota associated with diet, obesity and weight loss. *Int. J. Obes.* **32**, 1720–1724 (2008).
36. Minot, S. *et al.* The human gut virome: inter-individual variation and dynamic response to diet. *Genome Res.* **21**, 1616–1625 (2011).
37. Ryan, G. B. & Majno, G. Acute inflammation. A review. *Am. J. Pathol.* **86**, 183–276 (1977).
38. Goldman, H. *Acute versus chronic colitis: How and when to distinguish by biopsy*. *Gastroenterology* vol. 86 (1984).
39. Samanta, A. K., Torok, V. A., Percy, N. J., Abimosleh, S. M. & Howarth, G. S. Microbial fingerprinting detects unique bacterial communities in the faecal microbiota of rats with experimentally-induced colitis. *J. Microbiol.* **50**, 218–225 (2012).
40. Wen, Z. & Fiocchi, C. Inflammatory bowel disease: Autoimmune or immune-mediated pathogenesis? in *Clinical and Developmental Immunology* vol. 11 195–204 (2004).
41. Skaar, E. P. The Battle for Iron between Bacterial Pathogens and Their Vertebrate Hosts. *PLoS Pathog.* **6**, e1000949 (2010).
42. Ron, E. Z. Bacterial Stress Response. in *The Prokaryotes* 1012–1027 (Springer New

York, 2006). doi:10.1007/0-387-30742-7_32.
43. Wilson, B. A., Salyers, A. A., Whitt, D. D. & Winkler, M. E. *Bacterial Pathogenesis*. *Bacterial Pathogenesis* (American Society of Microbiology, 2011). doi:10.1128/9781555816162.
44. *Bacterial Stress Responses, Second Edition*. *Bacterial Stress Responses, Second Edition* (American Society of Microbiology, 2011). doi:10.1128/9781555816841.
45. Smith, C. L. & Oishi, M. Early events and mechanisms in the induction of bacterial SOS functions: Analysis of the phage repressor inactivation process in vivo. *Proc. Natl. Acad. Sci. U. S. A.* **75**, 1657–1661 (1978).
46. Gogokhia, L. *et al.* Expansion of Bacteriophages Is Linked to Aggravated Intestinal Inflammation and Colitis. *Cell Host Microbe* **25**, 285-299.e8 (2019).
47. Barr, J. J. *et al.* Bacteriophage adhering to mucus provide a non–host-derived immunity. *Proc. Natl. Acad. Sci.* **110**, 10771–10776 (2013).
48. Appelmans, R. Le dosage du bactériophage. *Compt Rend Soc Biol* **85**, 701 (1921).
49. World Health Organization. *Overweight and obesity fact sheet.* (2016).
50. Hales, C. M., Carroll, M. D., Fryar, C. D. & Ogden, C. L. *Prevalence of Obesity Among Adults and Youth: United States, 2015-2016 Key findings Data from the National Health and Nutrition Examination Survey*. https://www.cdc.gov/nchs/data/databriefs/db288_table.pdf#1. (2015).
51. Popkin, B. M. & Gordon-Larsen, P. The nutrition transition: Worldwide obesity dynamics and their determinants. *Int. J. Obes.* **28**, S2–S9 (2004).
52. Popkin, B. M., Adair, L. S. & Ng, S. W. Global nutrition transition and the pandemic of obesity in developing countries. *Nutr. Rev.* **70**, 3–21 (2012).
53. Klein, S. *et al.* Weight management through lifestyle modification for the prevention and management of type 2 diabetes: Rationale and strategies. A statement of the American Diabetes Association, the North American Association for the Study of Obesity, and the American Society for Clinical Nutrition. *American Journal of Clinical Nutrition* vol. 80 257–263 (2004).
54. Singh, S., Dulai, P. S., Zarrinpar, A., Ramamoorthy, S. & Sandborn, W. J. Obesity in IBD: Epidemiology, pathogenesis, disease course and treatment outcomes. *Nature Reviews Gastroenterology and Hepatology* vol. 14 110–121 (2017).
55. Goodwin, P. J. & Stambolic, V. Impact of the Obesity Epidemic on Cancer. *Annu. Rev. Med.* **66**, 281–296 (2015).
56. Hollister, E. B., Gao, C. & Versalovic, J. Compositional and functional features of the gastrointestinal microbiome and their effects on human health. *Gastroenterology* **146**, 1449–58 (2014).
57. Cantarel, B. L., Lombard, V. & Henrissat, B. Complex Carbohydrate Utilization by the Healthy Human Microbiome. *PLoS One* **7**, e28742 (2012).
58. Sonnenburg, E. D. *et al.* Diet-induced extinctions in the gut microbiota compound over generations. *Nature* **529**, 212–5 (2016).
59. Ul Haq, I., Chaudhry, W. N., Akhtar, M. N., Andleeb, S. & Qadri, I. Bacteriophages and their implications on future biotechnology: A review. *Virology Journal* vol. 9 (2012).
60. Reyes, A., Wu, M., McNulty, N. P., Rohwer, F. L. & Gordon, J. I. Gnotobiotic mouse model of phage-bacterial host dynamics in the human gut. *Proc. Natl. Acad. Sci. U. S. A.* **110**, 20236–41 (2013).
61. FASTX-Toolkit. http://hannonlab.cshl.edu/fastx_toolkit/.

62. Bolger, A. M., Lohse, M. & Usadel, B. Trimmomatic: a flexible trimmer for Illumina sequence data. *Bioinformatics* **30**, 2114–2120 (2014).
63. Meyer, F. *et al.* The metagenomics RAST server – a public resource for the automatic phylogenetic and functional analysis of metagenomes. *BMC Bioinformatics* **9**, 386 (2008).
64. International Committee on Taxonomy of Viruses. & King, A. *Virus taxonomy : ninth report of the International Committee on Taxonomy of Viruses*. (Elsevier, 2011).
65. R Core Team. R: A language and environment for statistical computing. (2014).
66. Dixon, P. VEGAN, a package of R functions for community ecology. *J. Veg. Sci.* **14**, 927–930 (2003).
67. Pohlert, T. trend: Non-Parametric Trend Tests and Change-Point Detection. *R Packag. version 1.1.0* (2018).
68. Revelle, W. R. psych: Procedures for Personality and Psychological Research. (2017).
69. Kassambara, A. ggcorrplot: Visualization of a correlation matrix using ggplot2. https://github.com/kassambara/ggcorrplot (2015).
70. Zhu, C. & Yu, J. Nonmetric multidimensional scaling corrects for population structure in association mapping with different sample types. *Genetics* **182**, 875–88 (2009).
71. Shreiner, A. B., Kao, J. Y. & Young, V. B. The gut microbiome in health and in disease. *Curr. Opin. Gastroenterol.* **31**, 69–75 (2015).
72. Ziętak, M. *et al.* Altered Microbiota Contributes to Reduced Diet-Induced Obesity upon Cold Exposure. *Cell Metab.* **23**, 1216–1223 (2016).
73. David, L. A. *et al.* Diet rapidly and reproducibly alters the human gut microbiome. *Nature* **505**, (2014).
74. Hargreaves, K. R. & Clokie, M. R. J. A Taxonomic Review of Clostridium difficile Phages and Proposal of a Novel Genus, "Phimmp04likevirus". *Viruses* **7**, 2534–41 (2015).
75. Lavigne, R. *et al.* Classification of Myoviridae bacteriophages using protein sequence similarity. *BMC Microbiol.* **9**, 224 (2009).
76. ACLAME: Phages lifestyle. http://aclame.ulb.ac.be/Classification/Phages/life_style.html.
77. Labrie, S. & Moineau, S. Multiplex PCR for Detection and Identification of Lactococcal Bacteriophages. *Appl. Environ. Microbiol.* **66**, 987–994 (2000).
78. Blatny, J. M., Godager, L., Lunde, M. & Nes, I. F. Complete genome sequence of the Lactococcus lactis temperate phage φLC3: comparative analysis of φLC3 and its relatives in lactococci and streptococci. *Virology* **318**, 231–244 (2004).
79. Samson, J. E. & Moineau, S. Characterization of Lactococcus lactis phage 949 and comparison with other lactococcal phages. *Appl. Environ. Microbiol.* **76**, 6843–52 (2010).
80. Christiansen, B., Johnsen, M. G., Stenby, E., Vogensen, F. K. & Hammer, K. Characterization of the lactococcal temperate phage TP901-1 and its site-specific integration. *J. Bacteriol.* **176**, 1069–76 (1994).
81. Everard, A. *et al.* Cross-talk between Akkermansia muciniphila and intestinal epithelium controls diet-induced obesity. *Proc. Natl. Acad. Sci. U. S. A.* **110**, 9066–71 (2013).
82. Jovel, J. *et al.* Characterization of the Gut Microbiome Using 16S or Shotgun Metagenomics. *Front. Microbiol.* **7**, 459 (2016).
83. Hakkak, R., Korourian, S., Foley, S. L. & Erickson, B. D. Assessment of gut microbiota populations in lean and obese Zucker rats. *PLoS One* **12**, e0181451 (2017).
84. Backhed, F. *et al.* The gut microbiota as an environmental factor that regulates fat storage. *Proc. Natl. Acad. Sci.* **101**, 15718–15723 (2004).

85. Scanlan, P. D. Bacteria–Bacteriophage Coevolution in the Human Gut: Implications for Microbial Diversity and Functionality. *Trends in Microbiology* vol. 25 614–623 (2017).
86. Hsu, B. B. *et al.* Dynamic Modulation of the Gut Microbiota and Metabolome by Bacteriophages in a Mouse Model. *Cell Host Microbe* **25**, 803-814.e5 (2019).
87. Hsu, B. B. *et al.* Dynamic Modulation of the Gut Microbiota and Metabolome by Bacteriophages in a Mouse Model. *Cell Host Microbe* **25**, 803-814.e5 (2019).
88. Sender, R., Fuchs, S. & Milo, R. Revised Estimates for the Number of Human and Bacteria Cells in the Body. *PLOS Biol.* **14**, e1002533 (2016).
89. Zuo, T. *et al.* Gut mucosal virome alterations in ulcerative colitis. *Gut* gutjnl-2018-318131 (2019) doi:10.1136/gutjnl-2018-318131.
90. Chang, J. Y. *et al.* Decreased Diversity of the Fecal Microbiome in Recurrent *Clostridium difficile* –Associated Diarrhea. *J. Infect. Dis.* **197**, 435–438 (2008).
91. Le Roy, T. *et al.* Intestinal microbiota determines development of non-alcoholic fatty liver disease in mice. *Gut* **62**, 1787–1794 (2013).
92. Zhu, W. *et al.* Gut Microbial Metabolite TMAO Enhances Platelet Hyperreactivity and Thrombosis Risk. *Cell* **165**, 111–124 (2016).
93. Hsiao, E. Y. *et al.* Microbiota modulate behavioral and physiological abnormalities associated with neurodevelopmental disorders. *Cell* **155**, 1451–1463 (2013).
94. Li, H. & Durbin, R. Fast and accurate short read alignment with Burrows-Wheeler transform. *Bioinformatics* **25**, 1754–1760 (2009).
95. Li, H. *et al.* The Sequence Alignment/Map format and SAMtools. *Bioinformatics* **25**, 2078–2079 (2009).
96. Kurtz, Z. D. *et al.* Sparse and Compositionally Robust Inference of Microbial Ecological Networks. *PLoS Comput. Biol.* **11**, (2015).
97. Csardi, G., & Nepusz, T. The Igraph Software Package for Complex Network Research. InterJournal 2006, Complex Systems, 1695. - References - Scientific Research Publishing. https://www.scirp.org/(S(vtj3fa45qm1ean45vvffcz55))/reference/ReferencesPapers.aspx?ReferenceID=1426710 (2006).
98. Ernst, J. & Bar-Joseph, Z. STEM: a tool for the analysis of short time series gene expression data. *BMC Bioinformatics* **7**, 191 (2006).
99. Klumpp, J., Calendar, R. & Loessner, M. J. Complete Nucleotide Sequence and Molecular Characterization of Bacillus Phage TP21 and its Relatedness to Other Phages with the Same Name. *Viruses* **2**, 961–71 (2010).
100. Thingstad, T. & Lignell, R. Theoretical models for the control of bacterial growth rate, abundance, diversity and carbon demand. *Aquat. Microb. Ecol.* **13**, 19–27 (1997).
101. Silveira, C. B. & Rohwer, F. L. Piggyback-the-Winner in host-associated microbial communities. *npj Biofilms Microbiomes* **2**, 16010 (2016).
102. Dutilh, B. E. *et al.* A highly abundant bacteriophage discovered in the unknown sequences of human faecal metagenomes. *Nat. Commun.* (2014) doi:10.1038/ncomms5498.
103. Mobberley, J. M., Authement, R. N., Segall, A. M. & Paul, J. H. The temperate marine phage PhiHAP-1 of Halomonas aquamarina possesses a linear plasmid-like prophage genome. *J. Virol.* **82**, 6618–30 (2008).
104. Knowles, B. *et al.* Lytic to temperate switching of viral communities. *Nature* (2016) doi:10.1038/nature17193.
105. Little, J. W. Chance phenotypic variation. *Trends Biochem. Sci.* **15**, 138 (1990).
106. Miyazaki, R. *et al.* Cellular Variability of RpoS Expression Underlies Subpopulation

Activation of an Integrative and Conjugative Element. *PLoS Genet.* **8**, e1002818 (2012).
107. Nanda, A. M. *et al.* Analysis of SOS-induced spontaneous prophage induction in Corynebacterium glutamicum at the single-cell level. *J. Bacteriol.* **196**, 180–188 (2014).
108. Broussard, G. W. *et al.* Integration-Dependent Bacteriophage Immunity Provides Insights into the Evolution of Genetic Switches. *Mol. Cell* **49**, 237–248 (2013).
109. Erez, Z. *et al.* Communication between viruses guides lysis-lysogeny decisions. *Nature* **541**, (2017).
110. Casjens, S. *et al.* The Chromosome of Shigella flexneri Bacteriophage Sf6: Complete Nucleotide Sequence, Genetic Mosaicism, and DNA Packaging. *J. Mol. Biol.* **339**, 379–394 (2004).
111. Lemire, S., Figueroa-Bossi, N. & Bossi, L. Bacteriophage crosstalk: Coordination of prophage induction by Trans-Acting antirepressors. *PLoS Genet.* **7**, e1002149 (2011).
112. Campoy, S. *et al.* Induction of the SOS response by bacteriophage lytic development in Salmonella enterica. *Virology* **351**, 360–367 (2006).
113. Anderson, T. F. The Influence of Temperature and Nutrients on Plaque Formation by Bacteriophages Active on Escherichia coli Strain B. *J. Bacteriol.* **55**, 659 (1948).
114. Moebus, K. Marine bacteriophage reproduction under nutrient-limited growth of host bacteria. II. Investigations with phage-host system [H3:H3/1]. *Mar. Ecol. Prog. Ser.* **144**, 13–22 (1996).
115. Barr, J. J., Youle, M. & Rohwer, F. Innate and acquired bacteriophage-mediated immunity. *Bacteriophage* **3**, e25857 (2013).
116. Hurst, J. K., Barrette, W. C., Michel, B. R. & Rosen, H. Hypochlorous acid and myeloperoxidase-catalyzed oxidation of iron-sulfur clusters in bacterial respiratory dehydrogenases. *Eur. J. Biochem.* **202**, 1275–82 (1991).
117. De Oliveira, S., Rosowski, E. E. & Huttenlocher, A. Neutrophil migration in infection and wound repair: Going forward in reverse. *Nature Reviews Immunology* vol. 16 378–391 (2016).
118. Dukan, S., Danie`, D. & Touati, D. *Hypochlorous Acid Stress in Escherichia coli: Resistance, DNA Damage, and Comparison with Hydrogen Peroxide Stress*. *JOURNAL OF BACTERIOLOGY* vol. 178 http://jb.asm.org/ (1996).
119. Howard-Varona, C., Hargreaves, K. R., Abedon, S. T. & Sullivan, M. B. Lysogeny in nature: Mechanisms, impact and ecology of temperate phages. *ISME Journal* (2017) doi:10.1038/ismej.2017.16.
120. Weber-Dabrowska, B., Zimecki, M., Mulczyk, M. & Górski, A. Effect of phage therapy on the turnover and function of peripheral neutrophils. *FEMS Immunol. Med. Microbiol.* **34**, 135–8 (2002).
121. One step multiplication curve for bacteriophages. – Biotech Khan. https://biotechkhan.wordpress.com/2014/07/01/one-step-multiplication-curve-for-bacteriophages/.
122. One step multiplication curve for bacteriophages. – Biotech Khan. https://biotechkhan.wordpress.com/2014/07/01/one-step-multiplication-curve-for-bacteriophages/.
123. Clokie, M. R. J., Kropinski, A. M. (Andrew M. B. & Lavigne, R. *Bacteriophages : methods and protocols*.
124. Hu, B., Margolin, W., Molineux, I. J. & Liu, J. The bacteriophage T7 virion undergoes extensive structural remodeling during infection. *Science (80-.).* **339**, 576–579 (2013).

125. McKenna, S. M. & Davies, K. J. A. The inhibition of bacterial growth by hypochlorous acid. Possible role in the bactericidal activity of phagocytes. *Biochem. J.* **254**, 685–692 (1988).
126. Storms, Z. J., Smith, L., Sauvageau, D. & Cooper, D. G. Modeling bacteriophage attachment using adsorption efficiency. *Biochem. Eng. J.* **64**, 22–29 (2012).
127. Jun, J. W. *et al.* Bacteriophage application to control the contaminated water with Shigella. *Sci. Rep.* **6**, 22636 (2016).
128. Selva, L. *et al.* Killing niche competitors by remote-control bacteriophage induction. *Proc. Natl. Acad. Sci. U. S. A.* **106**, 1234–1238 (2009).
129. Yamamoto, N. Damage, repair, and recombination. II. Effect of hydrogen peroxide on the bacteriophage genome. *Virology* **38**, 457–463 (1969).
130. Abedon, S. T. Kinetics of phage-mediated biocontrol of bacteria. *Foodborne Pathogens and Disease* vol. 6 807–815 (2009).
131. Hyman, P. Bacteriophages and Nanostructured Materials. in *Advances in Applied Microbiology* vol. 78 55–73 (Academic Press Inc., 2012).
132. Sybesma, W. *et al.* Bacteriophages as potential treatment for urinary tract infections. *Front. Microbiol.* **7**, (2016).
133. Campoy, S. *et al.* Induction of the SOS response by bacteriophage lytic development in Salmonella enterica. *Virology* **351**, 360–367 (2006).
134. Guenther, S., Huwyler, D., Richard, S. & Loessner, M. J. Virulent bacteriophage for efficient biocontrol of Listeria monocytogenes in ready-to-eat foods. *Appl. Environ. Microbiol.* **75**, 93–100 (2009).
135. Rodriguez-Valera, F. *et al.* Explaining microbial population genomics through phage predation. *Nat. Rev. Microbiol.* **7**, 828–836 (2009).
136. Muegge, B. D. *et al.* Diet Drives Convergence in Gut Microbiome Functions Across Mammalian Phylogeny and Within Humans. *Science (80-.).* **332**, 970–974 (2011).
137. McKenna, S. M. & Davies, K. J. The inhibition of bacterial growth by hypochlorous acid. Possible role in the bactericidal activity of phagocytes. *Biochem. J.* **254**, 685–92 (1988).
138. Houk, V. S. & DeMarini, D. M. Induction of prophage lambda by chlorinated pesticides. *Mutat. Res. Mutagen. Relat. Subj.* **182**, 193–201 (1987).
139. Frank, J. A. *et al.* Critical evaluation of two primers commonly used for amplification of bacterial 16S rRNA genes. *Appl. Environ. Microbiol.* **74**, 2461–2470 (2008).
140. David, L. A. *et al.* Diet rapidly and reproducibly alters the human gut microbiome. *Nature* **505**, 559–563 (2014).
141. Mai, V., Ukhanova, M., Reinhard, M. K., Li, M. & Sulakvelidze, A. Bacteriophage administration significantly reduces shigella colonization and shedding by shigella-challenged mice without deleterious side effects and distortions in the gut microbiota. *Bacteriophage* (2015) doi:10.1080/21597081.2015.1088124.
142. Danis-Wlodarczyk, K. *et al.* A proposed integrated approach for the preclinical evaluation of phage therapy in Pseudomonas infections. *Sci. Rep.* **6**, 28115 (2016).
143. Role of catalase in SOS induction by H2O2. (A) Survival of S. aureus... | Download Scientific Diagram. https://www.researchgate.net/figure/Role-of-catalase-in-SOS-induction-by-H2O2-A-Survival-of-S-aureus-strains-in-media_fig2_23785136.
144. International Committee on Taxonomy of Viruses (ICTV). https://talk.ictvonline.org/taxonomy/.
145. Serwer, P., Wright, E. T., Chang, J. T. & Liu, X. Enhancing and initiating phage-based

therapies. *Bacteriophage* **4**, e961869 (2014).
146. Garneau, J. E., Tremblay, D. M. & Moineau, S. Characterization of 1706, a virulent phage from Lactococcus lactis with similarities to prophages from other Firmicutes. *Virology* **373**, 298–309 (2008).
147. Bueno, E., García, P., Martínez, B. & Rodríguez, A. Phage inactivation of Staphylococcus aureus in fresh and hard-type cheeses. *Int. J. Food Microbiol.* **158**, 23–27 (2012).
148. Goerke, C. *et al.* Diversity of prophages in dominant Staphylococcus aureus clonal lineages. *J. Bacteriol.* **191**, 3462–8 (2009).
149. Michelsen, O., Cuesta-Dominguez, A., Albrechtsen, B. & Jensen, P. R. Detection of bacteriophage-infected cells of Lactococcus lactis by using flow cytometry. *Appl. Environ. Microbiol.* **73**, 7575–81 (2007).
150. Mahony, J. *et al.* Sequence and comparative genomic analysis of lactococcal bacteriophages jj50, 712 and P008: evolutionary insights into the 936 phage species. *FEMS Microbiol. Lett.* **261**, 253–261 (2006).
151. Gill, J. J. *et al.* Genomes and characterization of phages Bcep22 and BcepIL02, founders of a novel phage type in Burkholderia cenocepacia. *J. Bacteriol.* **193**, 5300–13 (2011).
152. Summer, E. J., Gill, J. J., Upton, C., Gonzalez, C. F. & Young, R. Role of phages in the pathogenesis of Burkholderia, or 'Where are the toxin genes in Burkholderia phages?'. *Curr. Opin. Microbiol.* **10**, 410–7 (2007).
153. Summer, E. J. *et al.* Divergence and mosaicism among virulent soil phages of the Burkholderia cepacia complex. *J. Bacteriol.* **188**, 255–68 (2006).
154. Langley, R. J., Kenna, D., Bartholdson, J., Campopiano, D. J. & Govan, J. R. W. Temperate bacteriophages DK4 and BcepMu from *Burkholderia cenocepacia* J2315 are identical. *FEMS Immunol. Med. Microbiol.* **45**, 349–350 (2005).
155. Liu, M. *et al.* Genomic and genetic analysis of Bordetella bacteriophages encoding reverse transcriptase-mediated tropism-switching cassettes. *J. Bacteriol.* **186**, 1503–17 (2004).
156. Rakonjac, J., O'Toole, P. W. & Lubbers, M. Isolation of lactococcal prolate phage-phage recombinants by an enrichment strategy reveals two novel host range determinants. *J. Bacteriol.* **187**, 3110–21 (2005).
157. Eraclio, G. *et al.* A virulent phage infecting Lactococcus garvieae, with homology to Lactococcus lactis phages. *Appl. Environ. Microbiol.* **81**, 8358–65 (2015).
158. Hatfull, G. F. The Secret Lives of Mycobacteriophages. **82**, 179–288 (2012).
159. Trigo, G. *et al.* Phage Therapy Is Effective against Infection by Mycobacterium ulcerans in a Murine Footpad Model. *PLoS Negl. Trop. Dis.* **7**, e2183 (2013).
160. Santos, T. M. A. & Bicalho, R. C. Complete genome sequence of vB_EcoM_ECO1230-10: A coliphage with therapeutic potential for bovine metritis. *Vet. Microbiol.* **148**, 267–275 (2011).
161. Sepúlveda-Robles, O., Kameyama, L. & Guarneros, G. High diversity and novel species of Pseudomonas aeruginosa bacteriophages. *Appl. Environ. Microbiol.* **78**, 4510–5 (2012).
162. Budzik, J. M., Rosche, W. A., Rietsch, A. & O'Toole, G. A. Isolation and characterization of a generalized transducing phage for Pseudomonas aeruginosa strains PAO1 and PA14. *J. Bacteriol.* **186**, 3270–3 (2004).
163. Kropinski, A. M. Sequence of the genome of the temperate, serotype-converting, Pseudomonas aeruginosa bacteriophage D3. *J. Bacteriol.* **182**, 6066–74 (2000).
164. Liao, W.-C. *et al.* T4-Like genome organization of the Escherichia coli O157:H7 lytic phage AR1. *J. Virol.* **85**, 6567–78 (2011).

165. Perry, L. L. *et al.* Sequence analysis of Escherichia coli O157:H7 bacteriophage PhiV10 and identification of a phage-encoded immunity protein that modifies the O157 antigen. *FEMS Microbiol. Lett.* **292**, 182–6 (2009).
166. Byrne, M. & Kropinski, A. M. The genome of the Pseudomonas aeruginosa generalized transducing bacteriophage F116. *Gene* **346**, 187–194 (2005).
167. Lehman, S. M., Kropinski, A. M., Castle, A. J. & Svircev, A. M. Complete genome of the broad-host-range Erwinia amylovora phage phiEa21-4 and its relationship to Salmonella phage felix O1. *Appl. Environ. Microbiol.* **75**, 2139–47 (2009).
168. Lan, S.-F. *et al.* Characterization of a new plasmid-like prophage in a pandemic Vibrio parahaemolyticus O3:K6 strain. *Appl. Environ. Microbiol.* **75**, 2659–67 (2009).
169. Carrias, A. *et al.* Comparative genomic analysis of bacteriophages specific to the channel catfish pathogen Edwardsiella ictaluri. *Virol. J.* **8**, 6 (2011).
170. Beilstein, F. & Dreiseikelmann, B. Temperate bacteriophage PhiO18P from an Aeromonas media isolate: characterization and complete genome sequence. *Virology* **373**, 25–9 (2008).
171. Campoy, S., Aranda, J., Alvarez, G., Barbé, J. & Llagostera, M. Isolation and sequencing of a temperate transducing phage for Pasteurella multocida. *Appl. Environ. Microbiol.* **72**, 3154–60 (2006).
172. Grose, J. H., Jensen, G. L., Burnett, S. H. & Breakwell, D. P. Genomic comparison of 93 Bacillus phages reveals 12 clusters, 14 singletons and remarkable diversity. *BMC Genomics* **15**, 855 (2014).
173. De Lappe, N., Doran, G., O'Connor, J., O'Hare, C. & Cormican, M. Characterization of bacteriophages used in the Salmonella enterica serovar Enteritidis phage-typing scheme. *J. Med. Microbiol.* **58**, 86–93 (2009).
174. Kim, S.-H. *et al.* Complete genome sequence of Salmonella bacteriophage SS3e. *J. Virol.* **86**, 10253–4 (2012).
175. Drulis-Kawa, Z. *et al.* Isolation and characterisation of KP34—a novel φKMV-like bacteriophage for Klebsiella pneumoniae. *Appl. Microbiol. Biotechnol.* **90**, 1333–1345 (2011).
176. Adriaenssens, E. M. *et al.* Bacteriophages LIMElight and LIMEzero of Pantoea agglomerans, belonging to the "phiKMV-like viruses". *Appl. Environ. Microbiol.* **77**, 3443–50 (2011).
177. Hassan, S. *et al.* Lytic Efficiency of Mycobacteriophages. *Open Syst. Biol. J.* **3**, 21–28 (2010).
178. Ellis, D. M. & Dean, D. H. Location of the Bacillus subtilis temperate bacteriophage phi 105 attP attachment site. *J. Virol.* **58**, 223–4 (1986).
179. Hemphill, H. E. & Whiteley, H. R. Bacteriophages of Bacillus subtilis. *Bacteriol. Rev.* **39**, 257–315 (1975).
180. Günthert, U. & Reiners, L. Bacillus subtilis phage SPR codes for a DNA methyltransferase with triple sequence specificity. *Nucleic Acids Res.* **15**, 3689–702 (1987).
181. Grose, J. H. & Casjens, S. R. Understanding the enormous diversity of bacteriophages: the tailed phages that infect the bacterial family Enterobacteriaceae. *Virology* **468–470**, 421–43 (2014).
182. Lynch, K. H., Seed, K. D., Stothard, P. & Dennis, J. J. Inactivation of Burkholderia cepacia complex phage KS9 gp41 identifies the phage repressor and generates lytic

virions. *J. Virol.* **84**, 1276–88 (2010).
183. Price-Carter, M. *et al.* The evolution and distribution of phage ST160 within Salmonella enterica serotype Typhimurium. doi:10.1017/S0950268810002335.
184. Shen, X. *et al.* Functional identification of the DNA packaging terminase from Pseudomonas aeruginosa phage PaP3. *Arch. Virol.* **157**, 2133–2141 (2012).
185. PhageSeed. http://www.phantome.org/PhageSeed/seedviewer.cgi?page=Subsystems&subsystem=T7-like_cyanophage_core_proteins.
186. Łobocka, M. B. *et al.* Genome of bacteriophage P1. *J. Bacteriol.* **186**, 7032–68 (2004).
187. Whichard, J. M. *et al.* Complete genomic sequence of bacteriophage felix o1. *Viruses* **2**, 710–30 (2010).
188. Villafane, R., Zayas, M., Gilcrease, E. B., Kropinski, A. M. & Casjens, S. R. Genomic analysis of bacteriophage epsilon 34 of Salmonella enterica serovar Anatum (15+). *BMC Microbiol.* **8**, 227 (2008).
189. Mmolawa, P. T., Schmieger, H., Tucker, C. P. & Heuzenroeder, M. W. Genomic structure of the Salmonella enterica serovar Typhimurium DT 64 bacteriophage ST64T: evidence for modular genetic architecture. *J. Bacteriol.* **185**, 3473–5 (2003).
190. Minakhin, L. *et al.* Genome comparison and proteomic characterization of Thermus thermophilus bacteriophages P23-45 and P74-26: siphoviruses with triplex-forming sequences and the longest known tails. *J. Mol. Biol.* **378**, 468–80 (2008).
191. Lynch, K. H., Stothard, P. & Dennis, J. J. Genomic analysis and relatedness of P2-like phages of the Burkholderia cepacia complex. *BMC Genomics* **11**, 599 (2010).
192. Urban-Chmiel, R. *et al.* Isolation and Characterization of Lytic Properties of Bacteriophages Specific for M. haemolytica Strains. *PLoS One* **10**, e0140140 (2015).
193. Deghorain, M. & Van Melderen, L. The Staphylococci phages family: an overview. *Viruses* **4**, 3316–35 (2012).
194. Nelson, D., Schuch, R., Zhu, S., Tscherne, D. M. & Fischetti, V. A. Genomic sequence of C1, the first streptococcal phage. *J. Bacteriol.* **185**, 3325–32 (2003).
195. Essoh, C. *et al.* Investigation of a Large Collection of Pseudomonas aeruginosa Bacteriophages Collected from a Single Environmental Source in Abidjan, Côte d'Ivoire. *PLoS One* **10**, e0130548 (2015).
196. Meijer, W. J., Horcajadas, J. A. & Salas, M. Phi29 family of phages. *Microbiol. Mol. Biol. Rev.* **65**, 261–87 ; second page, table of contents (2001).
197. Gregory, M. A., Till, R. & Smith, M. C. M. Integration site for Streptomyces phage phiBT1 and development of site-specific integrating vectors. *J. Bacteriol.* **185**, 5320–3 (2003).
198. Revathi, G., Fralick, J. A. & Rolfe, R. D. In vivo lysogenization of a Clostridium difficile bacteriophage ΦCD119. *Anaerobe* **17**, 125–9 (2011).
199. Sekulovic, O., Garneau, J. R., Néron, A. & Fortier, L.-C. Characterization of temperate phages infecting Clostridium difficile isolates of human and animal origins. *Appl. Environ. Microbiol.* **80**, 2555–63 (2014).
200. Hargreaves, K. R., Kropinski, A. M. & Clokie, M. R. J. What does the talking?: quorum sensing signalling genes discovered in a bacteriophage genome. *PLoS One* **9**, e85131 (2014).
201. Daniel, A., Bonnen, P. E. & Fischetti, V. A. First complete genome sequence of two Staphylococcus epidermidis bacteriophages. *J. Bacteriol.* **189**, 2086–100 (2007).

202. Bae, T., Baba, T., Hiramatsu, K. & Schneewind, O. Prophages of Staphylococcus aureus Newman and their contribution to virulence. *Mol. Microbiol.* **62**, 1035–47 (2006).
203. Adriaenssens, E. M. *et al.* Integration of genomic and proteomic analyses in the classification of the Siphoviridae family. *Virology* **477**, 144–154 (2015).
204. Lu, Z. *et al.* Sequence analysis of the Lactobacillus plantarum bacteriophage ΦJL-1. *Gene* **348**, 45–54 (2005).
205. Leblanc, C., Caumont-Sarcos, A., Comeau, A. M. & Krisch, H. M. Isolation and genomic characterization of the first phage infecting Iodobacteria: ϕPLPE, a myovirus having a novel set of features. *Environ. Microbiol. Rep.* **1**, 499–509 (2009).
206. Comeau, A. M. *et al.* Phage morphology recapitulates phylogeny: the comparative genomics of a new group of myoviruses. *PLoS One* **7**, e40102 (2012).
207. Petrov, V. M., Ratnayaka, S., Nolan, J. M., Miller, E. S. & Karam, J. D. Genomes of the T4-related bacteriophages as windows on microbial genome evolution. *Virol. J.* **7**, 292 (2010).
208. Kropinski, A. M. *et al.* The host-range, genomics and proteomics of Escherichia coli O157:H7 bacteriophage rV5. *Virol. J.* **10**, 76 (2013).
209. Deveau, H. *et al.* Phage response to CRISPR-encoded resistance in Streptococcus thermophilus. *J. Bacteriol.* **190**, 1390–400 (2008).
210. Guglielmotti, D. M. *et al.* Genome analysis of two virulent Streptococcus thermophilus phages isolated in Argentina. *Int. J. Food Microbiol.* **136**, 101–9 (2009).
211. Ali, Y. *et al.* Temperate Streptococcus thermophilus phages expressing superinfection exclusion proteins of the Ltp type. *Front. Microbiol.* **5**, 98 (2014).
212. Horgan, M. *et al.* Genome analysis of the Clostridium difficile phage PhiCD6356, a temperate phage of the Siphoviridae family. *Gene* **462**, 34–43 (2010).
213. Dalmasso, M. *et al.* Three New Escherichia coli Phages from the Human Gut Show Promising Potential for Phage Therapy. *PLoS One* **11**, e0156773 (2016).
214. Lim, J.-A. *et al.* Complete genome sequence of the Pectobacterium carotovorum subsp. carotovorum virulent bacteriophage PM1. *Arch. Virol.* **159**, 2185–2187 (2014).
215. McLaughlin, J. R., Wong, H. C., Ting, Y. E., Van Arsdell, J. N. & Chang, S. Control of lysogeny and immunity of Bacillus subtilis temperate bacteriophage SP beta by its d gene. *J. Bacteriol.* **167**, 952–9 (1986).
216. Jin, J. *et al.* Isolation and characterization of ZZ1, a novel lytic phage that infects Acinetobacter baumannii clinical isolates. *BMC Microbiol.* **12**, 156 (2012).
217. Ignacio-Espinoza, J. C. & Sullivan, M. B. Phylogenomics of T4 cyanophages: lateral gene transfer in the 'core' and origins of host genes. *Environ. Microbiol.* **14**, 2113–2126 (2012).
218. Shi, Y. *et al.* Characterization and determination of holin protein of Streptococcus suis bacteriophage SMP in heterologous host. *Virol. J.* **9**, 70 (2012).
219. Hong, J. *et al.* Identification of host receptor and receptor-binding module of a newly sequenced T5-like phage EPS7. *FEMS Microbiol. Lett.* **289**, 202–209 (2008).
220. Pickard, D. *et al.* A conserved acetyl esterase domain targets diverse bacteriophages to the Vi capsular receptor of Salmonella enterica serovar Typhi. *J. Bacteriol.* **192**, 5746–54 (2010).
221. Sillankorva, S., Neubauer, P. & Azeredo, J. Pseudomonas fluorescens biofilms subjected to phage phiIBB-PF7A. *BMC Biotechnol.* **8**, 79 (2008).
222. Zhao, X. *et al.* Outer membrane proteins ail and OmpF of Yersinia pestis are involved in the adsorption of T7-related bacteriophage Yep-phi. *J. Virol.* **87**, 12260–9 (2013).

223. Pope, W. H. *et al.* Cluster K Mycobacteriophages: Insights into the Evolutionary Origins of Mycobacteriophage TM4. *PLoS One* **6**, e26750 (2011).
224. Mihara, T. *et al.* A Ralstonia solanacearum phage ϕRP15 is closely related to Viunalikeviruses and encodes 19 tRNA-related sequences. *Virol. Reports* **6**, 61–73 (2016).
225. Lee, C.-N., Lin, J.-W., Weng, S.-F. & Tseng, Y.-H. Genomic characterization of the intron-containing T7-like phage phiL7 of Xanthomonas campestris. *Appl. Environ. Microbiol.* **75**, 7828–37 (2009).
226. Lohr, J. E., Chen, F. & Hill, R. T. Genomic analysis of bacteriophage PhiJL001: insights into its interaction with a sponge-associated alpha-proteobacterium. *Appl. Environ. Microbiol.* **71**, 1598–609 (2005).

Appendix 2. Supplemental Figures and Tables for Chapter 2

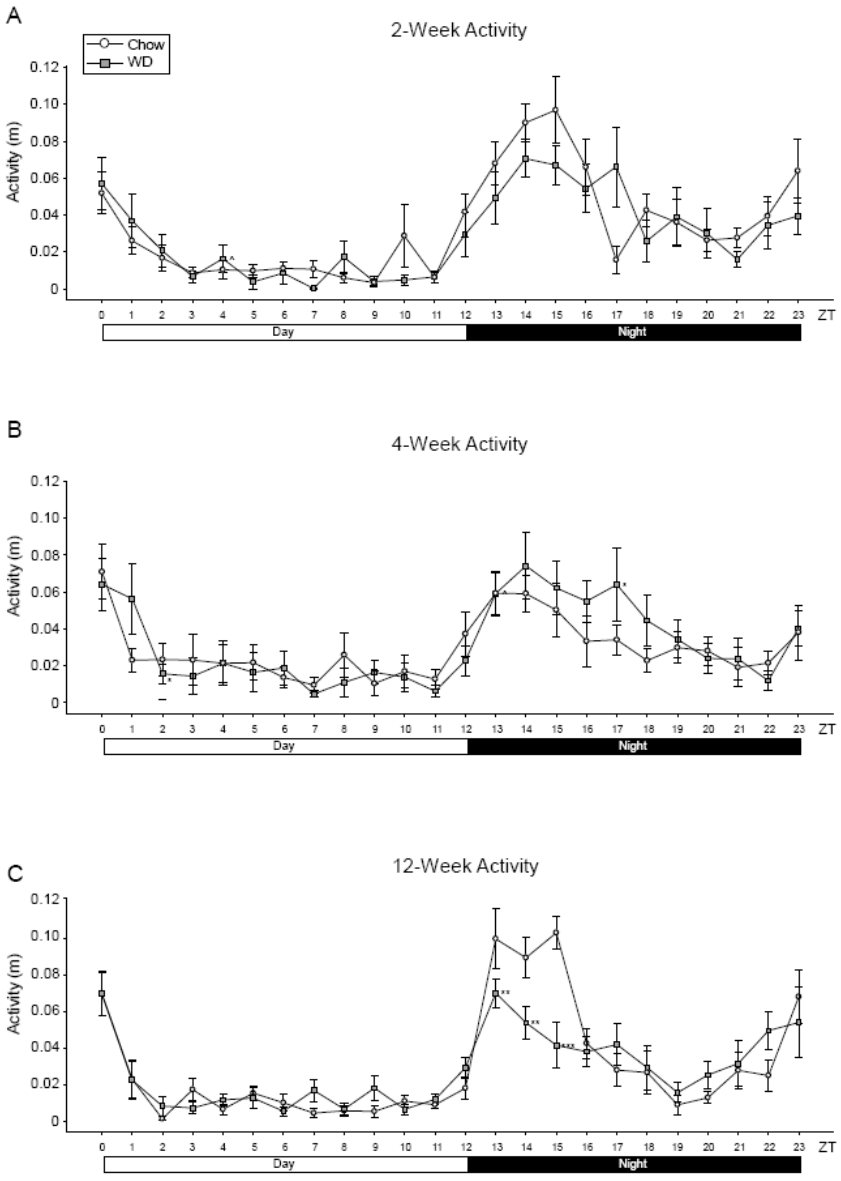

Supplemental Figure 1. Activity at 2-, 4- and 12-weeks. A. Mean circadian analysis of activity at each hour in the 24-hour cycle in the Chow and WD groups after 2-weeks of dietary exposure. B. Mean circadian analysis of activity at each hour in the 24-hour cycle in the Chow and WD groups after 4-weeks of dietary exposure. C. Mean circadian analysis of activity at each hour in the 24-hour cycle in the Chow and WD groups after 12-weeks of dietary exposure. All data points are shown as group mean ± SE. (* $p < 0.05$, ** $p < 0.01$, *** $p < 0.001$ compared to Chow).

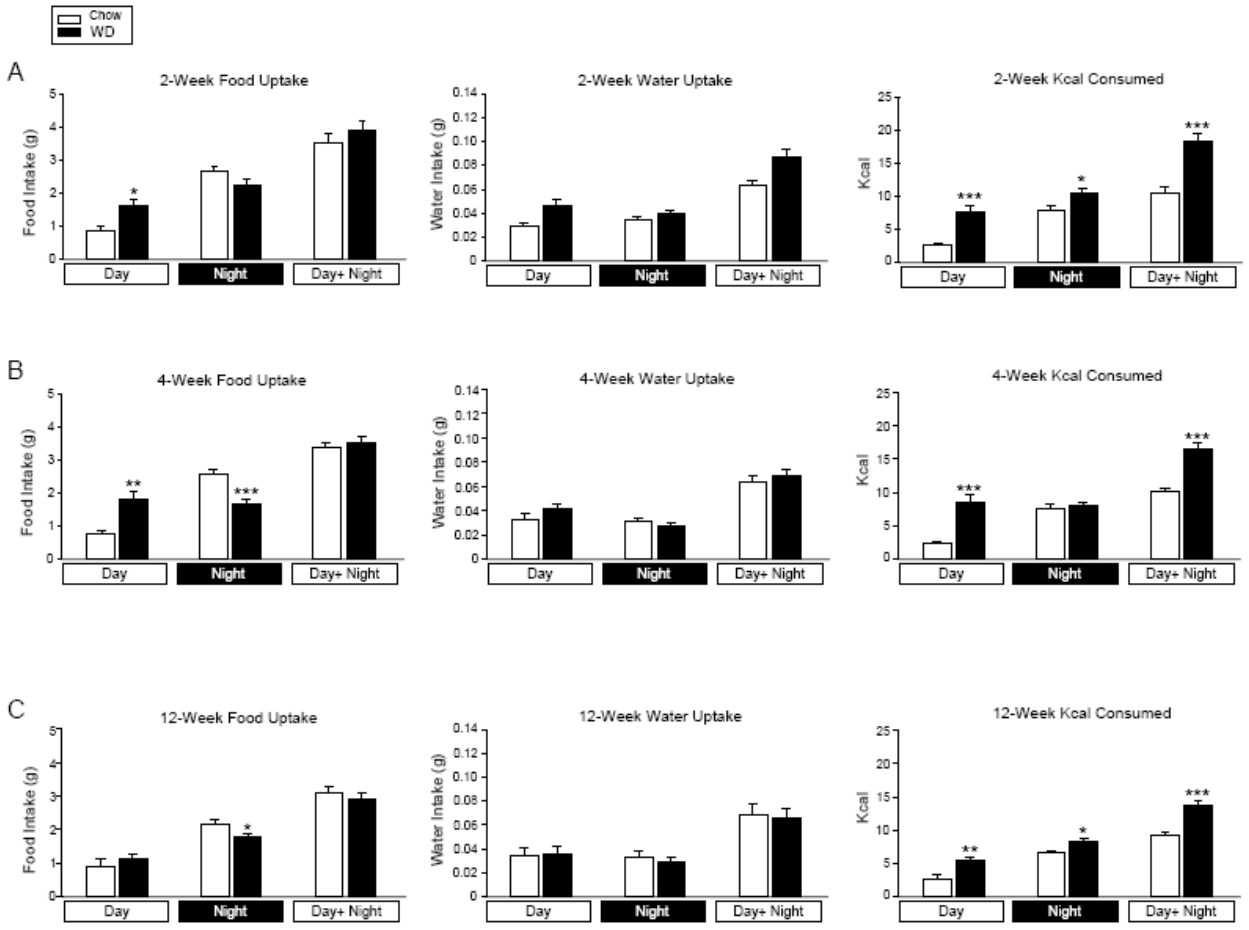

Supplemental Figure 2. Food and water uptake at 2-, 4- and 12-weeks. A. Circadian analysis of food uptake (*left panel*), water uptake (*middle panel*), and kcal consumed (*right panel*) for the day and night phases and total amount over a 24-hours in the Chow and WD groups after 2-weeks of dietary exposure. B. Circadian analysis of food uptake (*left panel*), water uptake (*middle panel*), and kcal consumed (*right panel*) for the day and night phases and total amount over a 24-hours in the Chow and WD groups after 4-weeks of dietary exposure. C. Circadian analysis of food uptake (*left panel*), water uptake (*middle panel*), and kcal consumed (*right panel*) for the day and night phases and total amount over a 24-hours in the Chow and WD groups after 12-weeks of dietary exposure. All data points are shown as group mean + SE. (* $p < 0.05$, ** $p < 0.01$, *** $p < 0.001$ compared to Chow).

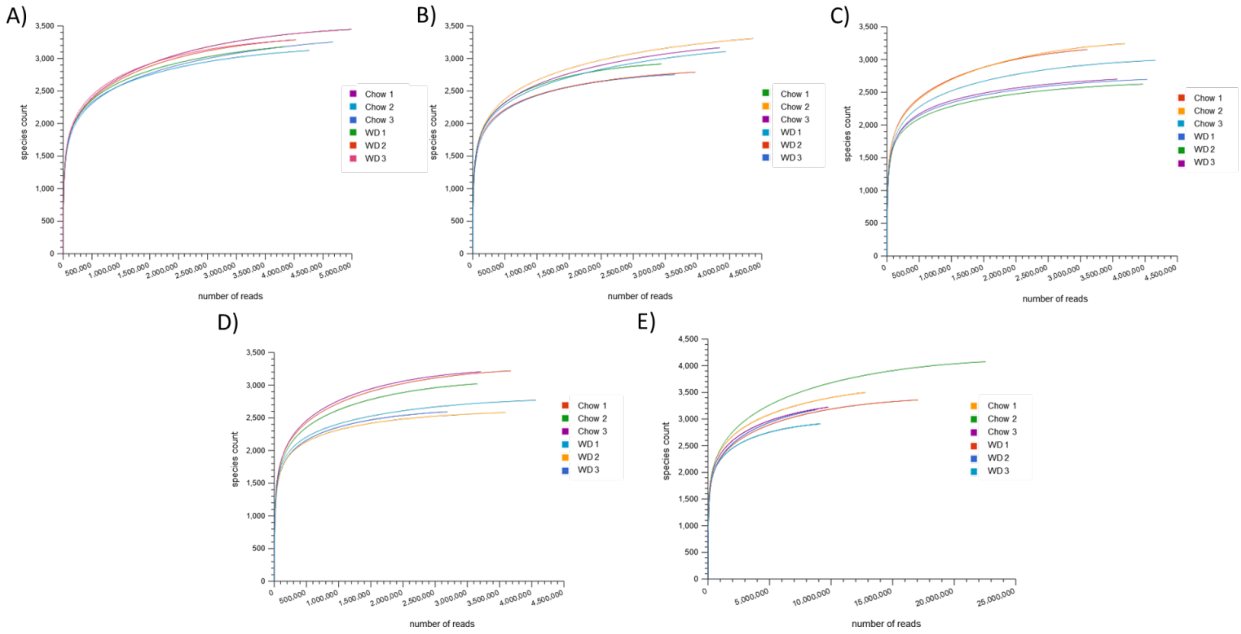

Supplemental Figure 3. Alpha diversity rarefaction curves overtime. Rarefaction curves comparing the number of reads with the number of species found in the DNA from feces in mice in the Chow and WD groups over time. Total species count from all domains and total number of reads were used to plot alpha diversity of all samples at (A) time 0, (B) 2 days, (C) 2 weeks, (D) 8 weeks, and (E) 12 weeks of dietary exposure.

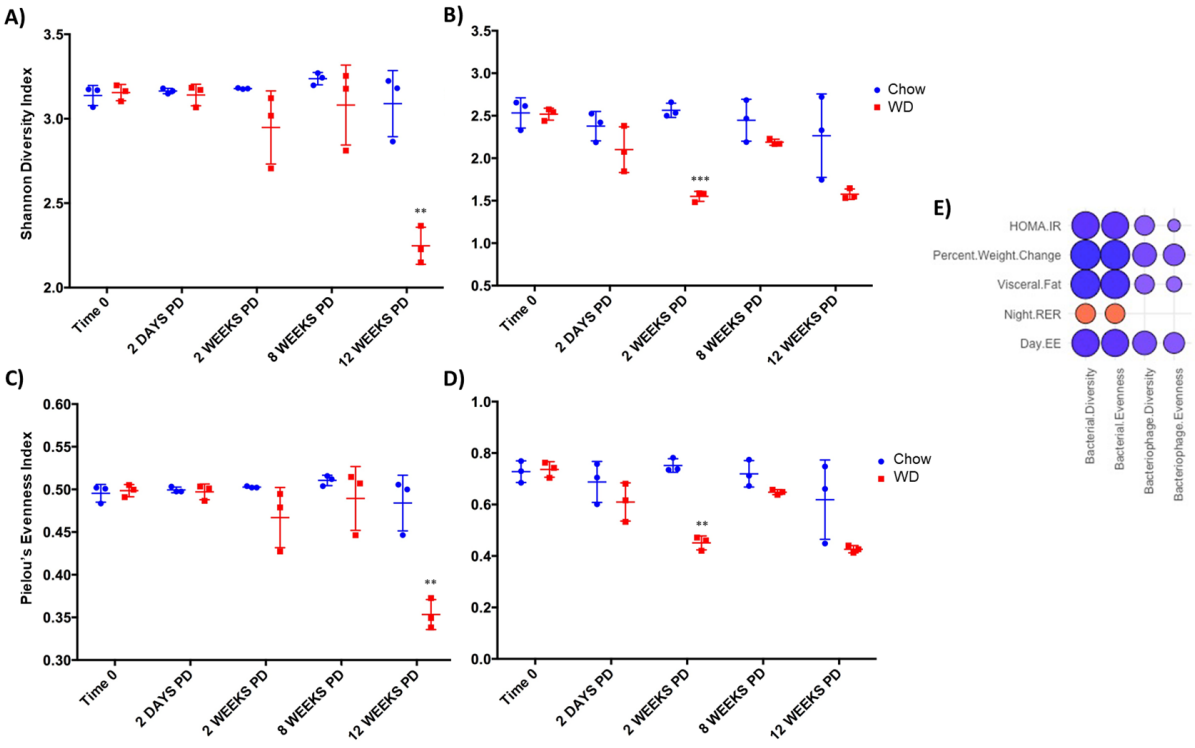

Supplemental Figure 4. Measure of diversity and evenness in microbial assemblages over time. Shannon diversity was used to estimate changes in diversity for A) Bacterial OTUs and B) Bacteriophage OTUs (Viral OTUs within the order Caudovirales) and Pielou's Evenness index was used to estimate changes in evenness for C) Bacterial OTUs and D) Bacteriophage OTUs within the fecal microbiota of mice in the Chow and WD groups at time 0, 2 days, 2, 8, and 12 weeks after diets began. *P < 0.05; **P < 0.01; ***P < 0.001. Pearson's correlation plot of E) Diversity and Evenness with Metabolic parameters.

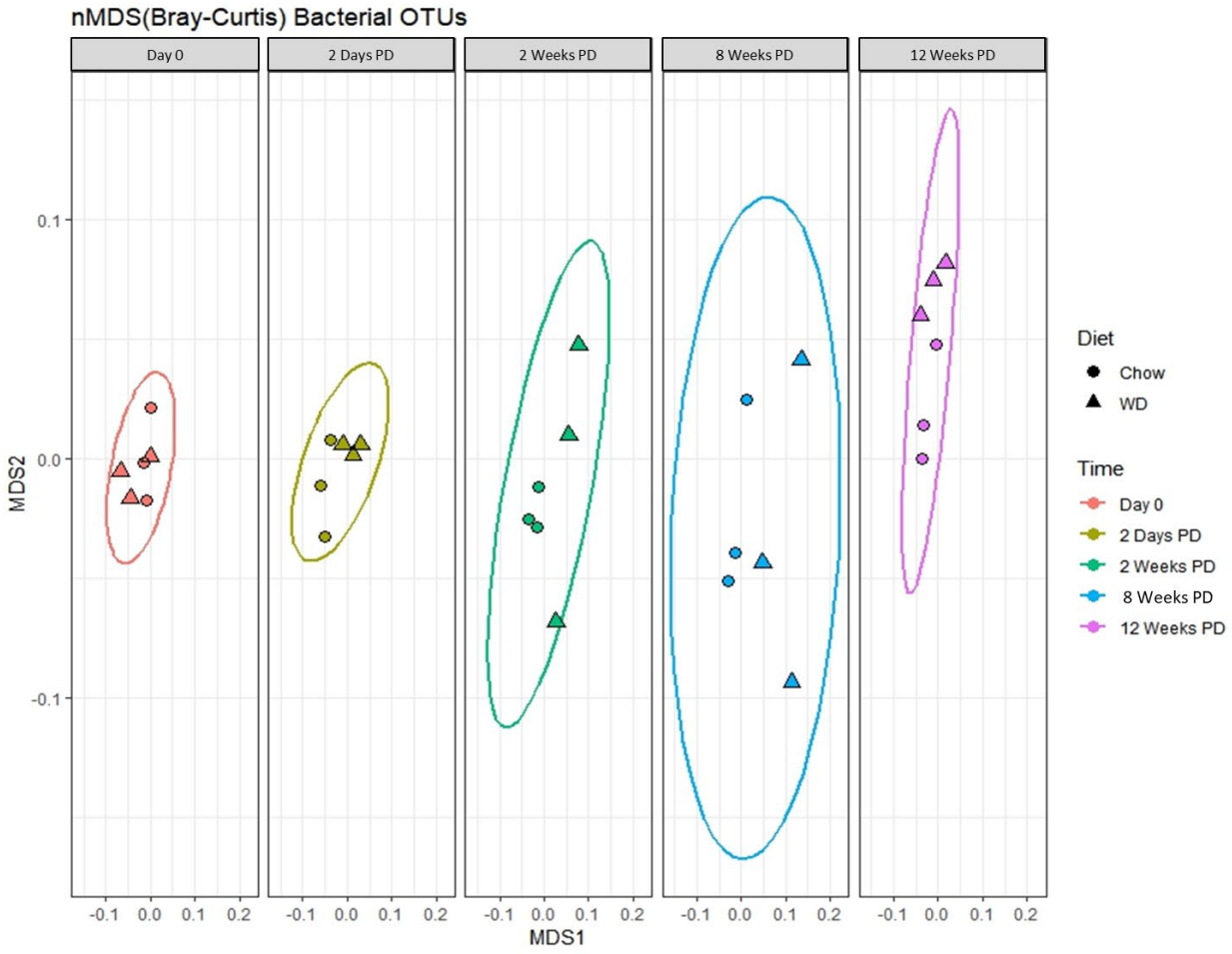

Supplemental Figure 5. nMDS ordination of the microbiota samples separated by time. The taxonomic profiles of the samples were used to compute the sample dissimilarity matrix using Bray-Curtis dissimilarity index. The matrix was used to compute an ordination of the samples in two dimensions (MDS1 and MDS2). The stress associated with this ordination is 0.168. The shapes in the plot denote the diet (Chow or WD). Plots are separated by time point (0 days, 2 days and 2, 8, 12 weeks after diets began).

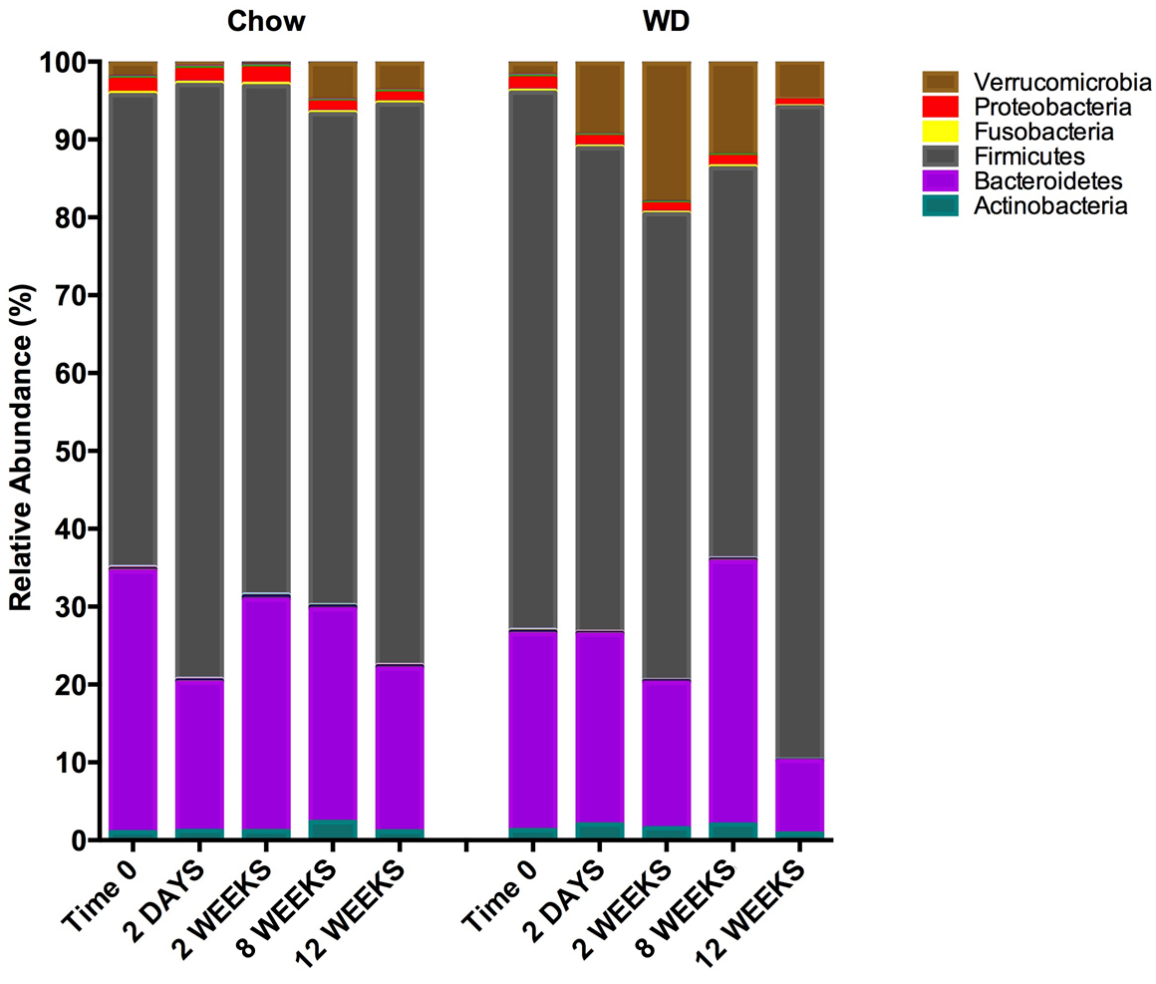

Supplemental Figure 6. Changes in relative abundance of microbial composition after administration of the Western diet. Phylum level bacterial composition in mice fed a Chow or WD at 0 days, 2 days and 2, 8 and 12 weeks after diets began. The mean relative abundance (%) of bacterial phyla are shown.

Appendix 3. Methods Diagram for HOCl Treatment for Modified One-Step Growth Curve